PI Passivity-Based Control : Application to Physical Systems

Rafael Cisneros Montoya

NNT : 2016SACLS187

THESE DE DOCTORAT
DE
L'UNIVERSITE PARIS-SACLAY
PREPAREE A
L'UNIVERSITE PARIS-SUD

LABORATOIRE DES SIGNAUX ET SYSTÈMES

ECOLE DOCTORALE N° 580
Sciences et Technologies de l'Information et de la Communication (STIC)

Automatique

Par

M. Rafael CISNEROS MONTOYA

Commande PI basée sur la Passivité : Application aux Systèmes Physiques

PI Passivity-Based Control : Application to Physical Systems

Thèse présentée et soutenue à Gif-sur-Yvette, le 13/07/16.

Composition du Jury :

M. Hugues MOUNIER	Professeur (LSS)	Président
M. Robert GRIÑÓ	Professeur (Polytechnique de Catalogne)	Rapporteur
Mme. Jacquelien SCHERPEN	Professeur (Université de Groningen)	Rapporteur
M. Stanislav ARANOVSKIY	Professeur (Université ITMO)	Examinateur
M. Romeo ORTEGA	Directeur de Recherche (LSS)	Directeur de thèse

Acknowledgments

I would like to express my gratitude to Prof. Ortega for his invaluable advices and assistance during this period. He was an example of rigourous research and hard work.

Thanks to Professors: R. Griñó, J. Scherpen, S. Aranovskiy and H. Mounier for being part of the Jury.

I also want to thank to my parents and sister for beeing always there, supporting me. To Sra. Amparo for her hospitality. To my laboratory collegues: Diego, Erik, Jonathan, Lupe, Mattia, Missie, Mohamed, Pablo, Víctor, for making this stay pleasant, creating a friendly environment both inside and outside the laboratory.

Finally, thanks to the Consejo National de Ciencia y Tecnología (CONACyT) for funding this thesis work.

Contents

Notations & Acronyms

Mathematical Notation

$\mathbb{R}$	Field of real numbers.
$\mathbb{R}^n$	Linear space of real vectors of dimension n.
$\mathbb{R}^{n\times m}$	Ring of matrices of size $n \times m$.
$\mathbb{R}^n_{\geq 0}$	For a vector x, $x_i \geq 0,\ i = 1, \ldots, n$.
x_i	The i-th element of the vector x.
x_{ij}	$x_{ij} = \text{col}(x_i, x_{i+1}, \ldots, x_j)$ where i, j are integers such that $1 \leq i < j \leq n$.
I_n	The identity matrix of size $n \times n$.
$\mathbf{0}_{n\times s}$	Matrix of zeros of $n \times s$
$\mathbf{0}_n$	column vector of zeros of dimension n.
$\text{diag}(\cdot)$	Diagonal matrix of the input arguments
$\text{col}(\cdot)$	Column vector of the input arguments
$\text{sym}(\cdot)$	Returns the symmetric part of a square matrix.
$\lvert x\rvert^2$	Square of the Euclidean norm, i.e., $\lvert x\rvert^2 := x^\top x$
$\lVert x\rVert_S^2$	The weighted square Euclidean norm, i.e., $\lVert x\rVert_S^2 := x^\top S x$.
$g^\dagger$	Pseudo inverse of the full-rank matrix g, i.e., $g^\dagger := (g^\top g)^{-1} g^\top$.
$F_\star,\ \tilde{F}(x)$	For the distinguished element $x_\star \in \mathbb{R}^n$ and any mapping $F : \mathbb{R}^n \to \mathbb{R}^s$, we denote $F^* := F(x^*)$ and $\tilde{F}(x) := F(x) - F^*$.
$g',\ g''$	For mappings of scalar argument $g : \mathbb{R} \to \mathbb{R}^s$ denote, respectively, first and second order differentiation.
$\nabla H(x)$	For $H : \mathbb{R}^n \to \mathbb{R}$, it refers to the gradient operator of a function, i.e., $\nabla H(x) := \left(\frac{\partial H(x)}{\partial x}\right)^\top$.

$\nabla^2 H(x)$	For $H : \mathbb{R}^n \to \mathbb{R}$, it refers to the Hessian operator of a function, i.e., $\nabla^2 H(x) := \left(\frac{\partial^2 H(x)}{\partial x^2}\right)^\top$.
$\nabla \mathcal{C}(x)$	For $\mathcal{C} : \mathbb{R}^n \to \mathbb{R}^m$, $\nabla \mathcal{C}(x) = [\nabla \mathcal{C}_1(x), \ldots, \nabla \mathcal{C}_m(x)]$.
$\arg\max f(x)$	Returns the argument x of the maxima of a function $f : \mathbb{R}^n \to \mathbb{R}$.

Acronyms

PBC	Passivity-Based Control
SPBC	Standard Passivity-Based Control
PMSG	Permanent Magnet Synchronous Generator
AS	Asymptotically Stable
UAS	Uniformly Asymptotically Stable
GAS	Global Asymptotically Stable
PI	Proportional and Integral
PID	Proportional-Integral-Derivative
PDE	Partial Differential Equations
LMI	Linear Matrix Inequalities

Aperçu de la thèse

Le régulateur PID (Proportionnel-Intégral-Dérivée) est la commande par retour d'état la plus connue. Elle permet d'aborder un bon nombre de problèmes de commande, particulièrement pour des systèmes faiblement non linéaires et dont la performance requise est relativement modeste. En plus, en raison de sa simplicité, la commande PID est largement utilisée dans l'industrie. Étant donné que les méthodes de réglage de la commande PID sont basées sur la linéarisation, la synthèse d'une commande autour d'un point d'équilibre est relativement simple, néanmoins, la performance sera faible dans des modes de fonctionnement loin du point d'équilibre. Pour surmonter ce désavantage, une pratique courante consiste à adapter les gains du PID, procédure connue sous le nom de séquencement de gain (ou gain-scheduling en anglais). Il y a plusieurs désavantages à cette procédure, comme la commutation des gains de la commande et la définition –non triviale– des régions de l'espace d'état dans lesquelles cette commutation aura lieu. Ces deux problèmes se compliquent quand la dynamique est fortement non linéaire.

L'un des avantages à utiliser la passivité est son caractère intuitif, qui exploite les propriétés physique des systèmes. Grosso modo, l'idée centrale d'un système passif est que le flux de puissance entrante au système n'est pas inférieur à l'incrément de son énergie de stockage. Par conséquence, ces systèmes ne peuvent pas stocker plus d'énergie que celle fournie, dont la différence correspond à l'énergie dissipée. En introduisant le concept d'énergie, cette méthodologie nous permet de formuler le problème de commande comme celui de trouver un système dynamique dont la fonction de stockage d'énergie prend la forme désirée. En incorporant le concept d'énergie, cette méthode devient accessible à la communauté de praticiens et permet de fournir des interprétations physiques de l'action de commande.

Dans ce contexte, ce travail de thèse a comme objectif de synthétiser des commandes PI, basées sur la passivité, de telle sorte que la stabilité globale du système en boucle fermé soit garantie.

Ce travail de thèse est principalement la continuation de [16,23,32,35,65,69]. Particulièrement dans [65], il est prouvé que si un système non-linéaire est rendu passif par

une loi de commande constante, il est stabilisable par une commande PI. En partant de ce résultat, dans [32], une commande PI pour une classe de systèmes bilinéaires est proposée pour traiter le problème de régulation et appliqué aux convertisseurs de puissance. Dans cette thèse nous étendons ce dernier résultat au problème de suivi.

D'autre part, dans [35], des conditions suffisantes pour une classe de système dynamique sont énoncées telles que s'il est passif, sa représentation incrémentale l'est aussi. Dans ce travail, en utilisant ce résultat, nous proposons une commande PI robuste qui dépend seulement des paramètres de la matrice d'entrée.

Une contribution finale concerne le domaine de recherche développée par [23]. Nous proposons une méthodologie constructive pour la synthèse d'une commande PI pour une classe de systèmes port-Hamiltoniens. Cette commande nous permet de façonner l'énergie du système en boucle fermée.

Présentation de la thèse

La thèse est organisée de la manière suivante :

- Dans le Chapitre 2, nous présentons la commande PI-PBC qui adresse le problème de suivi d'une classe de systèmes bilinéaires. Ce résultat est appliquée aux convertisseurs de puissance qui sont décrits par les équations dynamiques de la forme $\dot{x}(t) = [A + \sum_i u_i(t)B_i]x(t) + B_0u + d(t)$. L'approche est validée par des simulations numériques.

- En Chapitre 3 nous étudions le problème de commande des systèmes non linaires qui sont partiellement connus. Nous identifions une classe de systèmes dans laquelle une commande PI basée sur la passivité peut stabiliser les système autour d'un point d'équilibre désiré en connaissant seulement les paramètres de la matrice d'entrée.

- Le Chapitre 4 propose une commande PI, complètement constructive, pour une classe de systèmes porte-Hamiltoniens. En utilisant la *sortie passive de façonnage de puissance*, cette commande nous permet de assigner, au système en boucle fermée, le point minimum désiré de la fonction d'énergie du système en boucle fermée.

- Le Chapitre 5 est consacré à des applications de la commande PI-PBC. En utilisant la théorie des chapitres précédents, nous proposons deux systèmes d'énergie éolienne et faisons la synthèse de sa commande. Cette commande a comme objectif de garantir la l'extraction de la puissance maximale provenant du vent.

- Ce travail est terminé avec des conclusions et des travaux futurs, présentés dans le Chapitre 6.

Publications

Ce travail de thèse a fait l'objet des articles de conférence et revue suivantes.

Articles de conférence

- R. Cisneros, M. Pirro, G. Bergna, R. Ortega, G. Ippoliti and M. Molinas, Global Tracking Passivity-based PI Control of Bilinear Systems and its Application to the Boost and Modular Multilevel Converters, *Conf. on Modelling, Ident. and Cont. of Non Syst. (MICNON)*, vol. 48, no. 11, pp. 420-425, 2015.

- S. Aranovskiy, R. Ortega and R. Cisneros, Robust PI passivity-based control of nonlinear systems: Application to port-Hamiltonian systems and temperature regulation, *American Control Conference (ACC)*, pp. 434-439, 2015.

- P. Borja and R. Cisneros and R. Ortega, Shaping the energy of port-Hamiltonian systems without solving PDE's, *54th IEEE Conference on Decision and Control (CDC)*, pp. 5713-5718, 2015.

- R. Cisneros, R. Gao, R. Ortega and I. Husain, PI Passivity–Based Control for Maximum Power Extraction of a Wind Energy System with Guaranteed Stability Properties, *Int. Conf. on Renewable Energy : Generation and Appl. (ICREGA)(To be printed), 2015.*

Articles de revue

- R. Cisneros, F. Mancilla-David and R. Ortega,Passivity-Based Control of a Grid-Connected Small-Scale Windmill With Limited Control Authority ,*IEEE Journal of Emerging and Selected Topics in Power Electronics*, vol. 1, no. 4, pp. 247-259, 2013.

- R. Cisneros, M. Pirro, G. Bergna, R. Ortega, G. Ippoliti and M. Molinas, Global tracking passivity-based PI control of bilinear systems: Application to the interleaved boost and modular multilevel converters, *Control Engineering Practice*, vol. 46, pp. 109-119, 2015.

- S. Aranovskiy, R. Ortega and R. Cisneros, A robust PI passivity-based control of nonlinear systems and its application to temperature regulation, *International Journal of Robust and Nonlinear Control*, vol. 26, no. 10, pp. 2216–2231, 2015.

- P. Borja, R. Cisneros and R. Ortega, A Constructive Procedure for Energy Shaping of Port–Hamiltonian Systems, *Automatica*, vol. 72, pp. 230-234 , 2016.

.

Chapter 1

Introduction

Automatic feedback control systems have been known and used for more than 2000 years. There is evidence that the ancient romans and greeks developed devices to regulate the water level [10]. In late medieval, attempts to provide speed regulation by primitive feedback devices were made. Along the history, ingenious inventions concerning feedback control systems have been reported: mechanisms to control temperature, governors for steam engines, steering engines or servo-mechanisms, pneumatic feedback amplifiers, anti-aircraft control and many others. Actually, the word feedback is a 20th century neologism introduced in the 1920s by radio engineers to describe parasitic, positive feeding back of the signal from the output of an amplifier to the input circuit. Interested reader is referred to [9, 10], where an interesting monograph about the history of automatic control is presented.

The idea of feedback is at the same time, simple and powerful. It has had a profound influence on technology. Application of the feedback principle has resulted in major breakthroughs in control, communication, and instrumentation. The principle of the (negative) feedback relies on increasing a manipulated variable (control input) when the process variable is smaller than the setpoint (reference) and decrease the manipulated variable when the process variable is larger than the setpoint [6]. In general, a process or system to be controlled is fed-back by a function of its measured signals. One of the best known forms of feeding back a system is through a three-term control law known as PID (Proportional-Integral-Derivative) controller, which was firstly presented with an analytical formalism by N. Minorsky. In a traditional scheme, an error signal is derived from the difference between the measured signals and its desired values. In the *non-interacting PID*, the control signal is based on a sum of the weighted integral, proportional and derivative of the error. The transfer function of

this controller is of the form

$$H_{\texttt{PID}}(s) = K\left(1 + \frac{1}{T_I s} + T_D s\right).$$

The three term functionalities include:

1. The proportional term provides an overall control action proportional to the error signal through the allpass gain factor.

2. The integral term reduces steady-state errors through low-frequency compensation.

3. The derivative term improves transient response through high-frequency compensation.

Other classical PID realization is the *interacting PID*, which is implemented as a cascade of a PI and PD controller [6]. The transfer function of such PID is

$$H_{\texttt{PID}}(s) = K\left(1 + \frac{1}{T_I s}\right)(1 + sT_d).$$

Trying to improve transient performance has given rise to other control schemes such as PI-D (type B) or I-PD (type C) controllers, see [3,44] for a description.

PID controllers are sufficient for many control problems, particularly when process dynamics are not highly nonlinear and the performance requirements are modest. Besides, because of its simple structure, the PID controller is the most adopted control scheme by industry and practitioners. However, many practitioners opt to switch off the derivative term. Actually, many controllers applied in the industry are only PI controllers [7].

An important issue when implementing a PID is to determine its parameters that influence the performance of the system.In order to make this tuning of the PID gains more constructive, some procedures have been appear in the literature. This methods determine the gains values based on some parameters taken from the system response. They are divided in frequency and step response methods. The first and more classical method is the Ziegler-Nichols, which is frequently adopted because of its simplicity to implement. In its step response version, two parameters are registered from the straight line tangent at the inflection point of the step response of the system. Then, the PI(D) controller parameters are obtained from a table. In its frequency response version, the point at which the Nyquist curve intersects with the negative real axis is determined. To do so, the process is fed back with a proportional controller, the proportional gain is increased until the system and starts to oscillate. The proportional

gain and the period of the oscillations are registered and using a table, the parameter values of the PI(D) can be obtained. As discussed in [6], a fundamental drawback in the Ziegler-Nichols Method is that the design criterion is focused in the decay ratio, i.e., the ratio between two consecutive maxima of the error for a step change in set-point or load. In this method, the closed–loop system has a quarter amplitude decay ratio. This may cause good rejection of load disturbances but also poor damping and stability margins. In order to improve the control performance, new tuning methods have been developed [6]. In these methods the system response is characterized using three parameters instead of two, as in Ziegler-Nichols method. Even though these methods improves substantially the performance, there is a trade-off between the simplicity of the methods and its performance.

As stated in [6], many tuning strategies proposed can easily be eliminated if they are compared with a well–tuned PID. Also, since these methods are based on the linearization, commissioning a PI to operate around a single operating point is relatively easy, however, the performance will be below par in wide operating regimes, which is the scenario in modern high–performance applications. To overcome this drawback the current practice is to re–tune the gains of the PI controllers based on a linear model of the plant evaluated at various operating points, a procedure known as gain–scheduling. There are several disadvantages of gain–scheduling including the need to switch (or interpolate) the controller gains and the non–trivial definition of the regions in the plants state space where the switching takes place—both problems are exacerbated if the dynamics of the plant is highly nonlinear. Another common commissioning procedure is to use auto–tuners, that heavily rely on the availability of a "good" linear approximation of the plant dynamics. Besides, in other scenarios, a little or no information about the dynamics of the process/system is known, thus no stability of the system can be proved.

The current thesis work is aimed at the designing of PI controllers, based on the passivity theory, such that the stability of the closed–loop system is guarantied. The main objective is to develop constructive procedures that are applicable to physical systems.

1.1 Passivity : A Control Design Tool [58, 63, 73].

Passivity concepts offer a physical and intuitive appeal. This is one of its main advantage that explains the longevity of the concept from the time of its appearance —60 years ago. The primary idea in passive systems is that the power flowing into the system is not less that the increase of storage. Thus, they cannot store more energy than

is supplied to it from the outside, with the difference being the dissipated energy.

It is clear from this energy interpretation that the concept of passivity is related with the stability properties of the systems. For instance, rationalizing a feedback interconnection as a process of energy exchange it is not surprising to learn that passivity is invariant under negative feedback interconnection. In other words, the feedback interconnection of two passive systems is still passive. If the overall energy balance is positive, in the sense that the energy generated by one subsystem is dissipated by the other one, the closed loop will be stable.

Viewing dynamics systems as energy-transformation devices is particularly useful in studying complex nonlinear systems by decomposing them into simpler subsystems that,upon interconnection, add up their energies to determine the full system's behavior. This allows to recast the control problem as finding a dynamical system and an interconnection pattern such that the overall energy function takes the desired form. This "energy-shaping" approach is the essence of passivity-based control (PBC). Moreover, because of the universality of the concepts of energy, this formulation allows to facilitate the communication between practitioners and control theorists incorporating prior knowledge and providing physical interpretations of the control action.

The idea of energy shaping from a control point of view dates back to [77] where a robot manipulator control methodology was proposed using this philosophy. Using the fundamental notion of passivity, the principle was later formalized in [61], where the term PBC was coined to define a controller design methodology whose aim is to render the closed-loop system passive with a given storage function. Although there are many variations of this basic idea, PBCs may be broadly classified into two large groups, "classical" PBC where we a priori select the storage function to be assigned (typically quadratic in the increments) and then design the controller that renders the storage function non-increasing. This approach, clearly reminiscent of standard Lyapunov methods, has been very successful to control physical systems described by Euler-Lagrange equations of motion, which as thoroughly detailed in, includes mechanical, electrical and electromechanical applications. Approaches within this category are the energy balancing (EB), standard passivity based control (SPBC) [58] and the PI-PBCs. In the second class of PBCs we do not fix the closed-loop storage function, but instead select the desired structure of the closed- loop system, for example, Lagrangian or port-controlled Hamiltonian (PCH), and then characterize all assignable energy functions compatible with this structure. This characterization is given in terms of the solution of a partial differential equation (PDE). The most notable examples of this approach are the controlled Lagrangian, the interconnection and damping as-

signment (IDA) and power-shaping control methods which yields static controllers (see [13, 29, 54] for further details). There has been reported a dynamic version of the IDA-PBC, however as proved in [5], this extension is unnecessary since a system can be stabilized by IDA-PBC if and only if it can be stabilized by the dynamic IDA-PBC. In the same category is found the so-called control by interconnection (CBI). In this approach, a dynamic controller is obtained such that plant and the controller are coupled via a power-preserving interconnection-generating an overall PCH system with storage function the sum of the plant and controller storage functions. Roughly speaking, in this methodology it is desired to achieve stabilization making the desired equilibrium a minimum of the new storage function [53].

The present thesis work is placed within this line of research. Particularly, we are interested in deriving controllers, based on passivity theory, such that they admit a PI-like structure. We called these controllers PI passivity-based controllers or simple PI-PBC. The result presented is twofold. Firstly, we derived PI controllers that are widely accepted by practitioners due to its simplicity and then we find application of these controllers in physical systems. Secondly, the procedures here adopted encompass a large class of nonlinear dynamic systems and do not need to solve PDEs, a situation that commonly emerges when it is desired to shape the system energy.

1.2 Thesis Overview & Contributions

The work presented along this thesis follows mainly from [16, 23, 32, 35, 65, 69]. Thus, the PI controllers here formulated extend the methodology presented therein. A brief introduction of this line of research as well as the contributions of the thesis is described in the following.

Borrowing the concepts of *incremental passivity* and *energy in the increment* of [85], in [69] is shown that the energy in the increment of a broad class of switched converters is a Lyapunov function for a given nominal trajectory, so the nominal trajectory is stable. Furthermore, a control law of the incremental input is proposed to regulate switched converters. This incremental input is a deviation of the control signal from its value at the desired equilibrium (also known as nominal value). To represent the original system control input from its increment, the knowledge of its nominal value is needed.

In [65] is proved that if a nonlinear system is passifiable via a constant action, then it is stabilizable with a PI controller depending on its passive output. Using this result, in [32] is designed a completely constructive PI passivity-based controller for a class of bilinear system and motivated by the application to power converters.

On the other hand, in [35] sufficient conditions are stated under which a class of nonlinear systems defining a passive mapping $u \mapsto y$, also defines a passive mapping in its incremental representation, i.e. the mapping $\tilde{u} \mapsto \tilde{y}$ is passive —the symbol $\tilde{()}$ represents, respectively, the increments on the control input and output respect to their value at the desired equilibrium point.

In the current thesis is presented an extension of the regulation case of power converters system, addressed in [32], to the tracking problem. As a result, we prove that the fulfillment of some given conditions makes possible to obtain —time-varying— PIs controllers tracking admissible system trajectories. We apply this approach to some benchmark examples and a wind energy system. Furthermore, experimental applications were reported in [21]. Another contribution of this thesis is intended to robustify the PI-PBC controller introduced in [35]. To carry out this robustification we identify a class of systems to which this technique is applicable when the system parameters are unknown. This approach is motivated by its application to temperature regulation.

A final contribution of the thesis concerns the line of research developed in [23]. In that paper, it has been proposed for mechanical systems to abandon the objective of structure preservation and attention has been concentrated on the energy shaping objective only. That is, to look for a static state–feedback that stabilizes the desired equilibrium assigning to the closed-loop a Lyapunov function of the same form as the energy function of the open–loop system but with new, desired inertia matrix and potential energy function. However, it was not required that the closed-loop system is a mechanical system with this Lyapunov function qualifying as its energy function. In this way, the need to solve the matching equations is avoided. Under the same philosophy, we consider now the case of port–Hamiltonian (pH) systems. The starting point of the design is the well–known power shaping output [55]. Then, we construct the new storage function from the original energy function of the system and its power shaping output. We find out that under some conditions, PI controllers that regulate the system behavior and guarantee the stability of the system.

1.3 Outline of the Thesis

The current thesis is organized as follows.

- In Chapter 2, we present a PI-PBC for the tracking problem of a class of bilinear systems. We extend the result reported in [32], where a PI depending on a passive output is developed to solve the regulation problem in power converters . The class of systems under consideration has the form $\dot{x}(t) = [A + \sum_i u_i(t)B_i]x(t) + B_0u + d(t)$. A set of matrices $\{A, B_i\}$ are identified, via a linear

matrix inequalities, for which it is possible to ensure global tracking of (admissible, differentiable) trajectories with a simple linear time–varying PI controller. Instrumental to establish the result is the construction of an output signal with respect to which the incremental model is passive. The result is illustrated by the application to some conventional DC/DC converters.

- In Chapter 3, We deal with the problem of control of partially known nonlinear systems, which have an open–loop stable equilibrium, but we would like to add a *PI controller* to regulate its behavior around another operating point. We identify a class of nonlinear systems for which a globally stable PI can be designed knowing only the systems input matrix and measuring only the actuated coordinates.

- In Chapter 4 a new, fully constructive, procedure to shape the energy for a class of port–Hamiltonian systems that obviates the solution of partial differential equations is proposed. Proceeding from the well–known passive, power shaping output we propose a nonlinear static state–feedback that preserves passivity of this output but with a new storage function. A suitable selection of a controller gain makes this function positive definite, hence it is a suitable Lyapunov function for the closed–loop. The resulting controller may be interpreted as a classical PI—connections with other standard passivity–based controllers are also identified.

- Chapter 5 is advocated to the application of the PI-PBC. This chapter is mainly divided in two parts. First, we propose a maximum power extraction control with a PI-PBC for a wind system consisting of a turbine, a permanent magnet synchronous generator (PMSG), a rectifier, a load and one constant voltage source, which is used to form the DC bus. We propose a linear PI controller, based on passivity, whose stability is guaranteed under practically reasonable assumptions. In the second part, we consider the problem of controlling small–scale wind turbines providing energy to the grid. In this section, the overall system consists of a wind turbine plus a PMSG connected to a single–phase ac grid through a passive rectifier, a boost converter and an inverter. We present a high performance, nonlinear, passivity–based controller combining two Passivity-Based Control techniques: the Standard PBC and the tracking PI-PBC. Asymptotic convergence to the maximum power extraction point together with regulation of the dc link voltage and grid power factor to their desired values is ensured. The performance of the proposed controllers is compared via computer simulations.

- Finally, in Chapter 6, we wrap out the present thesis with some concluding remarks and possible future work in the same line of research.

Articles de conférence

- R. Cisneros, M. Pirro, G. Bergna, R. Ortega, G. Ippoliti and M. Molinas, Global Tracking Passivity-based PI Control of Bilinear Systems and its Application to the Boost and Modular Multilevel Converters, *Conf. on Modelling, Ident. and Cont. of Non Syst. (MICNON)*, vol. 48, no. 11, pp. 420-425, 2015.

- S. Aranovskiy, R. Ortega and R. Cisneros, Robust PI passivity-based control of nonlinear systems: Application to port-Hamiltonian systems and temperature regulation, *American Control Conference (ACC)*, pp. 434-439, 2015.

- P. Borja and R. Cisneros and R. Ortega, Shaping the energy of port-Hamiltonian systems without solving PDE's, *54th IEEE Conference on Decision and Control (CDC)* , pp. 5713-5718, 2015.

- R. Cisneros, R. Gao, R. Ortega and I. Husain, PI Passivity–Based Control for Maximum Power Extraction of a Wind Energy System with Guaranteed Stability Properties, *Int. Conf. on Renewable Energy : Generation and Appl. (ICREGA)(To be printed), 2015*

Articles de revue

- R. Cisneros, F. Mancilla-David and R. Ortega,Passivity-Based Control of a Grid-Connected Small-Scale Windmill With Limited Control Authority ,*IEEE Journal of Emerging and Selected Topics in Power Electronics*, vol. 1, no. 4, pp. 247-259, 2013.

- R. Cisneros, M. Pirro, G. Bergna, R. Ortega, G. Ippoliti and M. Molinas, Global tracking passivity-based PI control of bilinear systems: Application to the interleaved boost and modular multilevel converters, *Control Engineering Practice*, vol. 46, pp. 109-119, 2015.

- S. Aranovskiy, R. Ortega and R. Cisneros, A robust PI passivity-based control of nonlinear systems and its application to temperature regulation, *International Journal of Robust and Nonlinear Control*, vol. 26, no. 10, pp. 2216–2231, 2015.

- P. Borja, R. Cisneros and R. Ortega, A Constructive Procedure for Energy Shaping of Port–Hamiltonian Systems, *Automatica*, vol. 72, pp. 230-234 , 2016.

Chapter 2

The Tracking PI–PBC of Bilinear Systems : Application to Power Converters

Bilinear systems are a class of nonlinear systems that describe a broad variety of physical and biological phenomena [51] serving, sometimes, as a natural simplification of more complex nonlinear systems. In this chapter we propose a PI Passivity-Based controller for the global tracking of admissible, differentiable trajectories of a class of bilinear systems.

The objective of this chapter is to provide a theoretical framework—based on the property of passivity [34, 81] of the incremental model—to establish such a result. Our motivation to pursue a passivity framework is that it naturally leads to the design of PI controllers, which are known to be simple, robust and widely accepted by practitioners. The result presented in this chapter is an extension to the problem of tracking trajectories, of [32, 35] that treat the regulation case (see Section 2.3). The proposed result is illustrated by an application to power converters.

2.1 The PI-PBC of Bilinear system for the regulation and tracking problem

Consider the bilinear system[1]

$$\dot{x} = Ax + d + \sum_{i=1}^{m} u_i B_i x + B_0 u \tag{2.1}$$

[1]For brevity, in the sequel the time argument is omitted from all signals.

where $x \in \mathbb{R}^n, d \in \mathbb{R}^n$ are the state and the *known* time-varying signal vector, respectively, $u \in \mathbb{R}^m,\ m \leq n$, is the control vector, and $A \in \mathbb{R}^{n\times n}, B_i \in \mathbb{R}^{n\times n}, B_0 \in \mathbb{R}^{n\times m}$ are real constant matrices.

We will say that a function $x_\star : \mathbb{R}_+ \to \mathbb{R}^n$ is an *admissible trajectory* of (2.1), if it is differentiable, bounded and verifies

$$\dot{x}_\star = Ax_\star + d + \sum_{i=1}^{m} u_i^\star B_i x_\star + B_0 u_\star \tag{2.2}$$

for some bounded control signal $u_\star : \mathbb{R}_+ \to \mathbb{R}^m$.

The global tracking problem is to find, if possible, a dynamic state–feedback controller of the form

$$\dot{z} = F(x, x_\star, u_\star) \tag{2.3}$$

$$u = H(x, x_\star, z, u_\star), \tag{2.4}$$

where $F : \mathbb{R}^n \times \mathbb{R}^n \times \mathbb{R}^m \to \mathbb{R}^q,\ q \in \mathbb{Z}_+$, and $H : \mathbb{R}^n \times \mathbb{R}^n \times \mathbb{R}^m \to \mathbb{R}^m$, such that all signals remain bounded and

$$\lim_{t\to\infty}[x(t) - x_\star(t)] = 0, \tag{2.5}$$

for all initial conditions $(x(0), z(0)) \in \mathbb{R}^n \times \mathbb{R}^q$ and all admissible trajectories.

We characterize a set of matrices $\{A, B_i\}$ for which it is possible to solve the global tracking problem with a simple *linear time–varying PI controller*. The class is identified via the following LMI.

Assumption 2.1. $\exists P \in \mathbb{R}^{n\times n}$ such that

$$P = P^\top > 0 \tag{2.6}$$

$$\text{sym}(PA) \leq 0 \tag{2.7}$$

$$\text{sym}(PB_i) = 0, \tag{2.8}$$

where the operator sym : $\mathbb{R}^{n\times n} \to \mathbb{R}^{n\times n}$ computes the symmetric part of the matrix, that is

$$\text{sym}(PA) = \frac{1}{2}(PA + A^\top P).$$

To simplify the notation in the sequel the *positive semidefinite* matrix has been defined

$$Q := -\text{sym}(PA). \tag{2.9}$$

2.2 Passivity of the Bilinear Incremental Model

Instrumental to establish the main result of the paper is the following lemma.

Lemma 2.1. Consider the system (2.1) verifying the LMI of Assumption 2.1 and an admissible trajectory $x_\star$. Define the incremental signals $\tilde{(\cdot)} := (\cdot) - (\cdot)_\star$, and the m–dimensional output function

$$y := \mathcal{C}(x_\star)\tilde{x} \tag{2.10}$$

where the map $\mathcal{C} : \mathbb{R}^n \to \mathbb{R}^{m\times n}$ is defined as

$$\mathcal{C}(x_\star) := \left(\begin{bmatrix} x_\star^\top B_1^\top \\ \vdots \\ x_\star^\top B_m^\top \end{bmatrix} + B_0^\top \right) P. \tag{2.11}$$

The operator $\tilde{u} \mapsto y$ is *passive* with storage function

$$V(\tilde{x}) := \frac{1}{2}\tilde{x}^\top P \tilde{x}. \tag{2.12}$$

Hence, it verifies the dissipation inequality

$$\dot{V} \leq \tilde{u}^\top y.$$

Proof. Combining (2.1) and (3.30) yields

$$\dot{\tilde{x}} = (A + \sum_{i=1}^{m} u_i B_i)\tilde{x} + \sum_{i=1}^{m} \tilde{u}_i B_i x_\star + B_0 \tilde{u}. \tag{2.13}$$

Now, the time derivative of the storage function (2.12) along the trajectories of (2.13) is

$$\begin{aligned} \dot{V}(\tilde{x}) &= \tilde{x}^\top P \left[(A + \sum_{i=1}^{m} u_i B_i)\tilde{x} + \sum_{i=1}^{m} \tilde{u}_i B_i x_\star + B_0 \tilde{u} \right] \\ &= -\tilde{x}^\top Q \tilde{x} + \tilde{x}^\top P \left[\sum_{i=1}^{m} \tilde{u}_i B_i x_\star + B_0 \tilde{u} \right] \\ &\leq \tilde{x}^\top P \left[\sum_{i=1}^{m} \tilde{u}_i B_i x_\star + B_0 \tilde{u} \right] \\ &= \tilde{x}^\top P \left(\left[B_1 x_\star | \dots | B_m x_\star \right] + B_0 \right) \tilde{u} \\ &= y^\top \tilde{u}, \end{aligned}$$

where (2.8) of Assumption 2.1 has been used to get the second identity, (2.7) for the first inequality, (2.8) again for the third equation and (2.10) for the last identity. □□□

Remark 2.1. A key step for the utilization of the previous result is the derivation of the desired trajectories $x_\star$ and their corresponding control signals $u_\star$, which satisfy (3.30). As shown in the examples below this may prove to be a very complicated task and some approximations may be needed to derive them. Indeed, it is shown in [52] that even for the simple boost converter this task involves the search of a stable solution of an Abel ordinary differential equation, whose only stable trajectory is known to be highly sensitive to initial conditions.

2.3 A PI Global Regulating Controller [32]

In this section we recall the result reported in [32] about the regulation in systems of the form (2.1). For this case, we consider d and $x_\star$ constant vectors. Then, it can be seen that (3.30) becomes an algebraic equation, i.e., $x_\star$ is an admissible equilibrium point satisfying

$$0 = Ax_\star + d + \sum_{i=1}^{m} u_i^\star B_i x_\star + B_0 u_\star \tag{2.14}$$

for some $u_\star \in \mathbb{R}^m$.

Lemma 2.2. Consider the system (2.1) verifying Assumption 2.1 with d and $x_\star, u_\star$ such that (2.14). Then, the system (2.1) in closed–loop with the PI controller

$$\begin{aligned} \dot{z} &= -\, y \\ u &= -\, K_p y + K_i z \end{aligned} \tag{2.15}$$

with output y given in 2.10 and $K_p, K_i > 0$. For all initial conditions $(x(0), z(0)) \in \mathbb{R}^{n+m}$ the trajectories of the closed–loop system are bounded.

Proof: The reader is referred to [32].

2.4 A PI Global Tracking Controller

From Lemma 2.1 the next proposition follows immediately.

Proposition 2.1. Consider the system (2.1) verifying Assumption 2.1 and an admissible trajectory $x_\star$ in closed loop with the PI controller

$$\begin{aligned} \dot{z} &= -\, y \\ u &= -\, K_p y + K_i z + u_\star \end{aligned} \tag{2.16}$$

with output (2.10), (4.12) and $K_p > 0$, $K_i > 0$. For all initial conditions $(x(0), z(0)) \in \mathbb{R}^n \times \mathbb{R}^m$ the trajectories of the closed-loop system are bounded and

$$\lim_{t\to\infty} y_a(t) = 0, \tag{2.17}$$

where the augmented output $y_a : \mathbb{R}_+ \to \mathbb{R}^{m+n}$ is defined as

$$y_a := \begin{bmatrix} \mathcal{C}(x_\star) \\ Q^{\frac{1}{2}} \end{bmatrix} \tilde{x},$$

with $Q^{\frac{1}{2}}$ the square root of Q given in (2.9). Moreover, if

$$\text{rank} \begin{bmatrix} \mathcal{C}(x_\star) \\ Q^{\frac{1}{2}} \end{bmatrix} = n, \tag{2.18}$$

then state global tracking is achieved, *i.e.*, (2.5) holds.

Proof. The PI controller (2.16) is equivalent to

$$\begin{aligned} \tilde{u} &= -K_p y + K_i z \\ \dot{z} &= -y. \end{aligned} \tag{2.19}$$

Consider the following radially unbounded Lyapunov function candidate

$$W(\tilde{x}, z) := V(\tilde{x}) + \frac{1}{2} z^\top K_i z, \tag{2.20}$$

whose time derivative is

$$\begin{aligned} \dot{W} &= -\tilde{x}^\top Q \tilde{x} + y^\top \tilde{u} - z^\top K_i y \\ &= -\tilde{x}^\top Q \tilde{x} - y^\top K_p y \\ &\leq -\lambda_{\min}\{K_p\}|y|^2 - |Q^{\frac{1}{2}}\tilde{x}|^2 \leq 0. \end{aligned}$$

Notice that the closed-loop system (2.13) and (2.19) is non-autonomous because of its dependence on $u_\star$ and $x_\star$ which are time-varying signals. Consequently, we cannot invoke LaSalle's Invariance Principle and proceed, instead, applying the generalization of Barbalat's Lemma reported in [79] and some standard signal chasing. Invoking the aforementioned result, we must prove that $y_a \in \mathcal{L}_2$ and $\dot{y}_a \in \mathcal{L}_\infty$ to conclude that $\lim_{t\to\infty} y_a(t) = 0$. Since the derivative of the Lyapunov function is negative, the trajectories are bounded, namely, $z, \tilde{x} \in \mathcal{L}_\infty$. In the same way, from the last inequality we conclude that $y, Q^{\frac{1}{2}}\tilde{x} \in \mathcal{L}_2$, consequently $y_a \in \mathcal{L}_2$. To conclude that $\dot{y}_a \in \mathcal{L}_\infty$ first notice

that $\tilde{x}, x_\star \in \mathcal{L}_\infty$ implies $x \in \mathcal{L}_\infty$ and, this in its turn, implies from (2.10) that $y \in \mathcal{L}_\infty$. Now, $y, z, u_\star \in \mathcal{L}_\infty$ implies, from (2.16), $u \in \mathcal{L}_\infty$. That implies, from (2.13), $\dot{\tilde{x}} \in \mathcal{L}_\infty$. Now, compute

$$\dot{y} = \begin{bmatrix} \dot{x}_\star^\top B_1^\top \\ \vdots \\ \dot{x}_\star^\top B_m^\top \end{bmatrix} P\tilde{x} + \left(\begin{bmatrix} x_\star^\top B_1^\top \\ \vdots \\ x_\star^\top B_m^\top \end{bmatrix} + B_0^\top \right) P\dot{\tilde{x}}, \tag{2.21}$$

which is bounded because $\dot{x}_\star \in \mathcal{L}_\infty$. Then, $\dot{y}_a$ is bounded and it follows that $y_a(t) \to 0$.

The proof of global state tracking follows noting that $y_a(t) \to 0$ ensures (2.5) if the rank condition (2.18) holds. □□□

Remark 2.2. Notice that the matrix $\mathcal{C}$ depends on the reference trajectory. Therefore, the rank condition (2.18) identifies a class of trajectories for which global tracking is ensured.

Remark 2.3. To assess the effect of the approximations mentioned in Remark 2.1, consider the following scenario where $m = 1$ and $B_0 = 0$. Defining $\bar{x} = x_\star + \xi$ and $\bar{u} = u_\star + \varsigma$ as, respectively, the approximation of $x_\star$ and $u_\star$ with ξ and ς two bounded signals, the measurable output is

$$\begin{aligned} \bar{y} &= (x_\star + \xi)^\top B^\top P x \\ &= y + \xi^\top B^\top P x. \end{aligned}$$

Then, in this setting, the controller (2.19) becomes

$$\begin{aligned} \dot{z} &= -y + \xi^\top B^\top P(\tilde{x} + x_\star) \\ \tilde{u} &= -K_p y + K_i z - K_p \xi^\top B^\top P x + \varsigma. \end{aligned}$$

Furthermore, the derivative of (2.20) yields

$$\dot{W} = -\tilde{x}^\top Q \tilde{x} - y^\top K_p y + y^\top (\varsigma - K_p \xi^\top B^\top P x) + z^\top K_i \xi^\top B^\top P(\tilde{x} + x_\star).$$

Hence, from the latter, we cannot conclude stability since (2.20) is not a strict Lyapunov function and there is no way to dominate the new terms appearing in its derivative.

Notice that for simplicity we adopt the case $m = 1$ however, it can be readily extended for $m \geq 2$.

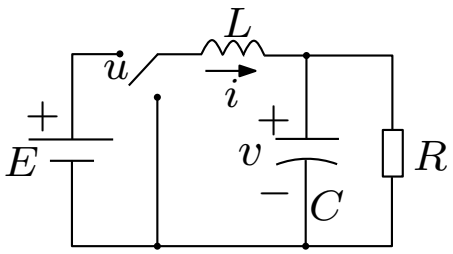

Figure 2.1: Representation of the ideal Buck Converter.

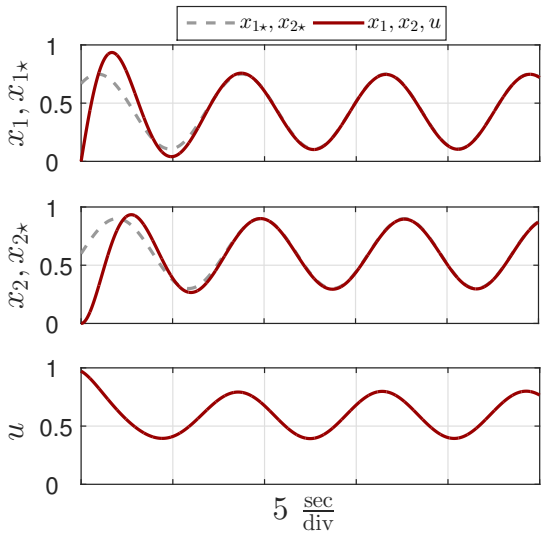

Figure 2.2: Simulation result of the tracking PI-PBC for the Buck Converter

2.5 Application to Power Converters

The present section is intended to exemplify the use approach proposed within this chapter. Experimental results have been reported in [21].

2.5.1 The Buck Converter

Consider the well-known normalized average model of the Buck Converter depicted in Fig. 2.1:

$$\begin{aligned} \dot{x}_1 &= -x_2 + u \\ \dot{x}_2 &= x_1 - \frac{x_2}{D}, \end{aligned} \tag{2.22}$$

where $D := R\sqrt{\frac{C}{L}}$. Also, E, C, L and R are the system parameters and u the control input. The relation between the physical variables i, v and x is given by the following transformation

$$\begin{bmatrix} x_1 \\ x_2 \end{bmatrix} = \begin{bmatrix} \frac{1}{E}\sqrt{\frac{L}{C}} & 0 \\ 0 & \frac{1}{E} \end{bmatrix} \begin{bmatrix} i \\ v \end{bmatrix}. \tag{2.23}$$

Clearly, defining

$$A = \begin{bmatrix} 0 & -1 \\ 1 & -\frac{1}{D} \end{bmatrix},\ B_0 = \begin{bmatrix} 1 \\ 0 \end{bmatrix}, Q = P = I_2, \tag{2.24}$$

the system satisfies Assumption 2.1. Furthermore,

$$y = B_0^\top P \tilde{x} = \tilde{x}_1. \tag{2.25}$$

The control objective is to drive x_2 to a desired time-varying reference $x_{2\star}$. Thus, from second equation of (2.22),

$$x_{1\star} = \dot{x}_{2\star} + \frac{x_{2\star}}{D}, \tag{2.26}$$

which substituted in the first equation of (2.22) yields

$$u_\star = \ddot{x}_{2\star} + \frac{\dot{x}_{2\star}}{D} + x_{2\star}. \tag{2.27}$$

Considering $x_{2\star} = V_0 + a\sin(\omega t)$, (2.26) and (2.27) becomes

$$\begin{aligned} u_\star &= -a\omega^2 \sin(\omega t) + \frac{a}{D}\omega\cos(\omega t) + a\sin(\omega t) + V_0 \\ x_{1\star} &= a\omega\cos(\omega t) + \frac{a}{D}\sin(\omega t) + \frac{V_0}{D}. \end{aligned}$$

Fig. 2.2 shows the simulation results of the system (2.22) in closed–loop with the controller (2.16). The system parameters are [75]: $R = 25\ \Omega,\ C = 50\ \mu\text{C},\ L = 19.91\ \text{mH},\ E = 24\ \text{V}$. Also, we select $a = 0.3,\ \omega = 0.8,\ V_0 = 0.6$, and gains $K_p = 0.3,\ K_i = 0.1$.

2.5.2 The Boost Converter

The well-known normalized average model of the Boost shown in Fig. 2.3 is

$$\begin{aligned} \dot{x}_1 &= -x_2 u + 1 \\ \dot{x}_2 &= x_1 u - \frac{x_2}{D} \end{aligned} \tag{2.28}$$

where $D := R\sqrt{\frac{C}{L}}$. Also, E, C, L and R are the system parameters and u the control input. The relation between the physical variables i, v and x is given by (2.23). Clearly,

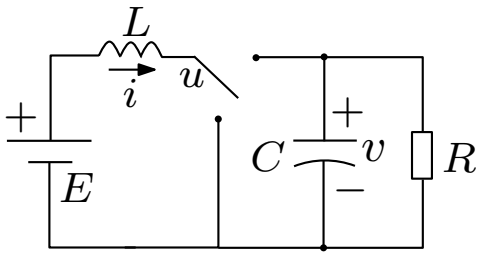

Figure 2.3: Representation of the ideal Boost Converter.

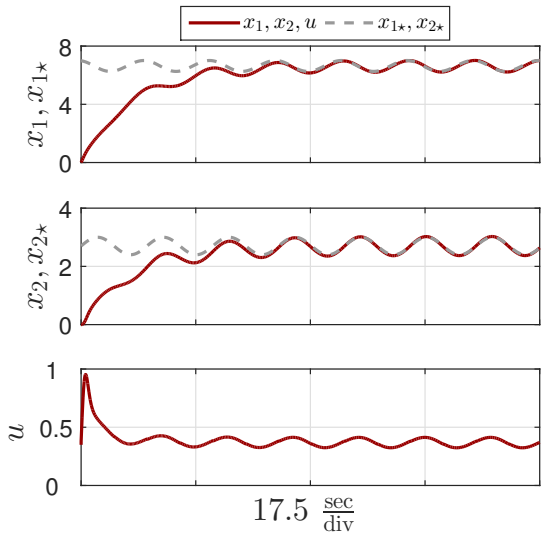

Figure 2.4: Simulation result of the tracking PI-PBC for the Boost Converter.

defining

$$A = \begin{bmatrix} 0 & 0 \\ 0 & -\frac{1}{D} \end{bmatrix}, \; B_1 = \begin{bmatrix} 0 & -1 \\ 1 & 0 \end{bmatrix}, Q = P = I_2, \tag{2.29}$$

the system satisfies Assumption 2.1. Furthermore,

$$y = x_\star^\top B_1^\top P \tilde{x} = \tilde{x}_2 x_{1\star} - \tilde{x}_1 x_{2\star}. \tag{2.30}$$

The control objective is x_2, which is selected as $x_{2\star} = V_0 + a\sin(\omega t)$. On the other hand, from the second equation of (2.28) we have

$$u_\star = \frac{1}{x_{1\star}} \left(\dot{x}_{2\star} + \frac{x_{2\star}}{D} \right). \tag{2.31}$$

Substituting the latter equation in the first equation of (2.28) yields

$$\dot{x}_{1\star} x_{1\star} = x_{1\star} - x_{2\star} \left(\dot{x}_{2\star} + \frac{x_{2\star}}{D} \right). \tag{2.32}$$

As claimed in Remark 2.1, since the system contains only one stable solution, finding $x_{1\star}$ from (2.32) is a difficult task. Instead, we take the approximation of the solution of

such system proposed in [27]. Here below we write the expression of $\hat{x}_{1\star}$, the approximation of $x_{1\star}$ —refer [27] for further details:

$$\hat{x}_{1\star} = c_0 + \frac{1}{2\omega c_0}\left[\frac{8V_0 a}{D}\cos(\omega t) - 4V_0 a\omega \sin(\omega t) + a^2\omega\cos(2\omega t) + \frac{a^2}{D}\sin(2\omega t)\right] \tag{2.33}$$

where $c_0 := \frac{1}{D}\left(V_0^2 + \frac{a^2}{2}\right)$.
Under this approximation, signal $\hat{u}_\star$, the approximation of (2.31), becomes

$$\hat{u}_\star = \frac{1}{\hat{x}_{1\star}}(\cos(\omega t) + \frac{1}{D}a\sin(\omega t) + V_0) \tag{2.34}$$

In Fig. 2.4 the simulation plots are shown for the system (2.28) in closed–loop with (2.16), when $L = 18\mathrm{m}H,\ C = 220\mu\mathrm{C},\ E = 50\ V_0 = 135\ \mathrm{V},\ a = 15,\ \omega = 0.6252\ K_p = K_i = 0.5$. A close-up view of the plot must reveal a steady-state error due to the approximation of $x_{1\star}$.

Chapter 3

A Robust PI Passivity–Based Control of a class of Nonlinear Systems : Application to Temperature Regulation

In many practical applications the plant to be controlled has an open–loop stable equilibrium, *e.g.*, at the origin, and we would like to add a controller to regulate its behavior around another operating point. In the case of linear systems the dynamics remains invariant under coordinate shifts, therefore this task can be easily accomplished using the incremental model of the plant. Unfortunately, this is not the case for nonlinear systems, for which there is no obvious advantage of working with the incremental model. To carry out this regulation task, in this chapter we identify a class of (input affine) nonlinear systems for which it is possible to design a PI controller with the following features.

F1 Regulation of the closed–loop system around the desired (non–zero) operating point should be guaranteed.

F2 The PI controller should be *robust*, in the sense that reduced knowledge of the system parameters is required.

F3 To simplify the controllers commissioning, a well defined admissible range of variation for the PI proportional and integral gains, preserving closed–loop stability, should be provided.

We propose the construction of a PI controller with the features F1–F3 for plants with unknown dynamics verifying the following assumptions.

A1 The open–loop system is *unknown* but has a stable equilibrium at the origin.

A2 The desired equilibrium belongs to the assignable set and admits a *convex* Lyapunov function.

A3 The Lyapunov function is the sum of two functions, depending on the un–actuated and actuated coordinates, respectively. The first function is *unknown* while the second one is separable and linearly parameterized in terms of some *unknown parameters*.

A4 The input matrix is constant, *known* and has $n - m$ zero rows, where n and m are the dimensions of the state and input vectors, respectively.

As indicated in the article's title we exploit the fundamental property of *passivity* to design the PI, which will be referred in the sequel as PI Passivity–based Control (PI–PBC). The first step in the design is to, relying on A1 above, invoke the celebrated theorem of Hill and Moylan [81] to identify a suitable passive output for the system, with storage function the Lyapunov function of the open–loop system. Since our interest is the regulation of non–zero equilibria, we then use the results of [35] to create a new passive output for the incremental model with a storage function that has a minimum at the desired equilibrium. As shown in [35], feeding back the passive output through a PI controller ensures stability of the desired equilibrium *for all* positive definite PI gains. It is important to underscore that, since the passivity property has been established for the incremental model, the equilibrium can also be stabilized setting the control input equal to the (constant) value that assigns the equilibrium, say $u_\star$, which is univocally defined. However, this open–loop control will, obviously, be non–robust. In the robustness context of the present chapter neither the plant dynamics nor the Lyapunov function are known and, consequently, we cannot compute neither the passive output nor $u_\star$. It is at this point that we invoke A3 and A4 above to prove that, under these assumptions, it is possible to define suitable proportional and integral gains that make the PI–PBC implementable and, consequently, guarantee stability of the equilibrium. Another important feature of the proposed PI–PBC is that it requires only partial measurement of the state, namely, only the m state variables associated to the non–zero rows of the input matrix, referred in the sequel as *actuated* coordinates. In this way, our approach is oriented towards a characterization of a class of systems that can be regulated by means of the PI–PBC with a minimum knowledge of the system parameters.

Several practical applications of PI–PBC have been reported in the literature. This include, RLC circuits [16], power converters [32], fuel cells [78], electric drives [47] and mechanical systems [49]. In [22] a procedure to add an integral action to a non–passive output for a class of port–Hamiltonian systems was first proposed, and later extended

in [60], [68]. To the best of our knowledge, the present result is the first attempt to design PI–PBCs with guaranteed stability properties for systems with partially known dynamics.

A natural question that arises at this point is the incorporation of adaptation in the design of the PI (or PID). In the power converter application of [32] a parameter that enters in the definition of the passive output, *i.e.*, the load resistance, is adaptively identified—however, all other parameters are assumed to be known. In the interesting paper [4] it is shown that it is possible to adaptively estimate $u_\star$ for a general nonlinear system with scalar input, keeping the estimate in a known interval, provided the passive output is known. In spite of a large number of publications the problem of designing a *provably stable* adaptive PID for systems with unknown parameters remains, as far as we know, open. The difficulty of this task was identified already in 1984 in [56]. As is well–known [70], the stability of indirect adaptive methods relies on parameter convergence that, in its turn, requires persistency of excitation—a property that is not satisfied in the regulation tasks where PI control is effective. On the other hand, the application of direct methods is stymied by the absence of a suitable parameterization of this structure–constrained controller. For the PI–PBC studied in this chapter the main difficulty is the need to estimate two objects, that appear multiplicatively in the Lyapunov analysis: the passive output and the ideal control signal $u_\star$. This point is further elaborated in Subsection 5.2.5.

3.1 Problem Formulation

In this section we formulate the control problem addressed along the chapter, enunciate the assumptions made on the plant to solve it and make some remarks on these assumptions.

3.1.1 Robust PI control problem

Consider the nonlinear, input affine, system

$$\dot{x} = f(x) + Gu, \tag{3.1}$$

where $x \in \mathbb{R}^n$, $u \in \mathbb{R}^m$, $n > m$, $f : \mathbb{R}^n \to \mathbb{R}^n$ is an *unknown* smooth mapping, $G \in \mathbb{R}^{n\times m}$ is *constant* verifying $\text{rank}(G) = m$.

The following is a key assumption made throughout the chapter.

Assumption 3.1. The matrix G has $n - m$ zero rows. Without lost of generality[1] it is assumed of the form

$$G = \begin{bmatrix} \mathbf{0}_{(n-m)\times m} \\ G_2 \end{bmatrix}, \tag{3.2}$$

where $G_2 \in \mathbb{R}^{m\times m}$ is *known*.

This assumption can be easily *obviated* introducing state and input changes of coordinates. Indeed, it is well–known—see, *e.g.*, Theorem 2 of Section 2.7 of [43]—that for any full rank, matrix $G \in \mathbb{R}^{n\times m}$ there exists (elementary) full rank matrices $T \in \mathbb{R}^{n\times n}$ and $S \in \mathbb{R}^{m\times m}$ such that

$$TGS = \begin{bmatrix} \mathbf{0}_{(n-m)\times m} \\ I_m \end{bmatrix}.$$

Consequently, introducing $z = Tx$ and $v = S^{-1}u$ the system (3.1) takes the desired form

$$\dot{z} = w(z) + \begin{bmatrix} \mathbf{0}_{(n-m)\times m} \\ I_m \end{bmatrix} v,$$

where $w(z) = Tf(T^{-1}z)$. We should note, however, that a change of state representation destroys—in general—the *original structure* of the system, whose knowledge may be critical for the verification of the second assumption below. This fact is clearly illustrated in the physical examples considered in Section 5.2.6. For this reason, we prefer to leave it as an standing assumption.

Motivated by Assumption 3.1 we find convenient to define a partition of the state vector into its un–actuated and actuated components as

$$x = \begin{bmatrix} x_u \\ x_a \end{bmatrix}, \; x_u := \begin{bmatrix} x_1 \\ x_2 \\ \vdots \\ x_{n-m} \end{bmatrix}, \; x_a := \begin{bmatrix} x_{n-m+1} \\ x_{n-m+2} \\ \vdots \\ x_n \end{bmatrix}.$$

It is assumed that *only x_a is available for measurement.*

The unforced system, that is, $\dot{x} = f(x)$, has a stable equilibrium at the origin with a *partially known* Lyapunov function. We are interested in controlling the system with a PI at a non–zero equilibrium—a situation that arises in most practical applications. Thus, we are given a desired equilibrium point, $x^\star \in \mathbb{R}^n$, and the control goal is to

[1] See R6 in the next subsection and Subsection 5.2.5 for more general forms of G.

ensure *stability* of this equilibrium using a PI control law of the form

$$\begin{aligned} \dot{z} &= -K_I \psi(x_a, x_\star) \\ u &= -K_P \psi(x_a, x_\star) + z \end{aligned}$$

where $z \in \mathbb{R}^m$ is the controller state, $K_P \in \mathbb{R}^{m\times m}$ and $K_I \in \mathbb{R}^{m\times m}$ are tuning gains and $\psi : \mathbb{R}^m \times \mathbb{R}^n \to \mathbb{R}^m$ is a mapping designed with the partial knowledge of the aforementioned Lyapunov function.

The following, practically reasonable, assumption is made throughout the chapter.

Assumption 3.2. The desired equilibrium point $x^\star$ belongs to the assignable equilibrium set, that is,

$$x^\star \in \mathcal{E} := \left\{ x \in \mathbb{R}^n \mid \left[\begin{array}{c|c} I_{n-m} & \mathbf{0}_{(n-m)\times n} \end{array} \right] f(x) = 0 \right\}. \tag{3.3}$$

3.1.2 Assumptions on the open–loop plant

The following assumption identifies the class of vector fields $f(x)$ for which we provide an answer to the problem.

Assumption 3.3. For the system (3.1) there exists a twice–differentiable, positive definite function $H : \mathbb{R}^n \to \mathbb{R}_{\geq 0}$, verifying the following.

(i) $[\nabla H(x)]^\top f(x) \leq 0$.

(ii) $[\nabla H(x) - \nabla H(x_\star)]^\top \tilde{f}(x) =: -Q(x) \leq 0$.

(iii) The function $H(x)$ is of the form

$$H(x) = H_u(x_u) + H_a(x_a) \tag{3.4}$$

with

$$H_a(x_a) = \sum_{i=n-m+1}^{n} d_i \phi_i(x_i), \tag{3.5}$$

where the function $H_u : \mathbb{R}^{n-m} \to \mathbb{R}$ and the constants $d_i > 0$ are *unknown* but the functions $\phi_i : \mathbb{R} \to \mathbb{R}$ are *known*.

(iv) The functions $H_u(x_u)$ and $\phi_i(x_i)$ are *convex*.

3.1.3 Discussion

The following remarks regarding the assumptions are in order.

R1 Although the set of assignable equilibria $\mathcal{E}$ is not known, it is reasonable to assume that we have enough prior knowledge about the plant to select the desired operating point as a feasible equilibrium. Hence, Assumption 3.2 is practically reasonable.

R2 A corollary of Assumption 3.2 is that the constant input $u^\star$, that assigns the equilibrium, is uniquely defined as

$$u^\star := \left(G_2^\top G_2\right)^{-1} \begin{bmatrix} \mathbf{0}_{m\times(n-m)} & G_2^\top \end{bmatrix} f^\star. \tag{3.6}$$

Notice that, without knowledge of $f(x)$, this constant cannot be computed.

R3 Since the open–loop system (3.1) has a stable equilibrium at the origin Assumption 3.3 (i) follows as a corollary of Lyapunov's converse theorems [39]. As will become clear below Assumption 3.3 (ii) and (iv) are required to prove passivity of the incremental model as done in [35].

R4 We underscore that no assumption, beyond twice differentiability and convexity, is imposed on the unknown component $H_u(x_u)$ of the Lyapunov function of the open–loop system $H(x)$. On the other hand, stricter conditions are imposed on the second component $H_a(x_a)$, with uncertainty captured by the unknown constants d_i.

R5 Assumptions 3.3 (iii) and Assumption 3.1 are the key requirements imposed on the plant to design the robust PI–PBC. This assumption is satisfied by a large class of physical systems, including the thermal systems studied in Section 5.2.6 and a class of port–Hamiltonian systems [81].

R6 It can be noticed that the class of port-Hamiltonian systems of the form:

$$\dot{x} = (\mathcal{J} - \mathcal{R})\nabla H(x) + Gu \tag{3.7}$$

with *constant* interconnection $\mathcal{J} = -\mathcal{J}^\top$ and damping $\mathcal{R} = \mathcal{R}^\top \geq 0$ matrices satisfies Assumption 3.3 (i) and (ii). Indeed, Assumption 3.3 (i) is satisfied since

$$[\nabla H(x)]^\top (\mathcal{J} - \mathcal{R})\nabla H(x) = -[\nabla H(x)]^\top \mathcal{R} \nabla H(x) \leq 0.$$

Similarly, Assumption 3.3 (ii) e

$$[\nabla H(x) - \nabla H(x_\star)]^\top (\mathcal{J} - \mathcal{R})[\nabla H(x) - \nabla H(x_\star)] = \\ -[\nabla H(x) - \nabla H(x_\star)]^\top \mathcal{R}[\nabla H(x) - \nabla H(x_\star)] \leq 0.$$

R7 Regarding Assumptions 3.1, in the more general case when G is not of the form (3.2) an additional shuffling of the rows of G is needed in the design. This procedure is explained in Subsection 5.2.5.

R8 For quadratic Lyapunov functions of the form $H(x) = x^\top P x$, with $P > 0$, Assumption 3.3 (ii) is satisfied if the open–loop system is *convergent* in the sense of Demidovich [64]. That is, if it satisfies

$$P\nabla f(x) + [\nabla f(x)]^\top P \leq 0.$$

3.2 Preliminary Lemmata

Unless otherwise indicated, throughout the rest of the chapter Assumption 3.1 holds. Define for the system (3.1) the output

$$y = G^\top \nabla H(x) = G_2^\top D\Phi(x_a), \tag{3.8}$$

where

$$D := \begin{bmatrix} d_{n-m+1} & 0 & \dots & 0 \\ 0 & d_{n-m+2} & \dots & 0 \\ \vdots & \vdots & \vdots & \vdots \\ 0 & 0 & \dots & d_n \end{bmatrix} > 0$$

$$\Phi(x_a) := \begin{bmatrix} \phi'_{n-m+1}(x_{n-m+1}) \\ \vdots \\ \phi'(x_n) \end{bmatrix}.$$

A corollary of the theorem of Hill and Moylan [81] is that, if Assumption 3.3 (i) holds, the system (3.1), (3.8) defines a passive mapping $u \mapsto y$ with storage function $H(x)$.

To operate the system at a non–zero equilibrium it is necessary to shift the minimum of the storage function and define the passivity property between the incremental input and the output error. Towards this end, we recall Proposition 1 of [35] and state it as a lemma below.

Lemma 3.1. Consider the incremental model of the system (3.1), (3.8)

$$\begin{aligned} \dot{x} &= f(x) + Gu^\star + G\tilde{u}, \\ e &= G_2^\top D\tilde{\Phi}(x_a), \end{aligned} \tag{3.9}$$

where $\tilde{u} = u - u^\star$ is the incremental input. Under Assumptions 3.1–3.3 the mapping $\tilde{u} \mapsto e$ is passive with storage function $U : \mathbb{R}^n \to \mathbb{R}_{\geq 0}$ given by

$$U(x) = H(x) - x_u^\top \nabla H_{u\star} - x_a^\top D\Phi_\star + k, \tag{3.10}$$

where k is a constant that ensures $U(x_\star) = 0$. More precisely,

$$\dot{U} = -Q(x) + e^\top \tilde{u}, \tag{3.11}$$

where $Q(x)$ is defined in Assumption 3.3 (ii).

One of the main interests of passive systems is that they can be globally stabilized with PI controls (with arbitrary positive definite gains). This well–known fact is stated in the lemma below, whose proof is given to streamline the presentation of our main result.

Lemma 3.2. Consider the system (3.1) verifying Assumptions 3.1–3.3 in closed–loop with the PI–PBC

$$\begin{aligned} e &= G_2^\top D\tilde{\Phi}(x_a) \\ \dot{z} &= -K_I e \\ u &= -K_P e + z. \end{aligned} \tag{3.12}$$

For all positive definite gain matrices $K_P \in \mathbb{R}^{m\times m}$ and $K_I \in \mathbb{R}^{m\times m}$ all trajectories are bounded, the equilibrium point $(x, z) = (x_\star, u_\star)$ is *globally stable* (in the sense of Lyapunov) and the augmented error signal

$$e_a := \begin{bmatrix} Q(x) \\ e \end{bmatrix} \tag{3.13}$$

where $Q(x)$ is defined in Assumption 3.3 (ii), verifies

$$\lim_{t\to\infty} e_a(t) = 0. \tag{3.14}$$

Moreover, if e_a is a detectable output for the closed–loop system then the equilibrium point is *asymptotically* stable.

Proof. Defining $\tilde{z} := z - u_\star$ the last two equations of the controller (3.12) may be written

in the form

$$\begin{aligned} \dot{\tilde{z}} &= -K_I e \\ \tilde{u} &= -K_P e + \tilde{z}. \end{aligned} \tag{3.15}$$

Consider the Lyapunov function candidate

$$W(\tilde{z}, x) = U(x) + \frac{1}{2}\tilde{z}^\top \Lambda_I \tilde{z}, \tag{3.16}$$

where $\Lambda_I > 0$. The time derivative of the Lyapunov function along the trajectories of the closed–loop system is

$$\begin{aligned} \dot{W} &= -Q(x) + e^\top \tilde{u} + \tilde{z}^\top \Lambda_I \dot{\tilde{z}} \\ &= -Q(x) - e^\top K_P e + \tilde{z}^\top e - \tilde{z}^\top \Lambda_I K_I e. \end{aligned} \tag{3.17}$$

Setting $\Lambda_I = K_I^{-1}$ yields

$$\dot{W} = -Q(x) - e^\top K_P e.$$

The proof is complete invoking standard Lyapunov arguments [39]. □□□

3.3 The Robust PI–PBC

As indicated in R4 of Subsection 5.2.2 the matrix D is unknown. Hence, the error signal e cannot be constructed and the PI–PBC (3.12) is not implementable. This motivates our main result given below.

Proposition 3.1. Consider system (3.1) verifying Assumptions 3.1–3.3 in closed–loop with the robust PI–PBC

$$\begin{aligned} u &= -K_P \widetilde{\Phi}(x_a) + z \\ \dot{z} &= -K_I \widetilde{\Phi}(x_a), \end{aligned} \tag{3.18}$$

with the controller gains

$$\begin{aligned} K_P &= G_2^{-1} \Gamma_P \\ K_I &= G_2^{-1} \Gamma_I. \end{aligned} \tag{3.19}$$

For all diagonal, positive definite matrices $\Gamma_P \in \mathbb{R}^{m \times m}$ and $\Gamma_I \in \mathbb{R}^{m \times m}$ we have the following.

(i) All trajectories are bounded and the equilibrium point $(x, z) = (x_\star, u_\star)$ is *globally stable* (in the sense of Lyapunov).

(ii) The augmented error signal e_a defined in (3.13) verifies (3.14).

(iii) If e_a is a detectable output for the closed–loop system then the equilibrium point is globally *asymptotically* stable.

Proof. Some simple manipulations prove that

$$K_P\widetilde{\Phi}(x_a) = G_2^{-1}\Gamma_P D^{-1} G_2^{-\top} G_2^{\top} D\widetilde{\Phi}(x_a) = \Lambda_P e, \tag{3.20}$$

where we defined the matrix

$$\Lambda_P := G_2^{-1}\Gamma_P D^{-1} G_2^{-\top}, \tag{3.21}$$

and used the definition of e in (3.12). Invoking Sylvester's Law of Inertia [43], and the fact that Γ_P and D are diagonal and positive definite, we have that $\Lambda_P > 0$.

Next choose

$$\Lambda_I := G_2^{\top} D\Gamma_I^{-1} G_2, \tag{3.22}$$

that is, also, positive definite for all diagonal, positive definite Γ_I. Then

$$\Lambda_I K_I\widetilde{\Phi}(x) = G_2^{\top} D\widetilde{\Phi}(x_a) = e. \tag{3.23}$$

Replacing (3.20) and (3.23) in the controller equations yields

$$\begin{aligned}\tilde{u} &= -\Lambda_P e + \tilde{z}\\ \dot{\tilde{z}} &= -\Lambda_I^{-1} e.\end{aligned}$$

Consequently, the time derivative of the Lyapunov function (3.17) becomes now

$$\dot{W} = -Q(x) - e^{\top}\Lambda_P e, \tag{3.24}$$

completing the proof. □□□

To obtain an implementable version of the robust PI–PBC it was necessary to carry–out two tasks. First, to make the damping injection, introduced by the proportional term, function of the unknown matrix D. Indeed, replacing (3.21) in (3.20) we get

$$K_P\widetilde{\Phi}(x) = G_2^{-1}\Gamma_P D^{-1} G_2^{-\top} e.$$

Second, make the gain Λ_I of the Lyapunov function (5.54) also a function of D—see (3.22).

An important observation is that, even though the controller only requires measurement of the actuated terms of the state x_a, it achieves regulation of the full state

vector.

3.4 Additional Remarks on the PI–PBC

In this section we explain how to proceed when G is not of the form (3.2), discuss the reasons that stymie the use of adaptation and the inability to state a robustness result based on continuity and approximate prior knowledge of the matrix D.

3.4.1 General G (with $n-m$ zero rows)

Instrumental to design the robust PI–PBC was the particular form of $H(x)$ defined in Assumption 3.3 (iii). In view of the construction of the robust PI–PBC, it is clear that if G is not of the form (3.2) the assumption must be modified redefining the actuated and un–actuated coordinates.

To avoid cluttering the notation we will explain the procedure only for the case when $n = 3$ and $m = 2$—the general case follows *verbatim*. Assume, furthermore, that G is of the form

$$G = \begin{bmatrix} g_1^\top \\ \mathbf{0}_{1\times 2} \\ g_3^\top \end{bmatrix}.$$

The form of $H(x)$ given in Assumption 3.3 (iii) must be, accordingly, modified to

$$H(x) = H_u(x_2) + d_1\phi(x_1) + d_3\phi(x_3).$$

In this case the passive output e for the incremental model becomes

$$G^\top[\nabla H(x) - \nabla H(x_\star)] = G_s \begin{bmatrix} d_1 & 0 \\ 0 & d_3 \end{bmatrix} \begin{bmatrix} \widetilde{\Phi}_1(x_1) \\ \widetilde{\Phi}_3(x_3) \end{bmatrix}.$$

where

$$G_s := \begin{bmatrix} g_1 & | & g_3 \end{bmatrix}.$$

The robust PI–PBC is given by

$$\begin{aligned} u &= -G_s^{-1}\Gamma_P \begin{bmatrix} \widetilde{\Phi}_1(x_1) \\ \widetilde{\Phi}_3(x_3) \end{bmatrix} + z \\ \dot{z} &= -G_s^{-1}\Gamma_I \begin{bmatrix} \widetilde{\Phi}_1(x_1) \\ \widetilde{\Phi}_3(x_3) \end{bmatrix}, \end{aligned}$$

where Γ_P and Γ_I are arbitrary, diagonal, positive definite matrices.

Before closing this subsection we remark that our construction *critically* relies on the assumption of existence of $n-m$ zero rows in G. Indeed, it is possible to show that if this is not the case, even assuming $H(x)$ of the form

$$H(x) = \sum_{i=1}^{n} d_i \phi_i(x_i)$$

it is not possible to find an $m \times m$ positive definite matrix Λ, which will depend on D, such that the matrix $\Lambda G^\top D$ is *independent* of D. The fact that this is *not possible* for all matrices G is obvious considering the counterexample $G = \text{col}(1,1)$. Hence, the assumption of existence of $n-m$ zero rows in G is *necessary* to solve the problem.

3.4.2 Difficulties for adaptation

A natural alternative to the robust PI–PBC presented above is to assume a parametrisation of $f(x)$ and try to estimate this parameters or, in a direct approach, estimate the matrix D that defines the passive output. The indirect approach, as is well–known, relies on parameter convergence that requires persistency of excitation—a property that is not satisfied in the regulation tasks where PI control is effective.

Let us see what are the difficulties for the application of a direct adaptation approach. Towards this end, we propose the adaptive PI–PBC

$$\begin{aligned}
\dot{\hat{D}} &= F(x,z) \\
\hat{e} &= G_2^\top \hat{D}\, \widetilde{\Phi}(x_a) \\
\dot{z} &= -K_I \hat{e} \\
u &= -K_P \hat{e} + z,
\end{aligned}$$

where the parameter adaptation law $F : \mathbb{R}^n \times \mathbb{R}^m \to \mathbb{R}^{m\times m}$ is to be defined.[2] Defining $\tilde{e} := \hat{e} - e$ the last two equations of the controller may be written in the form

$$\begin{aligned}
\dot{\tilde{z}} &= -K_I(e + \tilde{e}) \\
\tilde{u} &= -K_P(e + \tilde{e}) + \tilde{z}.
\end{aligned}$$

The time derivative of the Lyapunov function (5.54) with $\Lambda_I = K_I^{-1}$ is now

$$\begin{aligned}
\dot{W} &= -Q(x) - \hat{e}^\top K_P \hat{e} - \tilde{u}^\top \tilde{e} \\
&= -Q(x) - \hat{e}^\top K_P \hat{e} - \tilde{u}^\top G_2^\top \tilde{D} \widetilde{\Phi}(x_a)
\end{aligned}$$

[2]Notice that, in contrast to the robust PI–PBC, we have assumed that the full state is measurable.

where we underscore the presence of the last right hand term. If $\tilde{u}$ were known the standard procedure of augmenting the Lyapunov function with a term trace$(\tilde{D}^\top \tilde{D})$ and cancelling the sign–indefinite term with a suitable choice of $F(x, z)$ would do the job. Alas, $u_\star$ is not known, hence this approach is not feasible.

Adding an adaptation for the constant $u_\star$ is also not a trivial task, because of the bilinear nature of the joint estimation problem.

3.4.3 Comments on robustness based on continuity

The availability of a *bona fide* Lyapunov function for the known parameters PI–PBC, *i.e.*, $W(x, \tilde{z})$, suggests that stability will be preserved if the matrix D is replaced by a "good", *constant* estimate of it, say D_0. More precisely, it is expected that replacing the controller (3.12) by

$$\begin{aligned} e_0 &= G_2^\top D_0 \widetilde{\Phi}(x_a) \\ \dot{z} &= -K_I e_0 \\ u &= -K_P e_0 + z, \end{aligned}$$

where

$$D = D_0 + \Delta,\ \Delta := \text{diag}\{\delta_i\}$$

would ensure stability if $|\text{col}(\delta_i)|$ is sufficiently small. Unfortunately, since the Lyapunov function is *not strict*, this conjecture cannot be analytically validated. Indeed, in this case the time derivative of the Lyapunov function (5.54) with $\Lambda_I = K_I^{-1}$ is now

$$\begin{aligned} \dot{W} &= -Q(x) + e^\top \tilde{u} - \tilde{z}^\top (e - G_2^\top \Delta \widetilde{\Phi}(x_a)) \\ &= -Q(x) - e_0^\top K_P e_0 - (K_P e_0 - \tilde{z})^\top G_2^\top \Delta \widetilde{\Phi}(x_a). \end{aligned}$$

While the term $e_0^\top K_P G_2^\top \Delta \widetilde{\Phi}(x_a)$ can be dominated for "small" Δ, there is no way we can dominate the remaining term $\tilde{z}^\top K_I G_2^\top \Delta \widetilde{\Phi}(x_a)$ and the Lyapunov analysis cannot be completed with standard techniques.

This unfortunate situation does not mean, of course, that a continuity result of this type cannot be established. It simply reveals our inability to do it with the tools used to analyze the ideal case.

3.5 Application to Temperature Regulation

In this subsection we design a robust PI–PBC for the temperature regulation of a class of thermal systems—the so–called, Rapid Thermal Processes (RTP). Attention is concentrated on the verification of Assumption 3.3. Hence, unless otherwise indicated,

Assumption 3.1 is not imposed.

3.5.1 System Description

Similarly to [25, 72] we consider the following model of Rapid Thermal Processes

$$\dot{T} = A_1 \left[\Psi(T) - \Psi(T_{rad})\right] + A_2 \left(T - T_{conv}\right) + Gu, \tag{3.25}$$

where $T \in \mathbb{R}^n_{\geq 0}$ represents the vector of temperatures, $\Psi(T) := \text{col}(T_i^4)$ and $T_{rad},\ T_{conv} \in \mathbb{R}^n_{\geq 0}$ are, respectively, the vectors of temperatures related to the radiation heat emission from environment and the convection air flows. The constant matrices $A_1, A_2 \in \mathbb{R}^{n\times n}$ are *Hurwitz* and contain the radiation and the convection heat transfer coefficients. Also, the entries of $G \in \mathbb{R}^{n\times m}$ correspond to the heat transfer coefficients of the heating elements. Finally, $u \in \mathbb{R}^m$ is the controlled power applied to the heating elements. Physically, considering matrix G as (3.2) means that for m heating elements there are $n - m$ measured points that are not directly heated by these elements.

In the model above, as in [72], it is considered that the plant is heated almost uniformly so that the contribution of energy from conduction is too small with respect to the radiation transfer. Hence, the conduction heat transfer is neglected. We also assume the steady environment conditions, i.e., the values T_{rad} and T_{conv} are constant.

To simplify the notation we re–write the system (3.25) in the form

$$\dot{T} = A_1\Psi(T) + A_2T + E + Gu \tag{3.26}$$

where

$$E := -A_1\Psi(T_{rad}) - A_2T_{conv}.$$

Unlike A_1, A_2 and E that are highly uncertain, the input matrix G—that is defined by the induced heat flow—can be precisely identified. The *control objective* is then to design a robust PI, *i.e.*, that does not require the knowledge of the uncertain parameters, to regulate the process around some desired temperature, which is *not equal* to the open–loop equilibrium, but belongs to the assignable equilibrium set, that is,

$$T^\star \in \left\{T \in \mathbb{R}^n_{\geq 0} \mid G^\perp[A_1\Psi(T) + A_2T + E] = 0\right\}, \tag{3.27}$$

where $G^\perp \in \mathbb{R}^{(n-m)\times n}$ is a full-rank left-annihilator of G.

To place the problem in the context of Proposition 3.1 we first shift the equilibrium of the open–loop system to the origin and then proceed to verify Assumption 3.3. For,

we introduce the standard change of coordinates

$$x = T - \bar{T}$$

where $\bar{T}$ is the open–loop equilibrium that satisfies

$$A_1\Psi(\bar{T}) + A_2\bar{T} + E = 0. \tag{3.28}$$

Thus, the system (3.25) in the new coordinates takes the form (3.1) with

$$f(x) := A_1\Psi(x + \bar{T}) + A_2(x + \bar{T}) + E, \tag{3.29}$$

Associated to the desired temperature $T^\star$ we define the equilibrium to be stabilised

$$x^\star := T^\star - \bar{T}. \tag{3.30}$$

3.5.2 Passivity of the thermal system.

The lemma below identifies conditions under which the system (3.25) satisfies Assumption 3.3 *without* imposing Assumption 3.1, that is, avoiding the partition of the coordinates into actuated and un–actuated. Towards this end, the following assumption is needed.

Assumption 3.4. The matrix A_1 is *diagonally stable* [38]. That is, there exists $P \in \mathbb{R}^{n\times n}$, $P = \text{diag}\{p_i\} > 0$ such that

$$PA_1 + A_1^\top P =: -2S < 0. \tag{3.31}$$

Moreover, the matrix A_2 verifies

$$A_2^\top P\text{diag}\{T_i^3\} + \text{diag}\{T_i^3\}PA_2 \leq 0. \tag{3.32}$$

Conditions for diagonal stability of a matrix have been studied intensively, see [38] for a survey. Necessary and sufficient conditions were first reported in [8]—see also [74] for a simpler proof. For a Hurwitz matrix, a sufficient condition given in [26] is that it is a Metzler matrix (namely, its non diagonal elements are nonnegative). Note that due to physical nature of RTP systems the matrix A_1 usually belongs to this class.

Since A_2 is Hurwitz and $T_i \geq 0$, condition (3.32) is trivially satisfied if A_2 is *diagonal*, which is assumed in RTP models [71,72].

Lemma 3.3. If Assumption 3.4 holds the vector field (3.29) satisfies Assumption 3.3 with

$$H(x) = \sum_{i=1}^{n} p_i \phi_i(x_i) + k \tag{3.33}$$

where

$$\phi_i(x_i) = \frac{1}{5}(x_i + \bar{T}_i)^5 - \Psi_i(\bar{T})x_i. \tag{3.34}$$

and

$$k = -\frac{1}{5}\sum_{i=1}^{n} p_i \bar{T}_i^5.$$

Proof. Point (iii) of Assumption 3.3 is trivially satisfied by (3.33).

We proceed now to prove point (i). Replacing (3.34) in (3.33) and grouping terms yields

$$H(x) = \frac{1}{5}\sum_{i=1}^{n} p_i (x_i + \bar{T}_i)^5 - x^\top P \Psi(\bar{T}) + k,$$

Now, notice that

$$\nabla H(x) = P\Phi(x),$$

where

$$\Phi(x) := \Psi(x + \bar{T}) - \Psi(\bar{T}). \tag{3.35}$$

On the other hand, from (3.28) it follows that the systems vector field may be written as

$$f(x) = A_1 \Phi(x) + A_2 x.$$

Consequently,

$$\begin{aligned} [\nabla H(x)]^\top f(x,\theta) &= \Phi^\top(x) P [A_1 \Phi(x) + A_2 x] \\ &= -\Phi^\top(x) S \Phi(x) + \Phi^\top(x) P A_2 x, \end{aligned}$$

where we have used (3.31) to obtain the second identity. Now, condition (3.32) ensures that the function $h : \mathbb{R}^n \to \mathbb{R}^n$

$$h(x) := A_2^\top P \Psi(x),$$

is monotonically decreasing [64]. That is, for all $a, b \in \mathbb{R}^n$,

$$[h(a) - h(b)]^\top (a - b) \leq 0.$$

Consequently,

$$\Phi^\top(x) P A_2 x = [h(x + \bar{T}) - h(\bar{T})]^\top x \leq 0$$

completing the proof of point (i).

To prove point (ii) we notice that

$$\tilde{f}(x) = A_1\tilde{\Phi}(x) + A_2\tilde{x},$$

while

$$\nabla H(x) - \nabla H(x_\star) = P\tilde{\Phi}(x).$$

Hence, the claim is established invoking the same arguments used above and defining

$$Q(x) = \tilde{\Phi}^\top(x)S\tilde{\Phi}(x).$$

Finally, the second derivative of the functions $\phi_i(x_i)$ yields

$$\phi_i''(x_i) = 4(x_i + \bar{T}_i)^3 = 4T_i^3,$$

which is non–negative because $T_i \geq 0$. Hence, the functions $\phi_i(x_i)$ are convex as requested by condition (iv) of Assumption 3.3. This completes the proof. □□□

Direct application of Lemma 1 leads to the following.

Corollary 3.1. If Assumption 3.4 holds, the thermal system (3.25) defines a passive map $\tilde{u} \mapsto e$ with storage function $U(x)$, where

$$\begin{aligned} e &= G^\top P\tilde{\Phi}(x) \\ U(x) &= H(x) - x^\top P\Phi(x_\star) - H(x_\star) + (x_\star)^\top P\Phi(x_\star) \end{aligned}$$

3.5.3 Robust PI–PBC of the thermal system

To present the robust PI–PBC for systems verifying Assumption 3.1 we partition the vector of temperatures into its un–actuated and actuated components

$$T = \begin{bmatrix} T_u \\ T_a \end{bmatrix},\ T_u := \begin{bmatrix} T_1 \\ T_2 \\ \vdots \\ T_{n-m} \end{bmatrix},\ T_a := \begin{bmatrix} T_{n-m+1} \\ T_{n-m+2} \\ \vdots \\ T_n \end{bmatrix},$$

partition P as

$$P = \begin{bmatrix} P_1 & \mathbf{0}_{(n-m)\times m} \\ \mathbf{0}_{m\times(n-m)} & D \end{bmatrix},$$

and do the same with the vector function $\Psi(T)$.

The following proposition is a consequence of Lemma 3.3 and Proposition 3.1.

Proposition 3.2. Consider the system (3.25) verifying Assumptions 3.1 and 3.4. Fix any desired temperature $T_\star$ verifying (3.27) and define the PI–PBC

$$\begin{aligned} u &= -K_P\tilde{\Psi}_a(T_a) + z \\ \dot{z} &= -K_I\tilde{\Psi}_a(T_a), \end{aligned}$$

and the controller gains K_P and K_I are given by (3.19). *For all* diagonal, positive definite matrices $\Gamma_P \in \mathbb{R}^{m\times m}$ and $\Gamma_I \in \mathbb{R}^{m\times m}$ all trajectories are bounded and the equilibrium point $(T, z) = (T_\star, u_\star)$ is *globally asymptotically stable*.

Proof. The proof of stability is established invoking item (i) of Proposition 1 and identifying

$$\tilde{\Phi}_a(x_a)|_{x_a=T_a-\bar{T}_a} = \tilde{\Psi}_a(T_a).$$

To prove asymptotic stability we invoke item (ii) and observe that the augmented error signal (3.13) is given in this case by

$$e_a = \begin{bmatrix} \tilde{\Psi}^\top(T)S \\ G_2^\top D \end{bmatrix} \tilde{\Psi}(T).$$

Since e_a verifies (3.14) and S is positive definite we conclude that $\tilde{\Psi}(T(t)) \to 0$ and consequently $T(t) \to T^\star$. □□□

3.5.4 Numerical Simulation:

Consider the thermal system (3.26) with

$$A_1 = \begin{bmatrix} -a_{11} & a_{12} \\ a_{21} & -a_{22} \end{bmatrix},\ A_2 = \begin{bmatrix} -\alpha_1 & 0 \\ 0 & -\alpha_2 \end{bmatrix},\ G = \begin{bmatrix} 0 \\ g \end{bmatrix},\ C = \begin{bmatrix} c_1 \\ c_2 \end{bmatrix}$$

where $a_{ij} \geq 0,\ \alpha_i \geq 0$. Notice that the system satisfies Assumption 3.4. Then, the assignable equilibria set is

$$\mathcal{E} = \{T \ :\ T_2 \in \mathbb{R}_+,\ -a_{11}T_1^4 + a_{12}T_2^4 - \alpha_1 T_1 + c_1 = 0\} \tag{3.36}$$

From Proposition 3.2, the controller

$$\begin{aligned} \dot{z} &= -K_I\left(T_2^4 - (T_{2\star})^4\right) \\ u &= -K_P\left(T_2^4 - (T_{2\star})^4\right) + z \end{aligned}$$

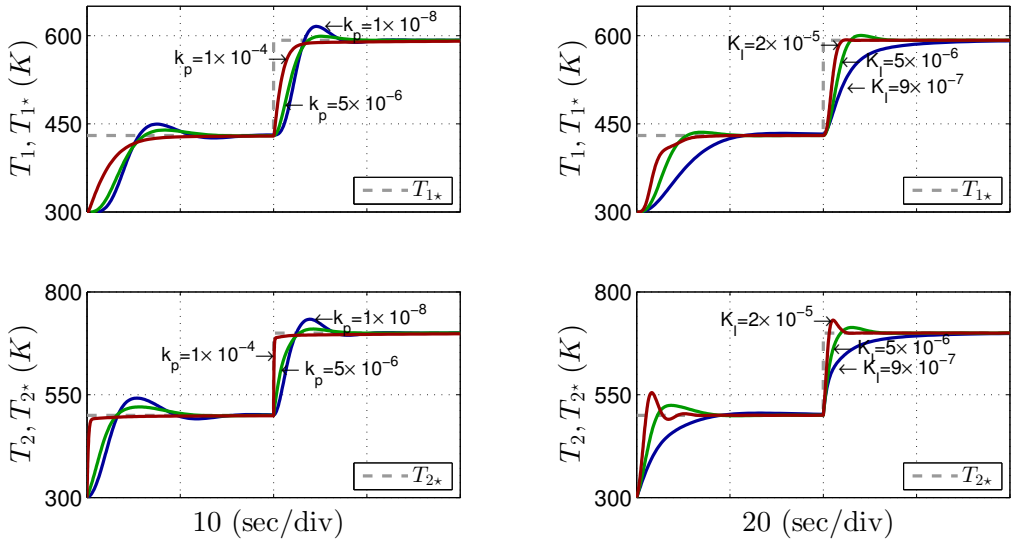

(a) (b)

Figure 3.1: Simulation Result showing the system response : (a) For different gains K_p letting $K_I = 3 \times 10^{-6}$. (b) For different gains K_I letting $K_p = 6 \times 10^{-6}$.

where $K_p = \frac{1}{g}\Gamma_p$, $K_I = \frac{1}{g}\Gamma_I$ and $\Gamma_P, \Gamma_I \in \mathbb{R}_+$ asymptotically stabilizes the system at $T = T_\star$. The parameter values used in the simulation where: $a_{11} = 1 \times 10^{-9}$, $a_{12} = \frac{1}{2} \times \times 10^{-9}$, $a_{21} = 1 \times 10^{-9}$, $a_{22} = 1 \times 10^{-9}$, $\alpha_1 = 1 \times 10^{-4}$, $\alpha_2 = \frac{1}{2} \times 10^{-4}$, $g = 1$, $c_1 = 3$, $c_2 = 1.7$, $\Gamma_p = 8 \times 10^{-5}$ and $\Gamma_I = 1 \times 10^{-5}$. In the simulation, the control objective is initially fixed at $T_{2\star} = 500\ K$, then it is suddenly changed to $T_{2\star} = 700\ K$. From (3.36), the corresponding values for $T_{1\star}$ are, respectively, $430.06\ K$ and $592.20\ K$. Fig. 3.1 shows the simulation results. In Fig. 3.1a the response of the system when varying control parameter K_p and letting $K_I = 3 \times 10^{-6}$ is depicted. As it can be noticed from the same figure, the larger is the value in K_p the faster is the convergence. In Fig. 3.1b it is shown the response of the system when K_I is varying while $K_P = 6 \times 10^{-6}$. From the figure, it can be seen that large values in K_I causes overshoots in the response of T_2.

Chapter 4

Energy Shaping PI of Port–Hamiltonian Systems

An energy shaping controller for *mechanical systems* that does not require the solution of partial differential equations (PDEs) has been recently proposed in [23]. In this chapter we pursue this research line considering the more general case of *port–Hamiltonian* (pH) systems [81].

The starting point of the design is the well–known *power shaping* output [55], which defines a passive output for the pH system with storage function its energy function. As is well–known a PI controller around this output preserves the passivity of the closed–loop. It is then shown that, if the power shaping output is "integrable", the integral action of the PI is passive with a storage function a quadratic term of the "integral" of the power shaping output, which depends on the plant state. In this way we can generate a *new storage function* for the closed–loop constructed as the sum of this function and the original energy function of the pH system. Adding a suitably chosen constant to the control makes this function *positive definite*, which then qualifies as a Lyapunov function for the closed–loop system. The condition imposed on the power shaping output boils down to a classical integrability condition of some computable vector fields, hence it can be readily verified.

.

4.1 Problem Formulation and Main Assumptions

The standard input–state representation of pH systems is of the form [24, 81]

$$\dot{x} = [\mathcal{J}(x) - \mathcal{R}(x)]\nabla H(x) + g(x)u, \tag{4.1}$$

where $x \in \mathbb{R}^n$ is the state vector, $u \in \mathbb{R}^m$, $m \leq n$, is the control vector, $H : \mathbb{R}^n \to \mathbb{R}$ is the systems Hamiltonian, $\mathcal{J}, \mathcal{R} : \mathbb{R}^n \to \mathbb{R}^{n \times n}$, with $\mathcal{J}(x) = -\mathcal{J}^\top(x)$ and $\mathcal{R}(x) = \mathcal{R}^\top(x) \geq 0$, are the interconnection and damping matrices, respectively, and $g : \mathbb{R}^n \to \mathbb{R}^{n \times m}$ is the input matrix, which is full rank. To simplify the notation in the sequel we define the matrix $F : \mathbb{R}^n \to \mathbb{R}^{n \times n}$

$$F(x) := \mathcal{J}(x) - \mathcal{R}(x).$$

The *control objective* is to stabilise an equilibrium $x_\star$, which is an element of the set of assignable equilibria defined as

$$\mathcal{E} := \left\{ x \in \mathbb{R}^n \mid g^\perp(x) F(x) \nabla H(x) = 0 \right\}, \tag{4.2}$$

where $g^\perp : \mathbb{R}^n \to \mathbb{R}^{(n-m) \times n}$ is a full–rank, left–annihilator of $g(x)$, that is, $g^\perp(x) g(x) = 0$ and rank$\{g^\perp(x)\} = n - m$.

The following assumptions identify the class of pH systems for which the proposed control strategy is applicable.

Assumption 4.1. The matrix $F(x)$ is *full rank*.

Assumption 4.2. The vector fields $F^{-1}(x) g_i(x)$, with $g_i(x),\ i = 1, \ldots, m$, the columns of the matrix $g(x)$, are *gradient vector fields.* That is,

$$\nabla \left(F^{-1}(x) g_i(x) \right) = [\nabla \left(F^{-1}(x) g_i(x) \right)]^\top.$$

If Assumption 4.1 holds, it is possible to define the *power shaping output* as follows

$$y_{\mathtt{PS}} := -g^\top(x) F^{-\top}(x) \left[F(x) \nabla H(x) + g(x) u \right]. \tag{4.3}$$

As shown in [55,62] $y_{\mathtt{PS}}$ is a cyclo–passive output[1] for the pH system (4.1) with storage function $H(x)$. More precisely, the following dissipation inequality holds

$$\dot{H} \leq u^\top y_{\mathtt{PS}}. \tag{4.4}$$

Noting that $y_{\mathtt{PS}}$ may be written as

$$y_{\mathtt{PS}} = -g^\top(x) F^{-\top}(x) \dot{x} \tag{4.5}$$

[1] We recall that, in contrast to passive systems where the storage function is bounded from below, in cyclo–passive systems this is not necessary [24].

and recalling Poincare's Lemma it is easy to see that Assumption 4.2 ensures the existence of a function $\gamma : \mathbb{R}^n \to \mathbb{R}^m$ such that

$$\dot{\gamma} = (\nabla\gamma)^\top \dot{x} = y_{\texttt{PS}}, \tag{4.6}$$

with $y_{\texttt{PS}}$ defined in (4.3).

4.2 Energy Shaping

In this section we define a static state–feedback such that the system (4.1) in closed–loop with this control preserves passivity of the mapping $v \mapsto y_{\texttt{PS}}$ but with a suitably *modified storage function*.

Proposition 4.1. Suppose Assumptions 4.1 and 4.2 hold. Define the mapping $u_{\texttt{PS}} : \mathbb{R}^n \to \mathbb{R}^m$

$$\begin{aligned} u_{\texttt{PS}}(x) :=& [I - K_P g^\top(x) F^{-\top}(x) g(x)]^{-1} \left[-K_I(\gamma(x) + C) + \right. \\ & \left. K_P g^\top(x) F^{-\top}(x) F(x) \nabla H(x)\right] \end{aligned} \tag{4.7}$$

where[2]

$$\nabla\gamma(x) := -F^{-1}(x) g(x) \tag{4.8}$$

and $C \in \mathbb{R}^m$ and $K_P, K_I \in \mathbb{R}^{m\times m}$, $K_I, K_P > 0$, are *free parameters*. The system (4.1) in closed–loop with the control $u = u_{\texttt{PS}}(x) + v$ defines a cyclo–passive mapping $v \mapsto y_{\texttt{PS}}$ with storage function

$$H_d(x) = H(x) + \frac{1}{2}\|\gamma(x) + C\|^2_{K_I}. \tag{4.9}$$

Proof. To establish the proof, first, notice that from (4.5) and (4.6) the control (4.7) reduces to

$$u_{\texttt{PS}}(x) = -\left[K_I(\gamma + C) + K_P y_{\texttt{PS}}\right]. \tag{4.10}$$

Therefore, differentiating (4.9) we get

$$\begin{aligned} \dot{H}_d &= \dot{H} + y_{\texttt{PS}}^\top K_I(\gamma + C) \\ &\leq y_{\texttt{PS}}^\top \left[u + K_I(\gamma + C)\right] \\ &= y_{\texttt{PS}}^\top (v - K_P y_{\texttt{PS}}) \\ &\leq y_{\texttt{PS}}^\top v, \end{aligned}$$

[2]Notice that the existence of $\gamma(x)$ is ensured by Assumption 4.2 and it can be computed via direct integration.

where we used (4.6) in the first equality, (4.4) in the first inequality, (4.10) for the second equality, respectively, and $K_P > 0$ for the last inequality. □□□

Remark 4.1. From (4.10) and (4.6) it is easy to see that the control $u = u_{\texttt{PS}}(x) + v$ is a PI of the form

$$u(t) = -K_P y_{\texttt{PS}}(t) - K_I \int_0^t y_{\texttt{PS}}(\tau) d\tau + D + v, \tag{4.11}$$

where $D := -K_I[C + \gamma(x(0))]$. This establishes the connection with the PI–like controller proposed for mechanical systems in [23]. Notice that in its state space realization (4.7) the pH structure is not preserved in closed–loop. However, it does if the PI (4.11) is implemented via a dynamic extension.

Remark 4.2. The condition of integrability of the vector fields $F^{-1}(x)g_i(x)$ appears also in the context of Control–by–Interconnection of pH systems, as a necessary and sufficient condition for existence of Casimir functions, see [53] for further details.

4.3 Stabilization

From Proposition 4.1 it is clear that if the new storage function $H_d(x)$ is positive definite (with respect to the desired equilibrium $x_\star$) it qualifies as a *bona fide* Lyapunov function for the closed–loop system (with $v = 0$) that ensures stability of $x_\star$. This fact is stated in the proposition below where we also give easily verifiable condition to check positivity of $H_d(x)$.

Proposition 4.2. Consider the system (4.1), verifying Assumptions 4.1 and 4.2, in closed–loop with the control $u = u_{\texttt{PS}}(x)$, where $u_{\texttt{PS}}(x)$ is given by (4.7). Fix

$$C := K_I^{-1} g_*^\dagger F_* (\nabla H)_* - \gamma_*. \tag{4.12}$$

If $x_* \in \mathcal{E}$ and

$$(\nabla^2 H_d)_* > 0 \tag{4.13}$$

with $H_d(x)$ defined in (4.9), then x_* is *stable* (in the sense of Lyapunov) with Lyapunov function $H_d(x)$. It is *asymptotically* stable if $y_{\texttt{PS}}$, defined in (4.3), is a detectable output, that is, if the following implication is true

$$y_{\texttt{PS}}(t) \equiv 0 \Rightarrow \lim_{t\to\infty} x(t) = x_*.$$

Proof. First, we will prove that x_* is an equilibrium point of the closed–loop system. From (4.3) we have that $y_{\texttt{PS}_*} = 0$, hence (4.10)—at the equilibrium—becomes

$u_{\mathtt{BC}_*} = -K_I(\gamma_* + C)$. The proof is completed noting that the choice of C given in (4.12), together with the fact that $x_* \in \mathcal{E}$, guarantees that

$$F_*(\nabla H)_* - g_* \left[K_I(\gamma_* + C)\right] = 0. \tag{4.14}$$

To prove the stability claim we recall that from Proposition 4.1 and $v = 0$ we have that $\dot{H}_d \leq -K_P|y_{\mathtt{PS}}|^2 \leq 0$. Hence, invoking classical Lyapunov theory [39], it suffices to prove that $H_d(x)$ is a positive definite function. From (4.14) we get

$$(\nabla H)_* = F_*^{-1} g_* K_I(\gamma_* + C). \tag{4.15}$$

Computing the gradient of $H_d(x)$ at the equilibrium yields

$$\begin{aligned}(\nabla H_d)_* &= (\nabla H)_* + (\nabla \gamma)_* K_I(\gamma_* + C) \\ &= (\nabla H)_* - F_*^{-1} g_* K_I(\gamma_* + C) = 0,\end{aligned}$$

where the second and third identities are obtained replacing (4.8) and (4.15), respectively. This ensures that x_* is a critical point of $H_d(x)$. The proof is completed recalling that (4.13) is a sufficient condition for x_* to be an isolated minimum of $H_d(x)$. □□□

Remark 4.3. From the proof of Proposition 4.2 it is clear that—for the purpose of stabilization—the constant vector C, which ensures $x_\star$ is an equilibrium point of the closed–loop, is *uniquely defined* by (4.12).

4.4 Relation with Classical PBCs

In this section we discuss the relationship between the new controller and the classical PBC techniques of EB and IDA.[3]

4.4.1 Energy–balancing PBC

The basic idea of EB–PBC (with the output $y_{\mathtt{PS}}$) is to look for a state feedback $u_{\mathtt{EB}} : \mathbb{R}^n \to \mathbb{R}^m$ such that

$$\dot{H}_a = -u_{\mathtt{EB}}^\top y_{\mathtt{PS}},$$

[3]The interested reader is referred to [54, 62, 63] for further details on EB–PBC and IDA–PBC.

for some "added" energy function $H_a : \mathbb{R}^n \to \mathbb{R}$. In this case, setting $u = u_{\texttt{EB}}(x)$ transforms the cyclo–pasivity inequality (4.4) into

$$\dot{H} + \dot{H}_a \leq 0,$$

and if $H(x) + H_a(x)$ is positive definite the closed–loop system will have a stable equilibrium at x_*. The following proposition states that, for a suitable choice of the tuning gains, the new controller is an EB–PBC.

Proposition 4.3. Consider the pH system (4.1) verifying Assumptions 4.1 and 4.2. Fix $K_P = 0$ in $u_{\texttt{PS}}(x)$. Then, the control $u = u_{\texttt{PS}}(x)$ is an EB–PBC with added energy function

$$H_a(x) := \frac{1}{2}\|\gamma(x) + C\|^2_{K_I}. \tag{4.16}$$

Proof. For $K_P = 0$ the mapping $u_{\texttt{PS}}(x)$, given in (4.10), reduces to

$$u_{\texttt{PS}}(x) = -K_I[\gamma(x) + C]. \tag{4.17}$$

On the other hand, from (4.6) and (4.16) we have

$$\dot{H}_a = y_{\texttt{PS}}^\top K_I(\gamma + C) = -y_{\texttt{PS}}^\top u_{\texttt{PS}},$$

completing the proof. □□□

4.4.2 Interconnection and damping assignment PBC

In IDA–PBC we fix the desired interconnection and damping matrices, hence, fix the matrix $F_d : \mathbb{R}^n \to \mathbb{R}^{n\times n}$ such that $F_d(x) + F_d^\top(x) \leq 0$, and look for a control $u = u_{\texttt{IDA}}(x)$ such that the closed–loop has the form

$$\dot{x} = F_d(x)\nabla H_{\texttt{IDA}}(x);$$

for some energy function $H_{\texttt{IDA}} : \mathbb{R}^n \to \mathbb{R}_{>0}$, which has a minimum at the desired equilibrium. It is easy to show that the assignable energy functions $H_{\texttt{IDA}}(x)$ are characterized by the solutions of the following PDE

$$g^\perp(x)\left[F_d(x)\nabla H_{\texttt{IDA}}(x) - F(x)\nabla H(x)\right] = 0, \tag{4.18}$$

and the control is uniquely defined as

$$u_{\texttt{IDA}}(x) := g^{\dagger}(x)\left[F_d(x)\nabla H_{\texttt{IDA}}(x) - F(x)\nabla H(x)\right]. \tag{4.19}$$

The proposition below establishes the relation between IDA–PBC and the controller of Proposition 4.1.

Proposition 4.4. Consider the pH system (4.1) verifying Assumptions 4.1 and 4.2. Fix $K_P = 0$ in $u_{\texttt{PS}}(x)$ and select the desired interconnection and damping matrices as

$$F_d(x) = F(x). \tag{4.20}$$

Then, the energy function $H_d(x)$ defined in (4.9) and the control $u = u_{\texttt{PS}}(x)$ given in (4.7) satisfy the IDA–PBC equations (4.18) and (4.19), respectively.

Proof. Replacing the gradient of $H_d(x)$, given by

$$\nabla H_d(x) = \nabla H(x) - F^{-1}(x)g(x)K_I(\gamma(x) + C),$$

in the PDE (4.18) we get

$$\begin{aligned} g^{\perp}\left\{F\left[\nabla H - F^{-1}gK_I(\gamma + C)\right] - F\nabla H\right\} &= g^{\perp}gK_I(\gamma + C) \\ &= 0. \end{aligned}$$

On the other hand, the control law (4.7) is given by (4.17), which satisfies (4.19) since, using (4.20),

$$\begin{aligned} u_{\texttt{IDA}} &= g^{\dagger}\left\{F\left[\nabla H - F^{-1}gK_I(\gamma + C)\right] - F\nabla H\right\} \\ &= -g^{\dagger}gK_I(\gamma + C) \\ &= u_{\texttt{PS}}. \end{aligned}$$

□□□

4.5 Examples

In this section we apply the proposed controller to three physical systems and investigate, with the example of LTI systems, some of the limitations of the method.

4.5.1 Micro electro–mechanical optical switch [14, 83]

Consider the optical switch system with pH model

$$\dot{x} = \begin{bmatrix} 0 & 1 & 0 \\ -1 & -b & 0 \\ 0 & 0 & -\frac{1}{r} \end{bmatrix} \nabla H(x) + \begin{bmatrix} 0 \\ 0 \\ 1 \end{bmatrix} u \tag{4.21}$$

where in order to simplify, the original control input $\bar{u}$ has been scaled, i.e. $u := \frac{1}{r}\bar{u}$. The energy function of the system is

$$H(x) = \frac{1}{2m}x_2^2 + \frac{1}{2}a_1 x_1^2 + \frac{1}{4}a_2 x_1^4 + \frac{1}{2c_1(x_1 + c_0)}x_3^2,$$

where x_1, x_2 are the mass of the comb driver actuator and its momentum, respectively; x_3 denotes the charge in the capacitor, u is the voltage applied o the electrodes, $a_1 > 0, a_2 > 0$ are the spring constants, $b > 0, r > 0$ are resistive elements, $c_0 > 0, c_1 > 0$ are constants that determine the capacitance function and, finally, $m > 0$ denotes the mass of the actuator. It is important to underscore the physical constraint $x_1 > 0$. See [14] for further details on the model.

The set of assignable equilibria for this system is

$$\begin{aligned} x_{2_\star} &= 0 \\ x_{3_\star} &= (c_0 + x_{1_\star})\sqrt{2c_1 x_{1_\star}(a_1 + a_2 x_{1_\star}^2)} \end{aligned} \tag{4.22}$$

and the goal is to stabilize at $x_{1_\star} > 0$.

Clearly, F is full rank. Also, some simple calculations using (4.3) prove that $y_{\mathtt{PS}} = r\dot{x}_3$, therefore $\gamma(x) = rx_3$. Hence, Assumptions 4.1 and 4.2 hold. It only remains to show that sufficient conditions of Proposition 4.2 holds. For this purpose, we evaluate the Hessian of H at the equilibrium. Some simple calculations yield

$$(\nabla^2 H_d)_\star = \begin{bmatrix} a_1 + 3a_2 x_{1_\star}^2 + d_1^2 d_2 & 0 & -d_1 d_2 \\ 0 & \frac{1}{m} & 0 \\ -d_1 d_2 & 0 & d_2 \end{bmatrix} + k_I \begin{bmatrix} 0 & 0 & 0 \\ 0 & 0 & 0 \\ 0 & 0 & r^2 \end{bmatrix}$$

where

$$d_1 := \sqrt{2c_1 x_{1_*}(a_1 + a_2 x_{1_*}^2)} \tag{4.23}$$

$$d_2 := \frac{1}{c_1(c_0 + x_{1_*})}. \tag{4.24}$$

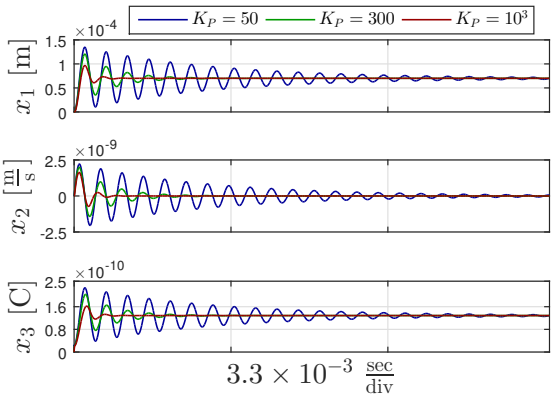

Figure 4.1: Simulation results when parameter K_P varies.

It can be seen that for all $K_I > 0$, the condition (4.13) holds. Hence, $x_\star$ is a stable equilibrium for the closed–loop system.

To prove asymptotic stability we verify the detectability of y_{PS}. First, from (4.12) we get

$$C = -\frac{1}{K_I}\frac{x_{3_*}}{rc_1(c_0 + x_{1_*})} - rx_{3_*}. \tag{4.25}$$

Second, in the residual set where $y_{\text{PS}} \equiv 0$, we have that x_3 is a constant, denoted $\bar{x}_3$. Thus, the control law is also a constant given by

$$u_{\text{BC}} = -K_I(r\bar{x}_3 + C), \tag{4.26}$$

which substituted in the third equation of (4.21) yields

$$-\frac{\bar{x}_3}{rc_1(\bar{x}_1 + c_0)} - K_I(r\bar{x}_3 + C) = 0. \tag{4.27}$$

From the latter equation is clear that $\bar{x}_1$ is a constant. Moreover, replacing (4.25) in (4.27) and using (4.21) we can conclude , invoking LaSalle's Invariance Principle, that $\bar{x}_1 = x_{1*}$ and $\bar{x}_3 = x_{3*}$ is an asymptotic equilibrium point.

Simulation results are presented in Fig. 4.1. Based on the results reported in [14], the system parameters were chosen as $c_0 = 15 \times 10^{-6}$, $c_1 = 35.6 \times 10^{-9}$, $m = 2.35 \times 10^{-9}$, $a_1 = 0.46$, $a_2 = 0.0973$, $b = 5.5 \times 10^{-7}$ and $r = 100$. Fig. 4.1 shows the system response for three different values of K_P when $K_I = 5 \times 10^{-3}$. The control objective is to stabilize x_1 at $x_{1*} = 7 \times 10^{-5}$. Thus, from (4.22), $x_{2*} = 0$ and $x_{3*} = 1.0601 \times 10^{-10}$. As it can be noticed from the plot, $x_1 > 0$, which agrees with the physical constraint.

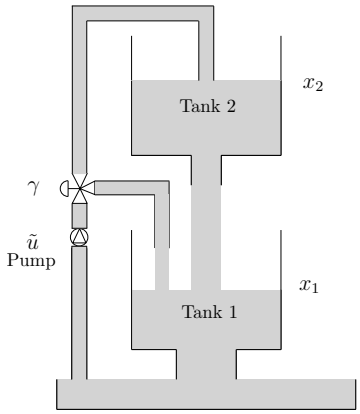

Figure 4.2: The two-tanks system

4.5.2 Two-Tanks Level Regulation Problem [62]

Consider the two-tank system shown in Fig. 4.2. The state variables $x_1,\ x_2 \in \mathbb{R}_+$ represent, respectively, the water level in Tank 1 and 2. the control action $\tilde{u} := \frac{A_1}{\Gamma} u \geq 0$ is the flow pumped from the reservoir. The valve parameter is a constant $1 \geq \Gamma \geq 0$, with $\Gamma = 0$ when the valve is fully open and $\Gamma = 1$ if it is closed. The pH model of system is

$$\dot{x} = \begin{bmatrix} -\alpha_1\sqrt{x_1} & \alpha_2\sqrt{x_2} \\ -\alpha_2\sqrt{x_2} & 0 \end{bmatrix} \nabla H(x) + \begin{bmatrix} 1 \\ g_2 \end{bmatrix} \tilde{u} \tag{4.28}$$

$$H(x) = x_1 + \frac{A_1}{A_2} x_2, \tag{4.29}$$

with the parameters

$$\alpha_i := \frac{a_i\sqrt{2G}}{A_i},\ i = 1, 2,\ g_2 := \frac{1-\Gamma}{\Gamma}, \tag{4.30}$$

where $a_i,\ A_i$ are the cross-sections of the outlet holes and the tanks, and G the gravitation constant. To simplify the notation, we assume $A_1 = A_2$. The assignable equilibrium set is given by

$$x_{2\star} = \left[\frac{a_1}{a_2}(1-\Gamma)\right]^2 x_{1\star},$$

and the control objective is to regulate the water level at some $x_{1_\star} > 0$.

As pointed out in [62] the vector field $F^{-1}(x)g$ is not integrable, as required by Assumption 4.2. However, the system dynamics can be alternatively written as

$$\dot{x} = \begin{bmatrix} -\frac{1}{a} & \frac{1}{d} \\ 0 & -\frac{1}{d} \end{bmatrix} \nabla \bar{H}(x) + \begin{bmatrix} 1 \\ g_2 \end{bmatrix} \tilde{u} \tag{4.31}$$

$$\bar{H}(x) = \frac{2}{3} a\alpha_1 x_1^{\frac{3}{2}} + \frac{2}{3} d\alpha_2 x_2^{\frac{3}{2}}$$

where a, d are free parameters satisfying $4d \geq a > 0$. In this form the obstacle can be overcome. Indeed, from (4.31) and (4.3) we get

$$y_{\texttt{PS}} = a(1+g_2)\dot{x}_1 + dg\dot{x}_2$$

and

$$\gamma(x) = a(1+g_2)x_1 + dgx_2.$$

After some computations we have

$$(\nabla^2 H_d)_\star = \begin{bmatrix} a\alpha_1 x_{1\star}^{\frac{1}{2}} & 0 \\ 0 & d\alpha_2 x_{2\star}^{\frac{1}{2}} \end{bmatrix} + K_I \begin{bmatrix} a^2(1+g_2)^2 & a(1+g_2)dg_2 \\ dg_2 a(1+g_2) & d^2 g_2^2, \end{bmatrix}$$

and clearly condition (4.13) holds. Therefore, the proposed controller will render $x_\star$ a stable equilibrium point for the closed–loop system.

4.5.3 LTI systems: Controllability is not enough

In the important paper [66] it was shown that IDA–PBC for LTI systems is a *universal stabiliser*, in the sense that it is applicable to all stabilisable systems. On the other hand, it was shown in [57] that stabilisability is *not enough* for IDA–PBC of mechanical system. Indeed, in Proposition 4.1 of [57] it is shown that if the system has *uncontrollable modes*, an additional condition of the pole location, which is stronger than stabilisability, must be imposed for stabilisation with IDA–PBC.

The difference between these two cases is that, while for general IDA–PBC there is no constraint on the structure of the desired energy function, for mechanical systems a *particular structure* is imposed to it. Since in the methodology proposed in this paper there is also a constraint on the desired energy function, namely (4.9), it is expected that a condition stronger than stabilisability should be imposed for the method to apply—a conjecture that we prove in this subsection via a counter–example. Actually, we will prove that unlike IDA–PBC for mechanical systems even controllability is not enough for the proposed method to work.

Now, recall that for LTI systems the energy function is of the form $H(x) = \frac{1}{2}x^\top Q x$, the matrices F and g are constant and, without loss of generality, we can take $x_\star = 0$. Therefore, the control (4.7) becomes a simple linear, state–feedback of the form $u_{\texttt{PS}}(x) = Kx$ with

$$K := \left(I - K_p g^\top F^{-\top} g\right)^{-1} (K_p g^\top F^{-\top} F Q + K_I g^\top F^{-\top}). \tag{4.32}$$

Notice that for linear systems, with $x_\star = 0$, the constant vector C given in (4.12) is equal to zero. To prove the aforementioned conjecture we will construct an LTI, controllable pH system for which the controller (4.32) yields an unstable closed–loop system *for all* values of the tuning gains K_p, K_I. It is important to note that the Lyapunov stability test utilised in Proposition 4.2 is sufficient, but not necessary—even for LTI systems. Therefore, instability must be proved checking directly the closed–loop system matrix. Also, the sign constraints imposed to the tuning gains, which are required to ensure positivity of the shaped energy function, need not be imposed in the LTI case where, as indicated above, a stability analysis—other than Lyapunov—will be carried out.

Consider the following *controllable*, LTI system

$$\dot{x} = \begin{bmatrix} 0 & 1 \\ a_1 & 1 - a_1 \end{bmatrix} x + \begin{bmatrix} 0 \\ 1 \end{bmatrix} u, \tag{4.33}$$

with $a_1 < 0$. Some simple calculations show that it admits a pH representation

$$\dot{x} = FQx + gu \tag{4.34}$$

with $g := \text{col}(0, 1)$,

$$\begin{aligned} F &:= \begin{bmatrix} -1 & a_1 \\ \frac{1}{2}a_1 & -a_1^2 \end{bmatrix} \\ Q &:= -\frac{2}{a_1^2} \begin{bmatrix} a_1^2 & a_1 \\ a_1 & 1 - \frac{a_1}{2} \end{bmatrix}, \end{aligned} \tag{4.35}$$

which satisfies $F + F^\top < 0$ and Assumption 4.1.[4]

Proposition 4.5. Consider the LTI, pH system (4.34), (4.35) in closed–loop with the controller (4.32). For all values of the controller gains K_p and K_I the closed–loop system is unstable.

Proof. The closed–loop system is given by

$$\dot{x} = \begin{bmatrix} 0 & 1 \\ a_1 - a_1\tilde{k} & 1 - a_1 - \tilde{k} \end{bmatrix} x$$

where

$$\tilde{k} := \frac{2}{a_1^2} \left(1 + \frac{2K_p}{a_1^2}\right)^{-1} (K_I + K_p).$$

[4] Assumption 4.2 is always satisfied for single input LTI systems.

Clearly, the closed–loop system matrix is Hurwitz if and only if the following conditions can be satisfied

$$\begin{aligned} a_1 - a_1\tilde{k} &< 0 \\ 1 - a_1 - \tilde{k} &< 0. \end{aligned}$$

Since $a_1 < 0$, these inequalities are equivalent to

$$\begin{aligned} \tilde{k} &< 1 \\ \tilde{k} &> 1 - a_1, \end{aligned}$$

Since $1 - a_1 > 1$ the inequalities cannot be simultaneously satisfied. □□□

Chapter 5

Applications of the PI-PBC to Wind Energy Systems

The concern over the environment has made us look for alternatives sources of power generation. Within this new tendency, electrical power generation from wind has become one of the most adopted. In both Europe, which has the greater wind source, and North America, large scale developments to exploit wind power have been undertaken from some time ago. Since then, the power electronics technologies used in wind power application have been dramatically changed due to the growing capacity and the increasing presence of wind turbine systems in the power grid. An evidence of this growth is the world wind power capacity cumulated during the first years of the current century, from 13.6 in 2000 GW to 370 GW in 2014 [11, 67]. Besides, it is expected that in 2020 this value ranges 760 MW. In fact, the wind power grows more significant compared to any other renewable source and it is an important component in the modern power supply system.

A wind energy system is composed of interconnected mechanical and electrical systems. The mechanical part consists of a turbine which captures energy from the wind. When the wind velocity is not too high to exceed the capacity limits of the —variable-speed— turbine and generator units, it is customary to require that the turbine operates at a rotational speed ensuring the maximum power extraction from the wind. This captured power is transform into electric energy and flows to the electrical system to which the wind system is connected. Common uses of this electrical energy include charging a battery in stand–alone windmill systems, injection of reactive power for grid–connected windmills or minimizing power losses for a given load.

In this chapter we address the control problem of two different wind energy system topologies, which will be detail in the sequel. One of the main difference in their topology is the rectification stage, being active for the first system and passive for the

second one. Indeed, active rectification offers more degrees of freedom when designing a controller at the expense of increasing the cost implementation of such systems.

Some previous work in the literature about control of windmill systems make use of MMPT algorithms based on the so–called Hill–climb search procedures. Many publications, including some variants of this approach, can be found. See, for instance, [1, 41, 86] and references therein. The most widely used method, the perturb & observe algorithm, presents some undesirable drawbacks. These include oscillations around the maximum power point [33] and the failure to track fast–changing wind [18]. There are also papers, like [18, 91], considering the linearization of the system dynamics. In [30, 40] the problem is tackled by means of the extremum seeking control technique. Some fuzzy logic–based schemes have been developed, for example [15, 89]. In the current chapter a passivity–based strategy is derived in order to tackle the problem. The control technique adopted follows mainly from Chapter 2. It is worth to mention that, in contrast with the previous approaches, our work is model–based, with all (relevant) nonlinearities of the dynamic system considered in the model.

5.1 PI–PBC for Maximum Power Extraction of a Wind Energy System with Guaranteed Stability Properties

In this section we propose a maximum power extraction control for a wind system The approach adopted in this paper follows the line pursued in [32, 35, 90]. The final objective is to design a simple linear PI with guaranteed stability properties. Towards this end, we identify a passive output for the nonlinear incremental model around to which the stabilizing PI is designed. Interestinlgy, as shown in [32, 90] the PI scheme that results from the application of this method is closely related to the well–known instantaneous active power control of [2]. In this way, an important connection with current practice is established.

5.1.1 System Modeling

Depicted in Fig. 5.1, the system consists of a turbine, surface-mounted PMSG and a rectifier connected to a load, a capacitor, a load and one constant voltage source, which is used to form the dc bus.

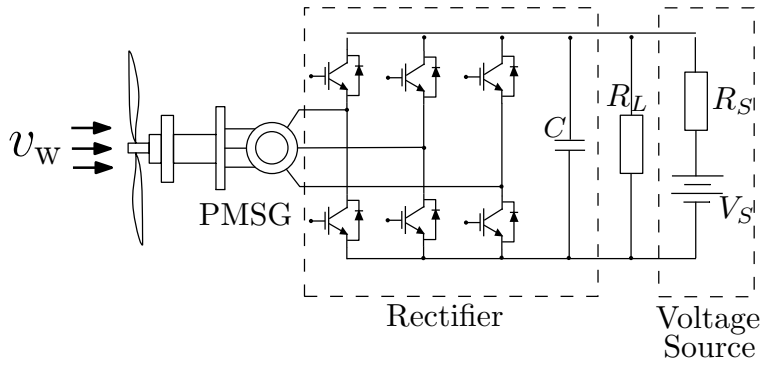

Figure 5.1: System under consideration

Wind Turbine

The mechanical power extracted from the wind is given by the power function

$$P_w = \frac{1}{2}\rho A C_p(\lambda) v_w^3,$$

where ω_m is the shaft's rotational speed, ρ is the air density, A is the area swept by the blades and C_p is the turbine's coefficient power[1], λ, which is defined as

$$\lambda := \frac{r\omega_m}{v_w}, \tag{5.1}$$

is the blades' tip speed, r the blades' radius, ρ the air density, and v_w the wind speed, which is assumed *constant and known*. The shape of the function $C_p(\lambda)$ depends on the geometry of the windmill. Fig. 5.2 shows a typical curve that can be obtained from experimental measurements. Since we are interested in the maximum power extraction, it is required that the system operates in the point

$$\lambda_\star = \arg\max C_p(\lambda). \tag{5.2}$$

which is assumed to be known. It is important to note that, if v_w is known the control task boils down, in view of (5.1), to regulation of the shaft's speed ω_m around the reference speed

$$\omega_{m\star} = \frac{\lambda_\star v_w}{r}. \tag{5.3}$$

The dynamic equation of a one-mass turbine is obtained from Newton's equation of motion

$$J\dot{\omega}_m = -f\omega_m + T_m - T_e \tag{5.4}$$

[1]The power coefficient is also a function of the blade pitch angle, which acts as an additional control input. We are interested in the operation regime where this angle is kept constant, consequently we have omitted this additional argument in the function C_p.

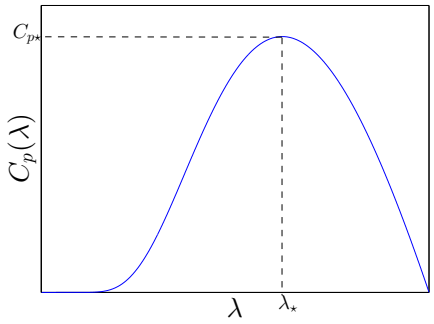

Figure 5.2: Function $C_p(\lambda)$

where J is the rotor inertia, $f > 0$ is a friction coefficient, T_m is the mechanical torque applied to the windmill shaft

$$T_m = \frac{P_w}{\omega_m} = \frac{1}{2}\rho A r v_w^2 \frac{C_p(\lambda)}{\lambda}, \tag{5.5}$$

and T_e is the electrical torque provided by the generator.

Permanent Magnet Synchronous Generator

The dynamic equations of the generator in dq-coordinates are

$$\begin{aligned} L\dot{i}_d &= -Ri_d + Li_q\omega_e - v_d \\ L\dot{i}_q &= -Ri_q - Li_d\omega_e + \phi\omega_e - v_q \end{aligned} \tag{5.6}$$

where i_q, i_d, v_q, v_d are respectively the q and d components of the current and voltage, R and L are the stator resistance and inductance respectively, ϕ is the permanent magnetic flux and ω_e is the electrical frequency. The electrical frequency satisfies the relation

$$\omega_e = \frac{P}{2}\omega_m. \tag{5.7}$$

where P is the number of pole pairs. The electrical torque T_e is given by

$$T_e = \frac{3}{2}\frac{P}{2}\phi i_q. \tag{5.8}$$

The input voltages in the generator are

$$v_d = v_C d_1, \; v_q = v_C d_2 \tag{5.9}$$

where d_1 and d_2 are duty ratio of the rectifier control signals in dq-coordinates. Finally, from Kirchhoff's current law we have

$$C\dot{v}_C = -R_e v_C + \frac{V_S}{R_S} + i_d d_1 + i_q d_2 \tag{5.10}$$

where C is the capacitance value, $R_e := \frac{R_L+R_S}{R_L R_S}$, R_L is a resistive load and R_S and V_S are, respectively, the supply internal resistance and dc voltage.

The Overall System

Subsituting (5.5) and (5.8) in (5.4), (5.9) and (5.7) in (5.6) and from (5.10), the overall system becomes

$$\begin{aligned}
L\dot{i}_d &= -Ri_d + \frac{P}{2}Li_q\omega_m - d_1 v_C \\
L\dot{i}_q &= -Ri_q - \frac{P}{2}Li_d\omega_m + \frac{P}{2}\phi\omega_m - d_2 v_C \\
J\dot{\omega}_m &= -f\omega_m + \frac{1}{2}\rho A v_m^3 \frac{1}{\omega_m} C_p\left(\frac{v_w\omega_m}{r}\right) - \frac{3}{2}\frac{P}{2}\phi i_q \\
C\dot{v}_C &= -R_e v_C + \frac{V_S}{R_S} + d_1 i_d + d_2 i_q
\end{aligned}$$

Introducing the following definitions

$$\phi_1 := \frac{\phi P}{2},\ \gamma := \frac{P}{2},\ J_1 := \frac{2}{3}J,\ f_1 := \frac{2}{3}f,$$

and the change of variables $x = \text{col}(Li_d,\ Li_q,\ J_1\omega_m,\ Cv_C),\ u = \text{col}(d_1, d_2)$, the system can be rewritten as

$$\dot{x}_1 = -\frac{R}{L}x_1 + \frac{\gamma}{J_1}x_2x_3 - \frac{x_4}{C}u_1 \tag{5.11}$$

$$\dot{x}_2 = -\frac{\gamma}{J_1}x_1x_3 - \frac{R}{L}x_2 + \frac{\phi_1}{J_1}x_3 - \frac{x_4}{C}u_2 \tag{5.12}$$

$$\dot{x}_3 = -f_1x_3 + \Phi(x_3) - \frac{\phi_1}{L}x_2 \tag{5.13}$$

$$\dot{x}_4 = -\frac{R_e}{C}x_4 + \frac{x_1}{L}u_1 + \frac{x_2}{L}u_2 + \frac{V_S}{R_S} \tag{5.14}$$

where

$$\Phi(x_3) := \frac{1}{3}\rho A J_1 v_w^3 \frac{1}{x_3} C_p\left(\frac{rx_3}{J_1 v_w}\right).$$

Now, notice that the system admits the following representation

$$\dot{x} = A_0(x_3)x + \sum_{i=1}^{2} B_i x u + E_0(x_3) \tag{5.15}$$

where $E_0(x_3) := \text{col}\left(0, 0, \Phi(x_3), \frac{V_S}{R_S}\right)$ and

$$A_0(x_3) := \begin{bmatrix} -\frac{R}{L} & \frac{\gamma}{J_1}x_3 & 0 & 0 \\ -\frac{\gamma}{J_1}x_3 & -\frac{R}{L} & \frac{\phi_1}{J_1} & 0 \\ 0 & -\frac{\phi}{J_1} & -f_1 & 0 \\ 0 & 0 & 0 & -\frac{R_e}{C} \end{bmatrix}, \; B_1 := \begin{bmatrix} 0 & 0 & 0 & -\frac{1}{C} \\ 0 & 0 & 0 & 0 \\ 0 & 0 & 0 & 0 \\ \frac{x_1}{L} & 0 & 0 & 0 \end{bmatrix} \; B_2 := \begin{bmatrix} 0 & 0 & 0 & 0 \\ 0 & 0 & 0 & -\frac{1}{C} \\ 0 & 0 & 0 & 0 \\ 0 & \frac{1}{L} & 0 & 0 \end{bmatrix},$$

Control Objectives as Desired Equilibrium Points

The control objectives are: 1) Minimize the copper loss and maximize the efficiency of the generator, this is carried out whenever $x_{1\star} = 0$; 2) Operate at the maximum power extraction point $x_{3\star} := \frac{J_1 \lambda_\star v_w}{r}$.

Lemma 5.1. The assignable equilibrium points of the system (5.11)-(5.14), compatible with the control objectives, are defined by the set

$$\mathcal{E} = \left\{ x | x_1 = 0, x_2 = \frac{L}{\phi_1}\left(\Phi_\star - f_1 x_{3\star}\right), x_3 = x_{3\star}, h_1(x_4) = 0 \right\}$$

where $\Phi_\star := \Phi(x_{3\star})$ and

$$h_1(x_4) := \frac{R_e}{C^2}x_4^2 - \frac{V_S}{R_S C}x_4 + \frac{R}{\phi_1^2}(\Phi_\star - f_1 x_{3\star})^2 + \frac{f_1}{J_1^2}x_{3\star}^2 - \frac{x_{3\star}}{J_1}\Phi_\star$$

Proof: At the equilibrium, (5.15) satisfies

$$\begin{aligned} 0 =& A_0(x_3)x + \sum_{i=1}^{2} B_i x u + E_0(x_3) \\ =& A_0(x_3)x + G(x)u + E_0(x_3) \end{aligned} \tag{5.16}$$

where

$$G(x) := \begin{bmatrix} -\frac{x_4}{C} & 0 \\ 0 & -\frac{x_4}{C} \\ 0 & 0 \\ \frac{x_1}{L} & \frac{x_2}{L} \end{bmatrix}. \tag{5.17}$$

A full–rank left–annihilator of $G(x)$ is

$$G^\perp(x) = \begin{bmatrix} x^\top P \\ e_3^\top \end{bmatrix}, \tag{5.18}$$

where $P := \text{diag}\left(\frac{1}{L}, \frac{1}{L}, \frac{1}{J_1}, \frac{1}{C}\right)$ and $e_3 := \text{col}(0, 0, 1, 0)$. Pre-multiplying (5.16) by $G^\perp(x)$

yields

$$\begin{bmatrix} -x^\top Qx + \frac{1}{J_1}x_3\Phi(x_3) + \frac{V_S}{R_S C}x_4 \\ -f_1 x_3 + \Phi(x_3) - \frac{\phi_1}{L}x_2 \end{bmatrix} = 0$$

where $Q := \text{diag}\,(R, R, f_1, R_e) = -\text{sym}(PA) > 0$. Then, fixing $x_1 = 0$ and $x_3 = x_{3\star}$, we get from the second equation, $x_2 = \frac{L}{\phi_1}\Phi_\star - f_1 x_{3\star} := x_{2\star}$. Substituting the last value in the first equation yields the expression for $h_1(x_4)$. □□□

Remark 5.1. The necessary and sufficient condition for the existence of the desired equilibrium point is

$$\frac{R}{\phi_1^2}(\Phi_\star - f_1 x_{3\star})^2 + \frac{f_1}{J_1^2}x_{3\star}^2 - \frac{x_{3\star}}{J_1}\Phi_\star \leq \frac{V_S^2}{4R_e R_S^2}$$

5.1.2 Control Design : The PI-PBC Approach

To proceed with the design of the PI–PBC we make the usual assumption that the mechanical dynamics is much slower than the electrical one, which translates into the following standing assumption.

Assumption 5.1. The system dynamics is represented by

$$\dot{x} = Ax + \sum_{i=1}^{2} B_i x u_i + E. \tag{5.19}$$

where we defined $A := A_0(x_{3\star})$ and $E := E_0(x_{3\star})$.

Notice that we assume x_3 to be constant only when it appears in the matrix A_0 and the external force E_0, but it remains a state variable in the overall dynamics.

Following [32,35], and also recalled in Section 2.2 , we prove the following passivity property.

Lemma 5.2. *(Passivity)* The system (5.19) defines a passive mapping $\tilde{u} \mapsto y$ with storage function

$$V(\tilde{x}) = \frac{1}{2}\tilde{x}^\top P\tilde{x}, \tag{5.20}$$

where $\tilde{(\cdot)} = (\cdot) - (\cdot)_\star$, $P := \text{diag}\left(\frac{1}{L}, \frac{1}{L}, \frac{1}{J_1}, \frac{1}{C}\right)$ and the passive output defined as

$$y := G^\top(x_\star)P\tilde{x}. \tag{5.21}$$

with $G(\cdot)$ defined in (5.17).

Proof. First, as in Section 2.2, we define the incremental system of (5.19) as

$$\dot{\tilde{x}} = (A + \sum_{i=1}^{2} B_i u_i)\tilde{x} + \sum_{i=1}^{2} B_i x_\star \tilde{u}_i. \tag{5.22}$$

Then, since that $\text{sym}(PA) = \text{diag}(R, R, f_1, R_e) =: Q > 0$ and $\text{sym}(PB) = 0$, proceeding as in Section 2.3 yields

$$\begin{aligned} \dot{V} &= -\tilde{x}^\top Q x + \tilde{x}^\top P \left[\sum_{i=1}^{2} B_i x_\star \tilde{u}_i\right] && (5.23)\\ &\leq \tilde{x}^\top P G^\top(x_\star)\tilde{u} && (5.24)\\ &= y^\top \tilde{u}, && (5.25) \end{aligned}$$

which completes the proof. □□□

From Section 2.2, we state the following proposition.

Proposition 5.1. *(PI-PBC)* Consider the system (5.19) in closed–loop with the PI controller

$$\begin{aligned} \dot{z} &= -y \\ u &= -K_p y + K_i z, \end{aligned} \tag{5.26}$$

where y is given in (5.21) and the tuning gains verify $K_p > 0$ and $K_i > 0$. For all initial conditions $(x(0), z(0))$ the trajectories of the closed-loop system are bounded and

$$\lim_{t\to\infty} \tilde{x}(t) = 0. \tag{5.27}$$

Proof. Notice that (5.26) can be expressed as

$$\begin{aligned} \dot{\tilde{z}} &= -y \\ \tilde{u} &= -K_p y + K_i \tilde{z}, \end{aligned} \tag{5.28}$$

where $z_\star := K_i^{-1} u_\star$. Consider the Lyapunov function candidate

$$W(\tilde{x}, \tilde{z}) = V(\tilde{x}) + \frac{1}{2}\tilde{z}^\top K_i \tilde{z}.$$

Differentiating this function and using (5.24) and (5.28) yields

$$\begin{aligned}\dot{W} &= -\tilde{x}^\top Q x + y^\top \tilde{u} - \tilde{z}^\top K_i y \\ &= -\tilde{x}^\top Q \tilde{x} - y^\top K_p y \\ &\leq -\alpha |\tilde{x}|^2,\end{aligned}$$

where $|\cdot|$ is the Euclidean norm and

$$\alpha := \lambda_{\min}\{Q\} > 0.$$

Boundedness of the trajectories follows from Lyapunov's Direct Method. The proof is completed from La Salle's Invariance Principle which implies (5.27). □□□

Remark 5.2. The passive output used in the PI controller of Proposition 5.1 is

$$y = \frac{1}{LC}\begin{bmatrix} x_{1\star}\tilde{x}_4 - \tilde{x}_1 x_{4\star} \\ x_{2\star}\tilde{x}_4 - \tilde{x}_2 x_{4\star} \end{bmatrix},$$

which in the original system coordinates becomes

$$y = \begin{bmatrix} i_{d\star}\tilde{v}_C - \tilde{i}_d v_{C\star} \\ i_{q\star}\tilde{v}_C - \tilde{i}_q v_{C\star} \end{bmatrix}.$$

As discussed in [32, 90] our PI scheme is closely related to the well–known instantaneous active power control of [2].

5.1.3 Simulation Results

The power coefficient is assumed to be given by [31]

$$C_p(\lambda) = c_1\left(\frac{c_2}{\lambda_i} - c_5\right)\exp\left(-\frac{c_6}{\lambda_i}\right),$$

where $c_1 = 0.5, c_2 = 116, c_5 = 5$, $c_6 = 21$ and

$$\lambda_i = \left(\frac{1}{\lambda} - 0.035\right)^{-1}.$$

The maximum value is $C_{p\star} = 0.411$ and $\lambda_\star = 7.954$.

The parameters of the system were taken from [20] and are shown in Table 5.1. To test the controller in a real scenario, the simulation setting was realized in a switching based model. The considered PMSG wind turbine rectifier system is shown in Fig.

Table 5.1: Wind system parameters

Item	Value
Turbine	
Inertia	$J = 7.856$ kg$\cdot$ m^2
Blades radius	$r = 1.84$ m
PMSG	
Nominal Power	$S_n = 5$ kVA
Poles	$P = 28$
Synchronous resistance	$R = 0.3676\ \Omega$
Synchronous inductance	$L = 3.55$ mH
Flux	$\phi = 0.2867$ Wb
Friction coefficient	$f = 3.035 \times 10^{-4}$ N$\cdot$m$\cdot$s
Rectifier & Electrical Parameters	
Capacitance	$C = 3.3$ mF
System Load	$R_L = 60\ \Omega$
Power Supply Voltage	V_S =400 V
Power Supply Resistance	$R_S = 0.1\ \Omega$

5.1. A constant voltage source is adopted at the dc output terminal to set the constant dc bus condition, which is normally maintained by the back-end converter. Space vector pulse width modulation was adopted to generate the gate signals in the rectifier switches.

The control implementation diagram is shown in Fig. 5.3. The wind profile is shown at the bottom of the figure. to verify the controller performance under changing conditions, the wind profile involves two step variations. As it can be noticed from the profiles of i_q and i_d currents in Fig. 5.4 , they present typical switching noise, which is maintained in small range. A good transient performance is seen without any overshoot and oscillation.

5.2 Passivity–Based Control of a Grid–Connected Small–Scale Windmill with Limited Control Authority

In the present section we design a passivity-based control of wind energy system consisting of a wind turbine plus a permanent magnet synchronous generator connected to a single–phase ac grid through a passive rectifier, a boost converter and an single–phase inverter. The control is intended to regulate the generator speed and the dc link

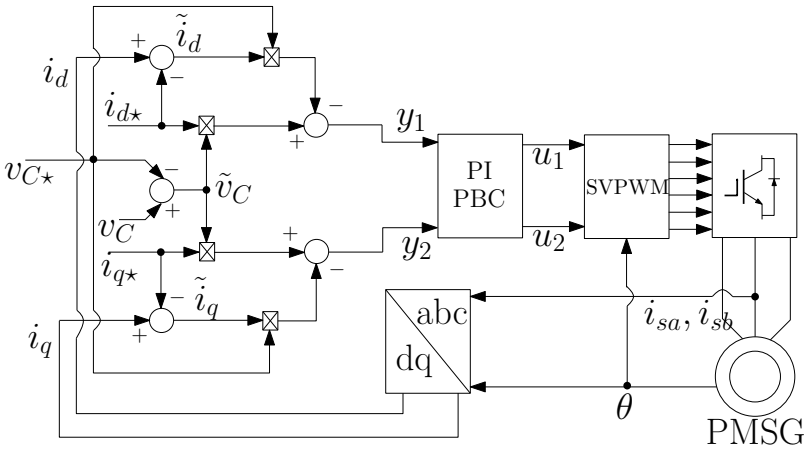

Figure 5.3: Block diagram of the control implementation of the PI-PBC

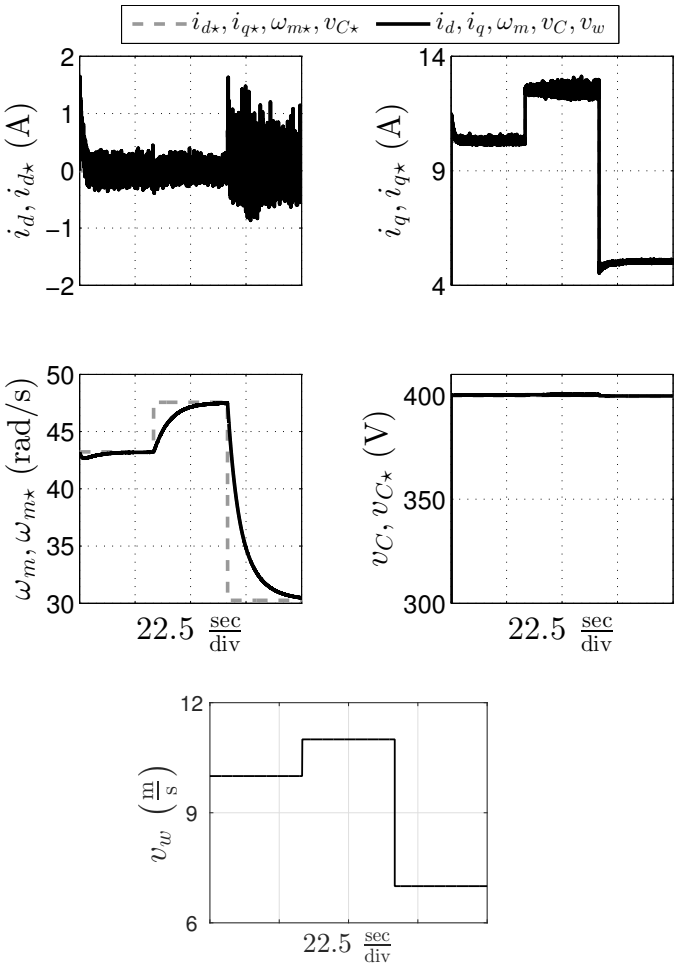

Figure 5.4: Simulation results.

voltage and power factor of the current injected into the ac grid. The controller design of the overall system becomes complicated for two reasons. On one hand, the generator dynamics cannot be neglected—as usually done for large wind turbines [19, 36]—leading to a system behavior described by highly–coupled set of nonlinear differential equations. On the other hand, due to the use of a "simple" generator and power elec-

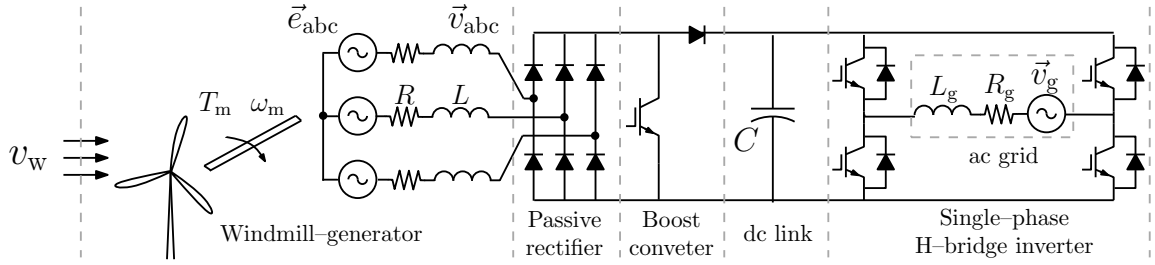

Figure 5.5: Circuit schematic of a grid–connected windmill system.

tronic interface, the control authority is quite restricted [2].

To design the controller, the overall system is decomposed as a cascade connection of two subsystems. One consisting of the windmill and PMSG and the other containing the boost converter and the inverter. The PMSG rotor speed of the first subsystem is regulated around the maximum power extraction point with a standard passivity–based controller (SPBC)—which is a nonlinear, dynamic, state feedback that shapes the energy of the subsystem and adds damping and an integral action [58]. The dc link voltage and the injection of reactive power to the grid is controlled in the second subsystem, via a tracking PI-PBC — see Chapter 2 — whose reference is suitably tailored to compensate for the coupling term coming from the first subsystem. The development of this tracking PI is an extension of the regulation PI schemes (for systems whose incremental model is passive) reported in [32, 35]. The main result in this section is the proof that the overall controlled system has an asymptotically stable equilibrium point at the desired operating regime. Simulation results are shown comparing the controllers performance with that of the typical PI control utilized in power engineering.

5.2.1 Mathematical Model of the System

In this section we describe the components of the system, whose schematic diagram is given in Fig.5.5. The system consists of a wind turbine with a PMSG, a passive diode bridge rectifier, a boost converter, a dc link and an inverter connected to the grid through a simple L filter. Although the passive rectifier injects current harmonics into the PMSG, this topology is preferred due to its low cost and simplicity of implementation. On the other hand, it is clear that it significantly reduces the available control authority.

In [46] we considered a similar system, replacing the dc link by a battery and removing the inverter and the grid. The reader is referred to [46] for additional details on

[2] More precisely, the number of control signals (three) is smaller than the order of the system (six) and equals the number of signals to be regulated.

the modeling of the first three elements that, in the interest of brevity, are only briefly summarized below.

5.2.2 Dynamics of the PMSG

The electrical equations which describe the behavior of the surface–mounted PMSG in the rotor (dq) reference frame are given by

$$\begin{aligned} L\,\dot{i}_d &= -Ri_d + Li_q\omega_e - v_d, \\ L\,\dot{i}_q &= -Ri_q - Li_d\omega_e + \phi\omega_e - v_q, \end{aligned} \tag{5.29}$$

where i_d, i_q, v_d, v_q, are the currents and voltages in the $d-q$ reference frame, L and R are the stator winding's inductance and resistance, ω_e is the electric frequency that is related to the mechanical speed via

$$\omega_e = \frac{P}{2}\omega_m,$$

ϕ is the permanent magnetic flux produced by the rotor magnets, and P is the number of poles. The magnetic flux ϕ is a constant that depends on the material used for the realization of the magnets. A detailed derivation of this standard model may be found in [42]. An important observation is that, in normal operating conditions, $i_d^2 + i_q^2 > 0$. See Remark 5.5 below.

Mechanical and wind turbine dynamics

The mechanical dynamics is described by

$$J\dot{\omega}_m = T_m - T_e. \tag{5.30}$$

where J is the rotor inertia, ω_m is the shaft's rotational speed, T_e is the electrical torque defined as

$$T_e = \frac{3}{2}\frac{P}{2}\phi i_q,$$

and T_m is the mechanical torque applied to the windmill shaft that, as in the Section 5.1, is given by

$$T_m = \frac{1}{2}\rho A r \frac{C_p(\lambda)}{\lambda} v_w^2,$$

where $C_p(\lambda)$ is the power coefficient, the blades' tip speed λ is defined in (5.1) — see Section 5.1 for the parameters descriptions and considerations. As in the last section,

we are interested in operating the system at the point of maximum power extraction.

$$\omega_{m\star} = \frac{\lambda_\star v_w}{r}.$$

Power electronic interface and grid

As shown in Fig. 5.5 the PMSG is linked to the grid through a passive rectifier a dc–dc boost converter, a dc link and an inverter. As discussed in [46], in this configuration the PMSG voltages may be expressed as

$$\begin{aligned} v_d &= \tfrac{i_d}{\sqrt{i_d^2+i_q^2}} M v_{dc} D, \\ v_q &= \tfrac{i_q}{\sqrt{i_d^2+i_q^2}} M v_{dc} D, \end{aligned} \tag{5.31}$$

where D is the duty ratio of the dc–dc boost converter, $M = \frac{\pi}{3\sqrt{3}}$ is the gain of the passive diode rectifier and v_{dc} is the voltage of the dc link. The well–known average model of the dc link and inverter (in dq coordinates) is given by

$$\begin{aligned} C\dot{v}_{dc} &= \frac{3M}{2}(i_d^2 + i_q^2)u_1 - \frac{1}{2}I_d u_2 - \frac{1}{2}I_q u_3, \\ L_g\dot{I}_d &= -R_g I_d + L_g\omega I_q - V_d + v_{dc}u_2, \\ L_g\dot{I}_q &= -L_g\omega I_d - R_g I_q + v_{dc}u_3, \end{aligned} \tag{5.32}$$

where C is the capacitance of the dc link, I_d, I_q are the d and q components of the grid currents, respectively, V_d is the amplitude of the grid's voltage, L_g, R_g are the inverter's inductance and resistance. We defined in (5.32)

$$u_1 := \frac{D}{\sqrt{i_d^2 + i_q^2}},$$

and u_2 and u_3 are the d and q components, respectively of the inverter modulating signal. Finally, ω is the (constant) frequency of the ac grid voltage. It is well–known that the inverter is operational only if the voltage of the dc link is kept above a minimal (positive) value. See Remark 5.5 below.

Overall dynamic model

Collecting (5.29), (5.30), (5.31) and (5.32), defining the state vector

$$x := \text{col}(i_d, i_q, r\omega_m, v_{dc}, I_d, I_q),$$

the constants $C_2 := \frac{\rho A}{3},\ L_1 := \frac{PL}{2r},\ \phi_1 := \frac{P\phi}{2r},\ J_1 := \frac{2J}{3r^2}$, and the function

$$\Phi(x_3) := C_2 \frac{v_w^3}{x_3} C_p\left(\frac{x_3}{v_w}\right). \tag{5.33}$$

the system state equations may be written as

$$\begin{aligned}
L\dot{x}_1 =& -Rx_1 + L_1 x_2 x_3 - M x_1 x_4 u_1 \\
L\dot{x}_2 =& -Rx_2 - L_1 x_1 x_3 + \phi_1 x_3 - M x_2 x_4 u_1 \\
J_1\dot{x}_3 =& -\phi_1 x_2 + \Phi(x_3) \\
C\dot{x}_4 =& \frac{3M}{2}(x_1^2 + x_2^2)u_1 - \frac{1}{2}x_5 u_2 - \frac{1}{2}x_6 u_3 \\
L_g\dot{x}_5 =& -R_g x_5 + L_g \omega x_6 - V_d + x_4 u_2 \\
L_g\dot{x}_6 =& -L_g \omega x_5 - R_g x_6 + x_4 u_3
\end{aligned} \tag{5.34}$$

where $u := \text{col}(u_1, u_2, u_3)$ is the control input vector.

Remark 5.3. The total energy of the system (5.34) is given by

$$H(x) = \frac{1}{4}x^\top \text{diag}\{3L, 3L, 3J_1, 2C, L_g, L_g\}x,$$

whose derivative, as expected, verifies the power balance equation

$$\dot{H} = \underbrace{-\frac{3R}{2}(x_1^2 + x_2^2) - \frac{R_g}{2}(x_5^2 + x_6^2)}_{\text{dissipation}} + \underbrace{\frac{3}{2}\Phi(x_3)x_3}_{\text{mechanical power}} - \underbrace{\frac{1}{2}x_5 V_d}_{\text{electrical power}}.$$

5.2.3 Assignable Equilibria and Problem Formulation

The control objective is three–fold: (*i*) to operate the system of (5.34) in the point of maximum wind power extraction which translates into an optimal shaft speed $x_{3\star}$; (*ii*) to keep the dc link voltage at a desired constant value $x_{4\star} > 0$; and (*iii*) to inject current in to the grid at a given power factor. It is assumed that the current is injected at unity power factor, that is, $x_{6\star} = 0$. These objective should be achieved independently of the wind speed.

Under the assumptions of known $\lambda_\star$ and v_w, the control task reduces to a standard problem of stabilization of an (assignable) equilibrium point $x_\star$ of the system (5.34) with

$$x_{3\star} := \lambda_\star v_w > 0, \quad x_{4\star} = v_{dc\star} > 0, \quad x_{6\star} = 0. \tag{5.35}$$

Assignable equilibria

The proposition below characterizes the set of assignable equilibria compatible with the constraint (5.35).

Lemma 5.3. Consider the system (5.34). Fix $x_{6\star} = 0$ and $x_{3\star} > 0$. Then, for any $x_{4\star} > 0$, the set of assignable equilibria is given by

$$\mathcal{E} := \{x \in \mathbb{R}^6 \mid \ell_1(x_1) = 0,\ x_2 = \frac{\Phi_\star}{\phi_1}, \ell_2(x_1, x_5) = 0\}, \tag{5.36}$$

where

$$\ell_1(x_1) := x_1^2 - \frac{\phi_1}{L_1}x_1 + \frac{\Phi_\star^2}{\phi_1^2} \tag{5.37}$$

$$\ell_2(x_1, x_5) := R_g x_5^2 + V_d x_5 + \frac{3R\phi_1}{L_1}x_1 - 3x_{3\star}\Phi_\star, \tag{5.38}$$

with $\Phi_\star := \Phi(x_{3\star})$.

Proof. Fix $x_3 = x_{3\star}$. From the third equation in (5.34) we get

$$x_{2\star} = \frac{\Phi_\star}{\phi_1}. \tag{5.39}$$

Then, eliminating u_1 from the first and second equations in (5.34) and using (5.39) we obtain

$$L_1(x_{1\star})^2 x_{3\star} - \phi_1 x_{1\star} x_3^\star + L_1 \frac{\Phi_\star^2}{\phi^2} x_3^\star = 0 \tag{5.40}$$

which is equivalent to $\ell_1(x_1^\star) = 0$.

Finally, at the equilibrium, the power balance equation of Remark 5.3 is equal to zero. Then, substituting $x_2^\star$ from (5.39), the balance equation becomes

$$0 = R_g(x_5^\star)^2 + V_d x_5^\star + 3R[(x_1^\star)^2 + \frac{\Phi_\star^2}{\phi^2}] - 3\Phi^\star x_3^\star. \tag{5.41}$$

Also, from (5.40)

$$(x_1^\star)^2 = \frac{\phi}{L_1}x_1^\star - \frac{\Phi_\star^2}{\phi_1^2}$$

which is substituted in (5.41) to complete the proof. □□□

Remark 5.4. Necessary and sufficient conditions for the existence of equilibria are

$$\begin{aligned} \frac{\phi_1^2}{2L_1} &\geq \Phi_\star \\ V_d^2 &\geq 12R_g\left(\frac{R\phi_1}{L_1}x_1^\star - x_3^\star\Phi_\star\right), \end{aligned} \tag{5.42}$$

where $x_{1\star}$ is a solution of $\ell_1(x_{1\star}) = 0$.

Control problem formulation

Given the system (5.34) and an equilibrium $x_\star \in \mathcal{E}$, verifying (5.35), find (if possible) a state–feedback controller that ensures *asymptotic stability* of the closed–loop system.

Remark 5.5. As explained in Section 5.2.1 the physical operation of the system is restricted to a subset of $\mathbb{R}^6$. In particular, it is necessary that

$$\begin{aligned} x_1^2(t) + x_2^2(t) &\geq \kappa_1 \\ x_4(t) &\geq \kappa_2, \end{aligned} \tag{5.43}$$

for some $\kappa_1, \kappa_2 > 0$, and all $t \geq 0$. We will prove below that the closed–loop system is asymptotically stable. This, together with the fact that $x_\star \in \mathbb{R}^6_+$, ensures that (5.43) holds if the initial conditions are sufficiently close to the equilibrium.

Remark 5.6. In reality the control signals, being duty cycles, live in a compact set. Unfortunately, the theoretical results presented later cannot take into account this consideration.

5.2.4 A Cascade Decomposition of the System

The following decomposition of the system allows us to simplify the controller design task. Recalling (5.43), and defining the new control signal

$$v_1 := -Mx_4u_1, \tag{5.44}$$

it is possible to write the overall system (5.34) as a *cascade connection* of the subsystem

$$\begin{aligned} L\dot{x}_1 &= -Rx_1 + L_1x_2x_3 + x_1v_1 \\ L\dot{x}_2 &= -Rx_2 - L_1x_1x_3 + \phi_1x_3 + x_2v_1 \\ J_1\dot{x}_3 &= -\phi_1x_2 + \Phi(x_3) \\ y_1 &= (x_1^2 + x_2^2)v_1, \end{aligned} \tag{5.45}$$

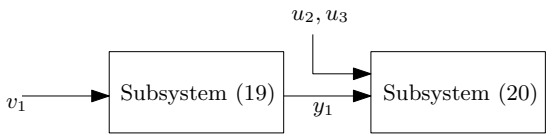

Figure 5.6: The cascade connection between subsystems (5.45) and (5.46).

with input v_1 and output y_1, and the subsystem

$$\begin{aligned} C\dot{x}_4 &= -\frac{1}{2}x_5u_2 - \frac{1}{2}x_6u_3 - \frac{3}{2x_4}y_1 \\ L_g\dot{x}_5 &= -R_gx_5 + L_g\omega x_6 - V_d + x_4u_2 \\ L_g\dot{x}_6 &= -L_g\omega x_5 - R_gx_6 + x_4u_3, \end{aligned} \tag{5.46}$$

with external input y_1 and controls u_2, u_3. A cascade connection between subsystems is presented in Fig. 5.6.

The cascade decomposition from Fig.5.6 suggests the following controller design procedure.

(S1) Design an SPBC to generate the control signal v_1 that renders the desired equilibrium $x_{13\star}$ of subsystem (5.45) asymptotically stable. This step is similar to the one done in [46], but with the difference that, to improve the transient performance of the closed–loop system, we have followed the suggestion made in the concluding remarks of [46] and explored an alternative construction of the SPBC. See Remark 5.7 below.

(S2) In the spirit of [32], design for the subsystem (5.46) a PI controller for an output with respect to which the incremental model is passive. Here, again, there is a fundamental difference with respect to the design proposed in [32]. Indeed, due to the presence of the term coupling the two subsystems, we are dealing now with a *tracking* and not a regulation problem like the one addressed in [32].

Since the controller design is based on the aforementioned decomposition, to enhance readability, we first present the individual controller designs in the next two sections. The main result of this section, given in Proposition 5.4, is the proof that the overall controller renders the equilibrium of the complete system (5.34) *asymptotically stable*.

5.2.5 Standard PBC of Subsystem (5.45)

The control design for the subsystem (5.45) is based on the SPBC, which is a variation of PBC that is particularly suited for systems described by Euler–Lagrange equations.

As shown in [58], it has been successful in a wide range of applications including mechanical, electromechanical and power electronic systems.

For the sake of clarity, we present in this section the three steps that are followed to design an SPBC. First, the Euler–Lagrange representation of (5.45) is given . Second, since SPBC requires a stable invertibility condition [58], the stability of the zero dynamics of (5.45)—for some suitably defined output—is studied and the design of the stabilizing SPBC is carried out. Finally, to improve performance, further damping and an integral robustifying term are added.

Euler–Lagrange model

In order to apply SPBC, the subsystem equations (5.45) are written in Euler–Lagrange form[3]

$$\mathcal{D}\dot{x}_{13} + [\mathcal{C}(x_3) + \mathcal{R}]x_{13} = G(x_{12})v_1 + b(x_3) \tag{5.47}$$

where we defined the generalized inertia, damping and interconnection matrices

$$\mathcal{D} := \text{diag}\{L, L, J_1\}, \mathcal{R} := \text{diag}\{R, R, 0\}$$

$$\mathcal{C}(x_3) := \begin{bmatrix} 0 & -L_1 x_3 & 0 \\ L_1 x_3 & 0 & -\phi_1 \\ 0 & \phi_1 & 0 \end{bmatrix}. \tag{5.48}$$

The right hand side terms in (5.47) are the external forces, where

$$b(x_3) := \begin{bmatrix} 0 \\ 0 \\ \Phi(x_3) \end{bmatrix}, \; G(x_{12}) := \begin{bmatrix} x_1 \\ x_2 \\ 0 \end{bmatrix}. \tag{5.49}$$

Notice that, consistent with their physical interpretation,

$$\mathcal{D} > 0, \; \mathcal{C}(x_3) = -\mathcal{C}^\top(x_3), \; \mathcal{R} \geq 0.$$

Hence, differentiating the systems energy function

$$H_1(x_{13}) = \frac{1}{2} x_{13}^\top \mathcal{D} x_{13}, \tag{5.50}$$

[3]See [58, 81] for further details on Euler–Lagrange systems in control applications.

yields the power–balance equation

$$\dot{H}_1 = \underbrace{-R|i_{dq}|^2}_{\text{dissipation}} - \underbrace{|v_{dq}||i_{dq}|}_{\text{elec. power}} + \underbrace{\frac{2}{3}T_m\omega_m}_{\text{mech. power}},$$

where $|\cdot|$ is the Euclidean norm.

A stable invertibility property of the system (5.47)

As explained in Section 3.1 of [58], SPBC performs a "partial inversion" of the system dynamics. Indeed, the controller is a copy of part of the system's equations with the remaining states set equal to constants—plus some damping injection terms which vanish at the equilibrium. Consequently, to ensure internal stability, it is necessary that the zero dynamics of the system, with respect to the "outputs" (the states that are fixed to constant) is asymptotically stable.

The SPBC proposed here takes as "output" the state x_1. Hence, the need of the lemma below.

Lemma 5.4. Given an assignable equilibrium $x_\star \in \mathcal{E}$ verifying (5.35). The zero dynamics of the system (5.45) with output $x_1 - x_{1\star}$ has an *asymptotically stable* equilibrium at $(x_{2\star}, x_{3\star})$.

Proof. Setting $x_1 = x_{1\star}$ and $\dot{x}_1 = 0$, in the first equation of (5.47) yields the (zeroing output) control[4]

$$v_1 = R - \frac{L_1}{x_{1\star}} x_2 x_3,$$

which replaced in $\dot{x}_2$ yields

$$\begin{aligned}
\dot{x}_2 &= -\frac{L_1}{L} x_{1\star} x_3 + \frac{\phi_1}{L} x_3 - \frac{L_1}{L x_{1\star}} x_2^2 x_3 \\
&= -\frac{L_1}{L x_{1\star}} x_3 \left((x_{1\star})^2 - \frac{\phi_1}{L_1} x_{1\star} + x_2^2 \right) \\
&= \frac{L_1}{x_{1\star}} x_3 [(x_{2\star})^2 - x_2^2] \\
&=: m_1(x_2, x_3),
\end{aligned} \tag{5.51}$$

where we have used (5.36) and (5.37) to get the second and third equations. The zero dynamics is completed with the third equation of (5.47)

$$\dot{x}_3 = -\frac{\phi_1}{J} x_2 + \frac{1}{J}\Phi(x_3) =: m_2(x_2, x_3). \tag{5.52}$$

[4]To avoid cluttering, but with some obvious abuse of notation, we use the same symbols for the system and its restricted dynamics.

The Jacobian of the zero dynamics vector field col$(m_1(x_2, x_3), m_2(x_2, x_3))$ is given by

$$\begin{bmatrix} -\frac{2L_1}{Lx_1^\star}x_2x_3 & \frac{L_1}{Lx_{1\star}}[(x_{2\star})^2 - x_2^2] \\ -\frac{\phi_1}{J_1} & \frac{1}{J_1}\Phi'(x_3) \end{bmatrix},$$

which evaluated at the equilibrium $(x_{2\star}, x_{3\star})$ yields

$$\begin{bmatrix} -\frac{2L_1}{Lx_{1\star}}x_{2\star}x_{3\star} & 0 \\ -\frac{\phi_1}{J_1} & \frac{1}{J_1}\Phi'(x_{3\star}) \end{bmatrix}. \tag{5.53}$$

Now, from the definition of $\Phi(x_3)$ given in (5.33) and the fact that $C_p(\lambda_\star) > 0$ and $C_p'(\lambda_\star) = 0$ we conclude that

$$\Phi'(x_3^\star) < 0.$$

This, together with the fact that $\frac{x_2^\star x_3^\star}{x_{1\star}} > 0$ ensures that (5.53) is a Hurwitz matrix. The proof is completed invoking Lyapunov's first method. □□□

Design of the SPBC

To enhance readability, the SPBC design is done in three steps: (*i*) energy–shaping, (*ii*) damping injection and (*iii*) explicit definition of the controller.

The first step in the SPBC procedure is to modify the energy function (5.50) assigning to the closed–loop system the energy function

$$W_1(e_{13}) := \frac{1}{2}e_{13}^\top \mathcal{D} e_{13}, \tag{5.54}$$

where

$$e_{13} := x_{13} - x_{13}^d. \tag{5.55}$$

is an error signal and the vector x_{13}^d, which is a signal that will converge to $x_{13\star}$, is defined below. Towards this end, a copy of the system dynamics is proposed

$$\mathcal{D}\dot{x}_{13}^d + [\mathcal{C}(x_3) + \mathcal{R}]x_{13}^d = b(x_3) + G(x_{12})v_1 + \begin{bmatrix} 0 \\ 0 \\ R_{3a}e_3 \end{bmatrix}, \tag{5.56}$$

where $R_{3a}e_3$, with $R_{3a} > 0$, is an additional damping injection signal. Substracting (5.47) and (5.56) and using (5.55) yields the error equation

$$\mathcal{D}\dot{e}_{13} + [\mathcal{C}(x_3) + \mathcal{R}_d]e_{13} = 0 \tag{5.57}$$

where

$$\mathcal{R}_d := \mathcal{R} + \text{diag}\{0, 0, R_{3a}\} > 0.$$

Taking the derivative of (5.54), along the trajectories of (5.57), yields

$$\begin{aligned} \dot{W}_1 &= -e_{13}^\top \mathcal{R}_d e_{13} \\ &\leq -2\frac{\min\{R, R_{3a}\}}{\max\{L, J_1\}} W_1 \end{aligned}$$

establishing that $e_{13}(t) \to 0$, exponentially fast.

The controller dynamics is obtained setting $x_1^d = x_{1\star}$ in (5.56), which yields

$$\begin{aligned} L\dot{x}_2^d &= -L_1 x_3 x_{1\star} - R x_2^d + \phi_1 x_3^d + x_2 v_1 \\ J_1 \dot{x}_3^d &= -\phi_1 x_2^d + \Phi(x_3) - R_{3a}(x_3 - x_3^d) \\ v_1 &= \frac{1}{x_1}(R x_1^\star - L_1 x_2^d x_3). \end{aligned} \tag{5.58}$$

Notice that the control signal v_1 is obtained from the first equation in (5.56), which becomes an algebraic equation because $x_1^\star$ is a constant.

The stability properties of this SPBC are summarized in the following.

Proposition 5.2. Consider the system (5.45) in closed–loop with the controller (5.58). The equilibrium $x_{13}^\star$ is *asymptotically stable*.

Proof. The derivations above established that $x_{13} - x_{13}^d$ is bounded, and $|x_{13}(t) - x_{13}^d(t)| \to 0$, exponentially fast. Therefore, it only remains to prove that, for a suitable set of initial conditions, x_{13}^d is bounded and $x_{13}^d(t) \to x_{13}^\star$. Towards this end, replace the control v_1 in the first equation of (5.58) and write—with obvious definitions—the controller equations in the compact form

$$\begin{aligned} \dot{x}_2^d &= f_1(x_1, x_3, x_2^d, x_3^d) \\ \dot{x}_3^d &= f_2(x_3, x_2^d, x_3^d). \end{aligned}$$

Make now the key observation that these functions verify

$$\begin{aligned} f_1(x_1^\star, x_3^d, x_2^d, x_3^d) &= m_1(x_2^d, x_3^d) \\ f_2(x_3^d, x_2^d, x_3^d) &= m_2(x_2^d, x_3^d), \end{aligned}$$

where the functions $m_i(x_2, x_3), i = 1, 2$ are defined in (5.51) and (5.52)—and correspond to the vector field of the *asymptotically stable* zero dynamics studied in Lemma 5.4. Adding and substracting the functions $m_i(x_2^d, x_3^d)$, the controller equations can be

written in the form

$$\begin{aligned}\dot{x}_2^d &= m_1(x_2^d, x_3^d) + \Delta_1(x_2^d, x_3^d, e_1, e_3)\\ \dot{x}_3^d &= m_2(x_2^d, x_3^d) + \Delta_2(x_2^d, x_3^d, e_3),\end{aligned}$$

with the signals

$$\begin{aligned}\Delta_1(x_2^d, x_3^d, e_1, e_3) &:= f_1(e_1 + x_1^\star, e_3 + x_3^d, x_2^d, x_3^d) - f_1(x_1^\star, x_3^d, x_2^d, x_3^d)\\ \Delta_2(x_2^d, x_3^d, e_3) &:= f_2(e_3 + x_3^d, x_2^d, x_3^d) - f_2(x_3^d, x_2^d, x_3^d)\end{aligned}$$

viewed as perturbations to an asymptotically stable system. The proof is completed recalling that $e_{13}(t) \to 0$ exponentially fast, noting that

$$\Delta_1(x_2^d, x_3^d, 0, 0) = 0, \quad \Delta_2(x_2^d, x_3^d, 0) = 0$$

and invoking standard results of (local) asymptotic stability of cascaded systems. □□□

The corollary below, is instrumental for the analysis of the overall closed–loop system. Its proof follows immediately from the definition of Lyapunov stability of an equilibrium, Lemma 5.3 and Proposition 5.2.

Corollary 5.1. Consider the system (5.45) in closed–loop with the controller (5.58). For any $\epsilon > 0$ there exists (sufficiently small) $\delta > 0$ such that for all initial conditions verifying

$$|\text{col}(x_{13}(0), x_2^d(0), x_3^d(0)) - \text{col}(x_{13}^\star, x_2^\star, x_3^\star)| \leq \delta$$

the corresponding trajectory satisfies the following.

(P1) $x_{13}(t) \in \mathbb{R}^3_+$ and $x_{23}^d(t) \in \mathbb{R}^2_+$ for all $t \geq 0$.

(P2) The error signal $\tilde{y}_1 := y_1 - y_1^\star$, with

$$y_1^\star := -\frac{1}{3}[R_g(x_5^\star)^2 + V_d x_5^\star] < 0, \tag{5.59}$$

verifies

$$\begin{aligned}|\tilde{y}_1(t)| &\leq \epsilon, \quad \forall t \geq 0\\ \lim_{t\to\infty} \tilde{y}_1(t) &= 0 \quad (\text{exp}).\end{aligned} \tag{5.60}$$

Remark 5.7. In the SPBC above we fixed $x_1^d = x_1^\star$, this should be contrasted with the SPBC of [46], where we fixed $x_2^d = x_2^\star$ instead. As discussed in [46] this was motivated by the fact that the zero dynamics of the system with the output $x_1 - x_1^\star$ has a

unique (asymptotically stable) equilibrium point in the operating region—as shown in Lemma 5.4. On the other hand, it was shown in Lemma 2 of [46], that the zero dynamics with output $x_2 - x_2^\star$ has two equilibria in the operating region, one of them *unstable*. Consequently, it is reasonable to expect that the domain of attraction of the new controller is larger than the one in [46].

Performance improvement

As usual in PBC, the performance of the controller can be improved injecting additional damping and incorporating integral actions [58]. In the present case, the third right hand side term in (5.56) can be replaced by $\text{col}(R_{1a}e_1, R_{2a}e_2, R_{3a}e_3)$, with $R_{1a}, R_{2a} > 0$, to inject additional damping and improve the convergence speed of the error e_{13}.[5]

An integral term can easily be added to the SPBC replacing the second equation in (5.58) by

$$J_1\dot{x}_3^d = -\phi_1 x_2^d + \Phi(x_3) - R_{3a}(x_3 - x_3^d) + z, \tag{5.61}$$

where z is an integral term defined by

$$\dot{z} = -K_{iw}e_3, \tag{5.62}$$

with $K_{iw} = K_{iw}^\top > 0$ an integral gain. The error equation (5.57) becomes

$$\mathcal{D}\dot{e}_{13} + [\mathcal{C}(x_3) + \mathcal{R} + \text{diag}\{R_{1a}, R_{2a}, R_{3a}\}]e_{13} = \begin{bmatrix} 0 \\ 0 \\ 1 \end{bmatrix} z \tag{5.63}$$

Stability of the modified scheme is established with the total energy function

$$V_1(e_{13}, z) = \frac{1}{2}e_{13}^\top \mathcal{D} e_{13} + \frac{1}{2K_{iw}}z^2,$$

whose derivative verifies

$$\dot{V}_1 \leq \min\{R + R_{1a}, R + R_{2a}, R_{3a}\}|e_{13}|^2.$$

The interested reader is referred to [58] for additional details.

[5] This fact, together with the performance improvement discussed in Remark 5.7, were verified by simulations, but are omitted from Section 5.2.9 for brevity.

5.2.6 A Tracking PI PBC for Subsystem (5.46)

In this section we design the controller for the subsystem (5.46). We notice that the subsystem is perturbed by the coupling term coming from the first subsystem, which we view as an additive (measurable) disturbance $y_1(t)$. In the absence of the latter, the *PI PBC* of [32] would solve the problem. In order to take into account this disturbance, we add to the regulation PI schemes of [32,35] a suitably tailored reference, yielding a *tracking PI PBC*.

Proposition 5.3. Consider subsystem (5.46) with y_1 and *external signal* verifying (5.60). Define the tracking PI controller

$$\begin{aligned} \dot{\xi} &= y_2 \\ u_{23} &= u_{23}^d - K_p y_2 - K_i \xi \end{aligned} \tag{5.64}$$

with $K_p = K_p^\top > 0$, $K_i = K_i^\top > 0$ and

$$y_2 = \frac{1}{2}\begin{bmatrix} x_4^\star x_5 - x_5^d x_4 \\ x_4^\star x_6 \end{bmatrix}, \tag{5.65}$$

$$u_{23}^d = \begin{bmatrix} -\frac{3}{x_4^\star x_5^d} y_1 \\ \\ L_g \omega \frac{x_5^d}{x_4^\star} \end{bmatrix} \tag{5.66}$$

and x_5^d the solution of the differential equation

$$L_g \dot{x}_5^d = -R_g x_5^d - V_d - \frac{3}{x_5^d} y_1, \ x_5^d(0) > 0. \tag{5.67}$$

There exists $\epsilon_c > 0$ such that for all $\epsilon \leq \epsilon_c$ the closed–loop system with state (x_{46}, ξ, x_5^d) has a *globally asymptotically stable* equilibrium point at $(x_{46}^\star, 0, x_5^\star)$.

Proof. First, we show that under the conditions of the proposition the solution of (5.67) is well–defined and verifies $x_5^d(t) > 0$, for all $t \geq 0$, and $x_5^d(t) \to x_5^\star$. Towards this end, we write (5.67) in the equivalent form

$$L_g \dot{x}_5^d = -R_g x_5^d - V_d - \frac{3}{x_5^d} y_1^* - \frac{3}{x_5^d} \tilde{y}_1. \tag{5.68}$$

Using (5.59) the equation above with $\tilde{y}_1 \equiv 0$ becomes

$$L_g \dot{x}_5^d = -R_g x_5^d - V_d + \frac{1}{x_5^d}[R_g (x_5^\star)^2 + V_d x_5^\star],$$

which has an asymptotically stable equilibrium at $x_5^\star$. Moreover, since $x_5^d(0) > 0$ and $x_5^\star > 0$, the set $\{x_5^d > 0\}$ is invariant. The proof that these properties are preserved for the perturbed equation is completed by invoking (5.60), a continuity argument and taking ϵ_c sufficiently small.

The subsystem (5.46) can be expressed in the following form

$$\dot{x}_{46} = A_d(u_{23})x_{46} + E \tag{5.69}$$

where $A_d(u_{23}) := A + B_2u_2 + B_3u_3$ and

$$E := -\begin{bmatrix} \frac{3}{2Cx_4}y_1 \\ \frac{V_d}{L_g} \\ 0 \end{bmatrix}, A := \begin{bmatrix} 0 & 0 & 0 \\ 0 & -\frac{R_g}{L_g} & \omega \\ 0 & -\omega & -\frac{R_g}{L_g} \end{bmatrix}, \; B_2 := \begin{bmatrix} 0 & -\frac{1}{2C} & 0 \\ \frac{1}{L_g} & 0 & 0 \\ 0 & 0 & 0 \end{bmatrix}, \; B_3 := \begin{bmatrix} 0 & 0 & -\frac{1}{2C} \\ 0 & 0 & 0 \\ \frac{1}{L_g} & 0 & 0 \end{bmatrix}.$$

Similarly to the construction in Chapter 2 —Section 2.1—, the key observation is that with the matrix

$$P := \begin{bmatrix} C & 0 & 0 \\ 0 & \frac{1}{2}L_g & 0 \\ 0 & 0 & \frac{1}{2}L_g \end{bmatrix} > 0,$$

Assumption 2.1 is verified, i.e.,

$$PA_d(u_{23}) + A_d^\top(u_{23})P = -\frac{1}{2}\text{diag}\{0, R_g, R_g\} \leq 0. \tag{5.70}$$

Now, define the vector $x_{46}^d := \text{col}(x_4^\star, x_5^d, 0)$. With (5.65)- (5.67), it is easy to prove that

$$\dot{x}_{46}^d = A_d(u_{23}^d)x_{46}^d + E.$$

Hence, the error $e_{46} := x_{46} - x_{46}^d$ verifies the equation

$$\dot{e}_{46} = A_d(u_{23})e_{46} + (e_2^uB_2 + e_3^uB_3)x_{46}^d, \tag{5.71}$$

where we defined the input error

$$e_{23}^u := u_{23} - u_{23}^d.$$

Notice that substituting y_1 of (5.45) and u_1 of (5.58), the vector u_{23}^d in (5.66) becomes

$$u_{23}^d = \begin{bmatrix} -\frac{3|x_{12}|^2}{x_1x_4^\star x_5^d}(Rx_1^\star - L_1x_2^dx_3) \\ L_g\omega\frac{x_5^d}{x_4^\star} \end{bmatrix}. \tag{5.72}$$

Motivated by (5.70) define the function

$$W_2(e_{46}) := \frac{1}{2} e_{46}^\top P e_{46},$$

whose derivative along the trajectories of (5.71) satisfies

$$\dot{W}_2 = -\frac{R_g}{2}|e_{56}|^2 + y_2^\top e_{23}^u.$$

This proves that (5.71) defines a passive map $e_{23}^u \mapsto y_2$, hence it can be controlled with a PI.

The proof is completed with the proper Lyapunov function candidate

$$V_2(e_{46}, \xi) = W_2(e_{46}) + \frac{1}{2}\xi^\top K_i \xi,$$

whose derivative yields

$$\begin{aligned} \dot{V}_2 &= -\frac{R_g}{2}|e_{56}|^2 + y_2^\top e_{23}^u + \xi^\top K_i y_2 \\ &= -\frac{R_g}{2}|e_{56}|^2 - y_2^\top K_p y_2, \end{aligned}$$

which establishes stability of the equilibrium. The proof of attractivity follows doing some standard signal chasing. □□□

Remark 5.8. The proof given above relies in a, far from elegant, perturbation argument. This argument is avoided in the proof of the main result in Section 5.2.7 where a basic lemma of cascades of asymptotically stable systems is invoked.

5.2.7 Main result

The proposition below shows that the combination of both controllers ensures the control objective is asymptotically achieved. The proof relies on the following lemma established in [84].

Lemma 5.5. Consider the following cascaded system

$$\begin{aligned} \dot{x} &= f(x, y, t) \\ \dot{y} &= g(y, t), \end{aligned}$$

with $|\frac{\partial f}{\partial x}|$ and $|\frac{\partial y}{\partial y}|$ bounded and

$$\begin{aligned} 0 &= f(x_\star, y_\star, t) \\ 0 &= g(y_\star, t). \end{aligned}$$

The following statements are *equivalent*.

(C1) $(x_\star, y_\star)$ is a uniformly asymptotically stable (UAS) equilibrium of the cascaded system.

(C2) $y_\star$ is a UAS equilibrium of $\dot{y} = g(y,t)$ and $x_\star$ is a UAS equilibrium of $\dot{x} = f(x, y_\star, t)$.

Proposition 5.4. Consider the system (5.34) and an equilibrium $x_\star \in \mathcal{E}$, verifying (5.35), in closed–loop with the dynamic state–feedback controller

Standard PBC:

$$\begin{aligned} L\dot{x}_2^d &= -L_1 x_3 x_1^\star - R x_2^d + \phi_1 x_3^d + \frac{x_2}{x_1}\left(R x_1^\star \right. \\ &\quad \left. - L_1 x_2^d x_3\right) && \text{(5.73a)} \\ J_1 \dot{x}_3^d &= -\phi_1 x_2^d + \Phi(x_3) - R_{3a}(x_3 - x_3^d) + z && \text{(5.73b)} \\ \dot{z} &= -K_{iw}(x_3 - x_3^d) && \text{(5.73c)} \\ u_1 &= -\frac{1}{M x_1 x_4}(R x_1^\star - L_1 x_2^d x_3) && \text{(5.73d)} \end{aligned}$$

PI PBC:

$$\begin{aligned} L_g \dot{x}_5^d &= -R_g x_5^d - V_d - \frac{3}{x_1 x_5^d}|x_{12}|^2 \left(R x_1^\star \right. \\ &\quad \left. - L_1 x_2^d x_3\right) && \text{(5.74a)} \\ \dot{\xi} &= \frac{1}{2}\begin{bmatrix} x_4^\star x_5 - x_5^d x_4 \\ x_4^\star x_6 \end{bmatrix} && \text{(5.74b)} \\ u_{23} &= \begin{bmatrix} -\frac{3|x_{12}|^2}{x_1 x_4^\star x_5^d}(R x_1^\star - L_1 x_2^d x_3) \\ L_g \omega \frac{x_5^d}{x_4^\star} \end{bmatrix} - K_p \begin{bmatrix} x_4^\star x_5 - x_5^d x_4 \\ x_4^\star x_6 \end{bmatrix} - K_i \xi \end{aligned}$$

with $x_5^d(0) > 0$, $R_{3a} > 0$, $K_p = K_p^\top > 0$, $K_i = K_i^\top > 0$. The equilibrium point of the closed–loop system

$$(x_\star, x_{23}^\star, 0, 0, x_5^\star) \in \mathbb{R}^{11}$$

is *asymptotically stable*.

Proof. From the derivations of Proposition 5.2 we identify the cascade of subsystems Σ_1 and Σ_2 given by

$$\begin{aligned}\Sigma_1 &: \dot{e}_{13} = A(t)e_{13}\\ \Sigma_2 &: \dot{x}^d_{23} = m_{12}(x^d_{23}) + \Delta_{12}(x^d_{23}, e_{13}),\end{aligned}$$

where

$$A(t) := -\mathcal{D}^{-1}[\mathcal{C}(x_3(t)) + \mathcal{R}_d],$$

and $m_{12}(x^d_{23}), \Delta_{12}(x^d_{23}, e_{13})$ are given in the proof. The cascade fits into the paradigm of Lemma 5.5, with Σ_1 UGAS (actually, exponentially) and Σ_2 AS, therefore the cascade is UAS—see Fig. 5.7.

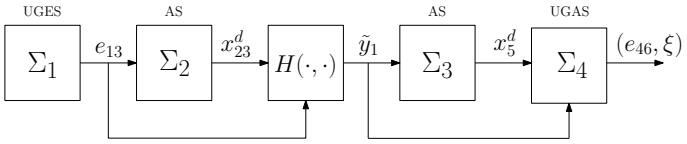

Figure 5.7: Block diagram of Proposition 5.4.

Now, from Proposition 5.2 we identify the cascade of a static map

$$\tilde{y}_1 = H(x^d_{23}, e_{13})$$

with the systems Σ_3 and Σ_4 given by

$$\begin{aligned}\Sigma_3 &: \dot{x}^d_5 = m_3(x^d_5) + \Delta_3(x^d_5, \tilde{y}_1)\\ \Sigma_4 &: \begin{bmatrix} \dot{e}_{46} \\ \dot{\xi} \end{bmatrix} = F(e_{46}, \xi x^d_5(t), \tilde{y}_1(t)).\end{aligned}$$

See (5.68) and (5.71). Σ_3 is AS and Σ_4 is UAS (actually, globally). Invoking Lemma 5.5 we conclude AS of the overall system. A block diagram of Proposition 5.4 is presented in Fig. 5.7. □□□

5.2.8 Control Implementation

In order to be implemented, the controller interconnection must have the structure depicted in Fig. 5.8. Of course, an implementation of the control implies the use of sensors that measure physical magnitudes as currents and angular velocities otherwise observers can also carry out this task. From this measurements the state variables of system (5.34) are derived.

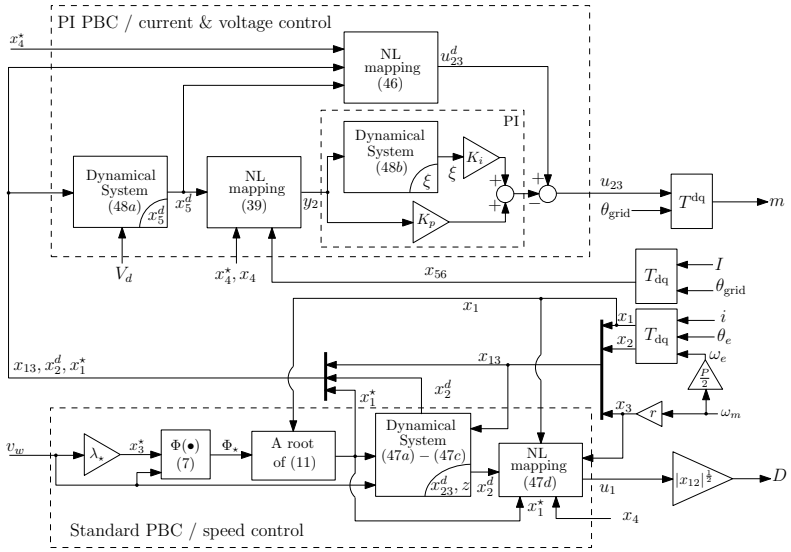

Figure 5.8: Implementation diagram of the passivity based controllers.

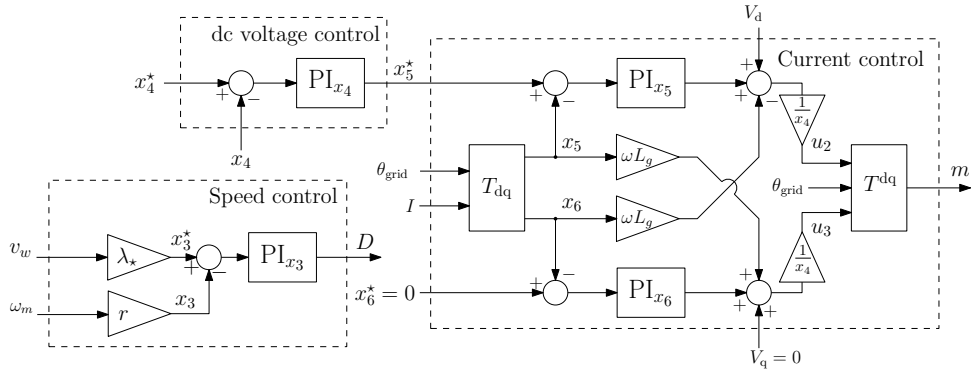

Figure 5.9: Block diagram of the PI–based benchmark control scheme. The matrices T_{dq}, T^{dq}, and the ac grid phase angle θ_{grid} represent a consistent transformation of variables in the single–phase time domain to the synchronous $d-q$ reference frame [12, 37].

As shown, the figure is mainly composed of two blocks representing the speed control (performed by the SPBC) and the current/speed control (performed by the PI PBC). The "dynamical system" blocks describes the dynamics of the variables written on the right corner in the bottom. The script "NL" means that the block represents a non-linear mapping of the input arguments. Notice that the PI PBC block is composed of two non-linear mappings, namely, the passive output y_2 in (5.65) and the term u_{23}^d showed in (5.72), a dynamical system which generates x_5^d (required by y_2) and the block containing the sum of the proportional and integral part (PI) of y_2. Therefore, this block output stands for equation (5.74c).

On the other hand, the standard PBC controller block is the dynamical system of equation (5.73) with an output u_1. This controller requires the value of $x_1^\star$. To compute it, it is necessary to solve the two degree equation (5.37) which depends on the value $\Phi_\star$, the evaluation of (5.33) in $x_3^\star$.

5.2.9 Benchmark system

The performance of the controller introduced in this section is compared against an industry standard PI control–based architecture [88]. The block diagram of the control scheme utilized as a benchmark is illustrated in Fig. 5.9.

Parameters of the system (5.34)

As is customary, the power coefficient is assumed to be given by the function

$$C_p(\lambda) = e^{-\frac{c_{p1}}{\lambda}}\left(\frac{c_{p2}}{\lambda} - c_{p3}\right) + c_{p4}\lambda, \tag{5.75}$$

where the coefficients $c_{pi}, i = 1, \ldots, 4$—that are windmill–specific, but independent of v_w and ω_m—are known. These coefficients were taken from [48, 87], and have the following values: $c_{p1} = 21.0000$, $c_{p2} = 125.229$, $c_{p3} = 9.7803$, and $c_{p4} = 0.0068$. This yields $\lambda_\star = 8.1$ and $C_p^\star = 0.48$. Parameters for the windmill system were taken from [80], and adapted to fit the physical constraints of the dc–dc converter. Table 5.2 shows the various numerical values. In order to use a boost dc–dc converter, a larger dc link voltage of $v_{dc}^\star = 400$ (V), is considered—this can be implemented with just a diode and a MOSFET as suggested in Fig. 5.5 [82]. The stiffness constraints required by the converter [50] are naturally given by the inductor of the PMSG on the pole side of the converter, and by the dc link capacitor in the throw side.

Controllers

As stated, the performance of two different schemes of control are compared. For simplicity, we will refer as *PBC controllers* for the controllers whose methodology is proposed in the current section. The structure of this scheme has been defined in the previous sections. On the other hand, the PI–based benchmark control scheme of Fig. 5.9 will be labelled as *PI controllers*. The various gains of both controllers were tuned using the well–known pole placement method. Numerical values are given below.

PBC controller gains

$$R_{3a} = 0.8;\ K_{iw} = 0.5;$$
$$K_p = \begin{bmatrix} 0.007 & 0 \\ 0 & 0.009 \end{bmatrix};\ K_i = \begin{bmatrix} 1 & 0 \\ 0 & 0.90 \end{bmatrix}.$$

Table 5.2: Grid–connected windmill system parameters

Item	Value
Turbine	
Inertia	$J = 7.856$ (kg m^2)
Blades radius	$r = 1.84$ (m)
PMSG	
Nominal Power	$S_n = 5$ (kVA)
Poles	$P = 28$
Synchronous resistance	$R = 0.3676$ (Ω)
Synchronous reactance	$L = 3.55$ (mH)
Flux	$\phi = 0.2867$ (Wb)
H–bridge inverter	
dc link voltage	$v_{dc}^{\star} = 400$ (V)
dc link capacitance	C =800 (μF)
L–filter	$L_g = 5$ (mH)
R–filter	$R_g = 0.1$ (Ω)
Single–phase ac grid	
Nominal voltage	$V_g = 240$ (V)
Frequency	$F_g = 60$ (Hz)

PI controllers gains

$$K_{p\_x3} = 0.00967472; \;\; K_{i\_x3} = 0.10516;$$

$$K_{p\_x4} = -4; \qquad K_{i\_x4} = -5;$$

$$K_{p\_x5} = 0.05; \quad K_{i\_x5} = 0.8;$$

$$K_{p\_x6} = 0.05; \quad K_{i\_x6} = 0.8.$$

Wind speed profile

The wind speed profile illustrated in Fig. 5.10 is utilized for the simulation studies. It was constructed using *real* measurements collected by the National Wind Technology Center in Boulder, Colorado, USA. The wind speed was measured at 100Hz at 36.6m above the ground using a cup anemometer. As may be observed in the figure, the profile is rich in turbulence and exhibits gusty behavior at times.

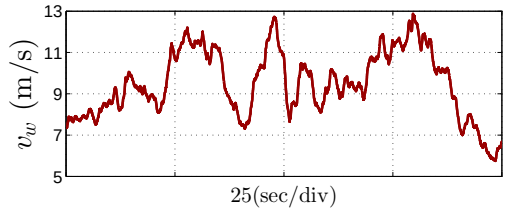

Figure 5.10: Real wind speed profile utilized in the simulation studies.

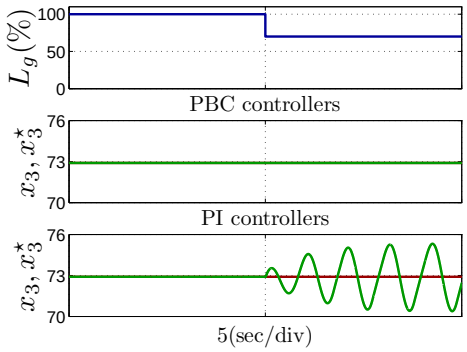

Figure 5.11: Robustness test. — $x_3^\star$ — x_3. A 30% step–like change in L_g is applied. We show the response of x_3. It may be observed that under the PBC controllers, x_3 is able to follow $x_3^\star$ indifferent to the variation of L_g. On the other hand, the PI controllers are unable to perform the tracking function, rendering the system unstable.

5.2.10 Computer simulations

In this section, the performance of both the PBC (defined by (5.73)-(5.74)) and PI (Fig. 5.9) controllers are tested via computer simulations considering a detailed model for the system of Fig. 5.5, with parameters specified in Section 5.2.9. All simulations are executed using the Matlab–Simulink® mathematical analysis software package.

Recalling (5.35), the theoretical considerations for PBC design were developed assuming $x_3^\star = \lambda_\star v_w$, that is, the reference for the optimal shaft rotational speed shall be computed using the actual wind speed. However, in a real setting the wind speed will likely be filtered before being utilized to track x_3. This is performed in order to provide smooth power to the turbine shaft. Alternatively, if the wind speed is unavailable for measurement —which will very likely be the case for a small–scale wind turbine— one could estimate its value and utilized it for tracking purposes. Several estimation algorithms featuring an acceptable performance have been proposed in the literature [76]. In the simulation study we consider all three cases. We study the system's response utilizing to generate $x_3^\star$ the actual wind speed ($x_3^\star = \lambda_\star v_w$), a filtered wind speed ($x_3^\star = \lambda_\star v_w^f$) and an estimated wind speed ($x_3^\star = \lambda_\star \hat{v}_w$). The filtered wind speed is computed utilizing a simple low–pass filter,

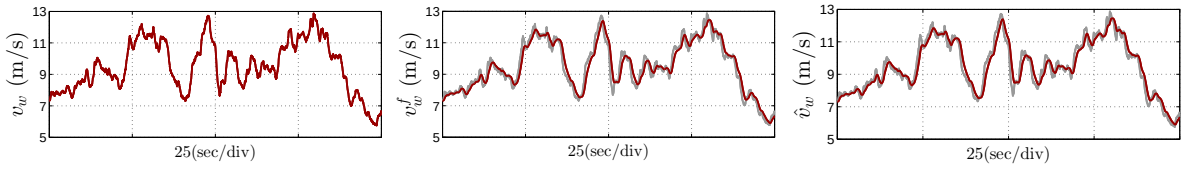

(a) Actual wind speed. (b) Filt. wind speed — v_w^f — v_w. (c) Estim. wind speed — $\hat{v}_w$ — v_w.

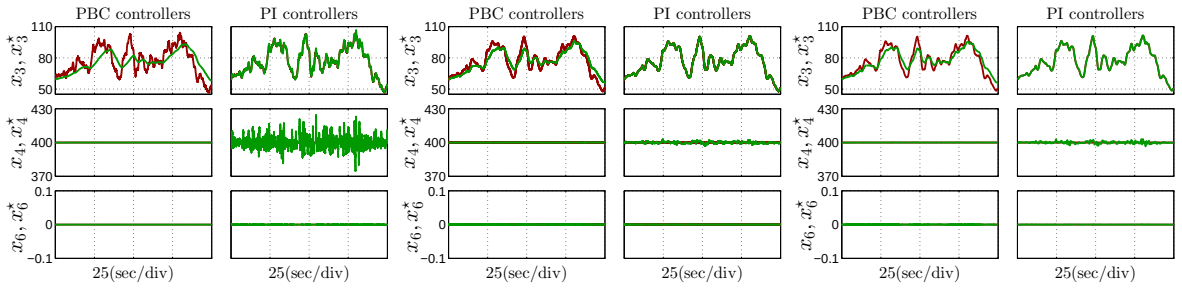

(d) Tracking states — x_3 — $x_3^\star$. (e) Tracking states — x_3 — $x_3^\star$. (f) Tracking states — x_3 — $x_3^\star$.

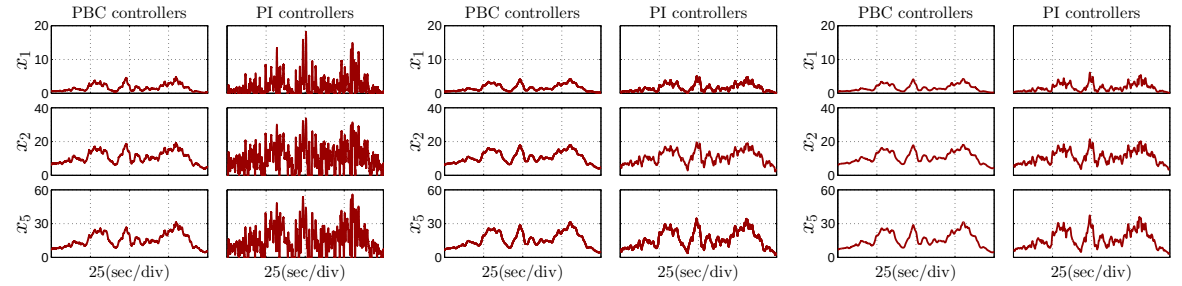

(g) Remaining states. (h) Remaining states. (i) Remaining states.

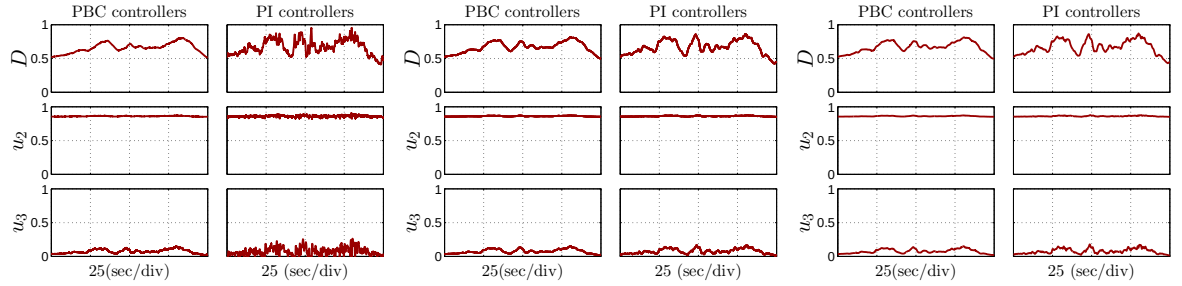

(j) Control signals. (k) Control signals. (l) Control signals.

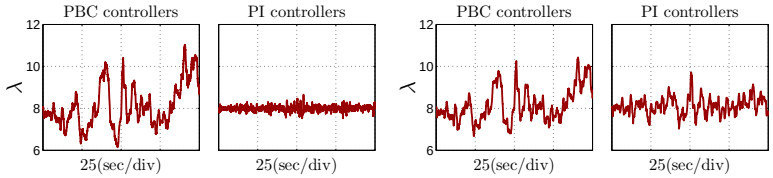

(m) Tip–speed ratio ($\lambda_\star = 8.1$). (n) Tip–speed ratio ($\lambda_\star = 8.1$).

Figure 5.12: Simulation results. The left, middle and right columns presents the comparative evaluation utilizing the actual, filtered and estimated wind speed, respectively. Recall $x := \text{col}(i_d, i_q, r\omega_m, v_{dc}, I_d, I_q)$, hence the units for the various plots are: x_1 (A), x_2 (A), x_3 (m/s), x_4 (V), x_5 (A), x_6 (A). Control signals are unitless and because of their physical interpretation they must be contained within 0 and 1.

$$v_w^f(s) = \frac{1}{1+\tau s} v_w(s),$$

with $\tau = 0.7$s. The estimation of the wind speed is performed through the Immersion & Invariance (I&I) estimator proposed in [59],

$$\dot{\hat{v}}_w = \frac{\gamma}{J_1}[\phi_1 x_2 - \Phi(x_3, \hat{v}_w + \gamma x_3)],$$

where $\gamma = 0.2$ is an adaptation gain.

Fig. 8 shows the results. The left, middle and right columns presents the comparative evaluation utilizing the actual, filtered and estimated wind speed, respectively. PBC controllers rely on a copy of the system's zero dynamics to generate references. Because of this, when using the actual wind speed the PBC controller is unable to accurately track $x_3^\star$. As a result, the efficiency of the power extraction process is sacrificed as observed in the tip–speed ratio plot. On the other hand, PI controllers are able to quickly respond and properly perform the tracking function. This comes at a cost of introducing large noise levels on the states and control signals. However, when using a filtered or estimated wind speed signals to feed the control schemes, the PBC controller approximately matches the tracking performance of the PI controllers. Both controllers track the tip–speed ratio to a similar degree of accuracy, and the compromise between speed and noise still exists. It is worth mentioning that the system's response was very sensitive to the gain's tuning for the PI controller, while the PBC controller exhibited an acceptable performance throughout a large range of gains' selection. Furthermore, the robustness of both controllers was tested by introducing a 30% disturbance in the value of the filter/grid inductance. Results are presented in Fig. 5.11. It may be observed that, unlike the PI controller, the PBC controller is able to remain stable.

Chapter 6

Conclusions & Future Work

The following concluding remarks are in order.

In Chapter 2, the trajectory tracking problem for power converters based on passivity foundations has been solved. The resulting controller is a simple PI and the stability results are global and hold for all positive definite gains of the PI. In fact, this outcome extends previous results obtained for the regulation case.

In Chapter 3, we identify a class of nonlinear systems for which it is possible to design robust PI controllers with guaranteed stability properties. The class consists of input affine systems with known, constant input matrix G and $n - m$ zero rows. We assume that only the states associated to the non–zero rows of G are measurable.The systems have an open–loop stable equilibrium, but is different from the desired operating point. To handle this situation, we follow [35] and generate new passive outputs for the incremental model, hence the name PI–PBC. Associated to the open–loop stable equilibrium a Lyapunov function of the form (3.4) is assumed to exist. We underscore that, besides convexity, there is no assumption on the function $H_u(x_u)$, which is unknown. Moreover, the controller does not require the measurement of x_u. The functions $\phi_i(x_i)$ are assumed convex and known, but the coefficient d_i are unknown. Under these conditions, we show that, for a well identified class of PI tuning gains, global stability of the proposed PI–PBC is guaranteed. Conditions that ensure global asymptotic stability, are also derived.

In Chapter 4, we have presented a new energy shaping method to stabilize pH systems that, in contrast with the classical PBC methods, does not require the solution of PDEs. The key modification introduced here is to abandon the objective of preservation in closed–loop of the pH structure, which is the condition that gives rise to the PDEs.

The class of systems for which the method is applicable is identified by Assumptions 4.1 and 4.2, which can be easily verified from the systems data. The invertibility

Assumption 4.1 is rather weak, and is satisfied in many practical examples. Notice that if it does not hold then there exists equilibria for the open–loop system, which are not *extrema* of the energy function—a situation that its not expected to happen in physical systems. The integrability Assumption 2 is a technical condition needed to create the term added to the open–loop energy function (4.9). As indicated at the end of Section 5.2.1, this term may be interpreted as an integral term on the power shaping output. Unfortunately, besides this nice interpretation, we don't have at this point any physical, nor practical motivation, for Assumption 4.2. The controller design parameters are introduced to ensure that $H_d(x)$ is positive definite, hence, it qualifies as a Lyapunov function.

Finally, in Chapter 5, we present two different wind energy systems to which we control by means of PBC controllers. In Section 5.1 we present a maximum power extraction PI-PBC control for a wind energy system consisting of a turbine, a permanent magnet synchronous generator, a rectifier, a load and one constant voltage source, which is used to form the DC bus. Invoking practically considerations we proved stability. In Section 5.2 an asymptotically convergent PBC for a basic windmill system connected to the grid which ensures maximum power extraction and regulation of the dc link voltage and injection of reactive power has been proposed.

In order to design the controller, the overall systems has been divided in two coupled subsystems: the windmill with the PMSG and the power converters with the grid. For the first subsystem a SPBC, similar to that of [46], was realized. The second subsystem was controlled by means of a tracking PI-PBC controller presented in Chapter 2. Endowing the PI controller with tracking capabilities allows for a faster response with respect to the standard regulation PI of [32].

These results have motivated the following future work.

- From Chapter 4, a future research is intended to construct not only PIs but also PIDs controllers based on other passive outputs besides $y_{\mathtt{ps}}$. It was recently revealed in [53,83] that there exists a large class of passive outputs that can be used for this purpose.

- To develop an unifying theoretical framework for the PIDs based on passivity.

- Proposed alternative PBC methods to address the wind energy systems than those introduced in Chapter 5 and make a comparative study between them.

- Also, a future work could include a comparative performance between our control approach and the standard one implemented by the power engineering com-

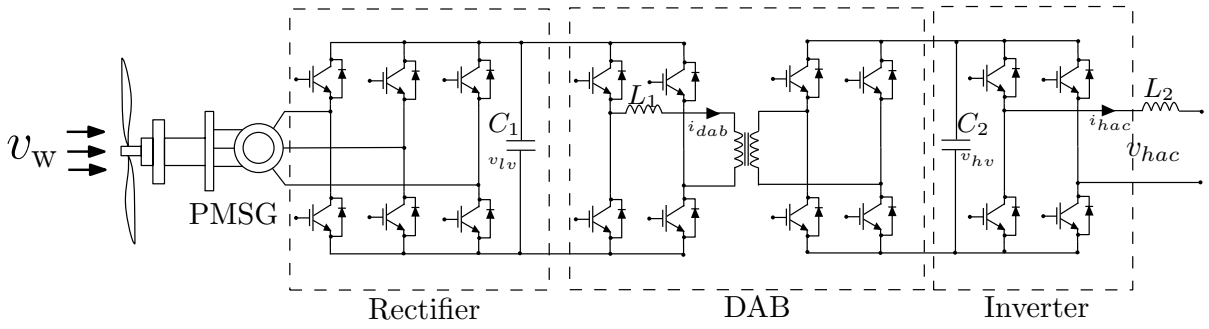

Figure 6.1: A scheme of the complete wind generation system

munity [17].

- To validate the proposed controller through experimentation. Particularly, that of Section 5.1 is part of the research carried out within the framework of the FREEDM System Center whose main objective is the implementation and testing of a solid–state transformer enabled microgrid. A complete picture of the system model is depicted in Fig. 6.1. As shown in the figure, the configuration consists of a surface-mounted PMSG, the SST and a load [28]. The SST is constituted by three stages: an AC-DC rectifier, a Dual Active Bridge (DAB) converter with a high frequency transformer and a DC-AC inverter. Besides, unlike the classical topologies using a diode bridge rectifier with a DC-DC converter [46, 80], one of the advantages in the SST topology is due to its larger number of control inputs. Indeed, it offers more degrees of freedom when designing a controller. It can be noticed from the figure that there are control inputs at each stage. Other advantage is that the DAB topology allows seamless control for bidirection power flow. Real power flows from the bridge with leading phase angle to the bridge with lagging phase angle.

Bibliography

[1] T. Ahmed, K. Nishida, and M. Nakaoka. MPPT control algorithm for grid integration of variable speed wind energy conversion system. In *Industrial Electronics, 2009. IECON '09. 35th Annual Conference of IEEE*, pages 645–650, 2009.

[2] A. Akagi. *Instantaneous Power Theory and Applications to Power Conditioning*. Wiley, 2007.

[3] K. H. Ang, G. Chong, and Y. Li. PID control system analysis, design, and technology. *IEEE Transactions on Control Systems Technology*, 13(4):559–576, July 2005.

[4] R. Antonelli and A. Astolfi. Continuous stirred tank reactors: Easy to stabilise? *Automatica*, 39(10):1817 – 1827, 2003.

[5] A. Astolfi and R. Ortega. Dynamic extension is unnecessary for stabilization via interconnection and damping assignment passivity-based control. *Systems & Control Letters*, 58(2):133 – 135, 2009.

[6] K. J. Astrom and T. Hagglund. *PID Controllers*. ISA: The Instrumentation, Systems, and Automation Society, 1995.

[7] K. J. Astrom and T. Hagglund. The future of PID control. *Control Engineering Practice*, 9(11):1163 – 1175, 2001.

[8] G. P. Barker, A. Berman, and R. J. Plemmons. Positive diagonal solutions to the Lyapunov equations. *Linear and Multilinear Algebra*, 5(4):249–256, 1978.

[9] S. Bennett. Development of the pid controller. *IEEE Control Systems*, 13(6):58–62, Dec 1993.

[10] S. Bennett. A brief history of automatic control. *IEEE Control Systems*, 16(3):17–25, Jun 1996.

[11] F. Blaabjerg and K. Ma. Future on power electronics for wind turbine systems. *Emerging and Selected Topics in Power Electronics, IEEE Journal of*, 1(3):139–152, Sept 2013.

[12] F. Blaabjerg, R. Teodorescu, M. Liserre, and A. V. Timbus. Overview of control and grid synchronization for distributed power generation systems. *IEEE Transactions on Industrial Electronics*, 53(5):1398–1409, October 2006.

[13] G. Blankenstein, R. Ortega, and A. van der Schaft. The matching conditions of controlled Lagrangians and IDA-Passivity based control. *International Journal of Control*, 75(9):645–665, 2002.

[14] B. Borovic, C. Hong, A. Q. Liu, L. Xie, and F.L. Lewis. Control of a MEMS optical switch. In *Decision and Control, 2004. CDC. 43rd IEEE Conference on*, volume 3, pages 3039–3044, Dec 2004.

[15] V. Calderaro, V. Galdi, A. Piccolo, and P. Siano. A fuzzy controller for maximum energy extraction from variable speed wind power generation systems. *Electric Power Systems Research*, 78(6):1109 – 1118, 2008.

[16] F. Castaños, B. Jayawardhana, R. Ortega, and E. García-Canseco. Proportional plus integral control for set–point regulation of a class of nonlinear RLC circuits. *Circuits, Systems and Signal Processing*, 28(4):609–623, 2009.

[17] M. Chinchilla, S. Arnaltes, and J. C. Burgos. Control of permanent-magnet generators applied to variable-speed wind-energy systems connected to the grid. *IEEE Transactions on Energy Conversion*, 21(1):130–135, 2006.

[18] G. Chun, P. Ganeshkumar, A. Ahmed, and J. Park. Design of MPPT controller for small scale wind power system with PMSG. In *Electrical Machines and Systems (ICEMS), 2012 15th International Conference on*, pages 1–4, 2012.

[19] CIGRE. Technical brochure, modeling and dynamic behavior of wind generation as it relates to power system control and dynamic performance. Working Group 601 of Study Committee C4, Final Report, January 2007.

[20] R. Cisneros, F. Mancilla-David, and R. Ortega. Passivity-based control of a grid-connected small-scale windmill with limited control authority. *Emerging and Selected Topics in Power Electronics, IEEE Journal of*, 1(4):247– 259, Dec 2013.

[21] R. Cisneros, M. Pirro, G. Bergna, R. Ortega, G. Ippoliti, and M. Molinas. Global tracking passivity-based PI control of bilinear systems: Application to the interleaved boost and modular multilevel converters. *Control Engineering Practice*, 43:109 – 119, 2015.

[22] A. Donaire and S. Junco. On the addition of integral action to port–controlled Hamiltonian systems. *Automatica*, 45(8):1910 – 1916, 2009.

[23] A. Donaire, R. Mehra, R. Ortega, S. Satpute, J. G. Romero, F. Kazi, and N. M. Singh. Shaping the energy of mechanical systems without solving partial differential Equations. *Automatic Control, IEEE Transactions on*, To appear.

[24] V. Duindam, A. Macchelli, S. Stramigioli, and H. Bruyninckx. *Modeling and Control of Complex Physical Systems: The Port-Hamiltonian Approach*. Springer Science & Business Media, 2009.

[25] J. L. Ebert, D. De Roover, L.L. Porter, V. A Lisiewicz, S. Ghosal, R.L. Kosut, and A Emami-Naeini. Model–based control of rapid thermal processing for semiconductor wafers. In *American Control Conference, 2004. Proceedings of the 2004*, volume 5, pages 3910–3921, June 2004.

[26] L. Farina and S. Rinaldi. *Positive Linear Systems: Theory and Applications*. John Wiley & Sons, Inc, 2000.

[27] E. Fossas, J. M. Olm, and H. Sira-Ramírez. Iterative approximation of limit cycles for a class of abel equations. *Physica D: Nonlinear Phenomena*, 237(23):3159–3164, 2008.

[28] R. Gao, I. Husain, F. Wang, and A.Q. Huang. Solid-State Transformer Interfaced PMSG Wind Energy Conversion System. In *Applied Power Electronics Conference and Exposition (APEC), 2015 IEEE*, pages 1310–1317, March 2015.

[29] E. García-Canseco, R. Ortega, J. M. A. Scherpen, and D. Jeltsema. *Lagrangian and Hamiltonian Methods for Nonlinear Control 2006: Proceedings from the 3rd IFAC Workshop, Nagoya, Japan, July 2006*, chapter Power Shaping Control of Nonlinear Systems: A Benchmark Example. 2007.

[30] A. Ghaffari, M. Krstic, and S. Seshagiri. Power optimization and control in wind energy conversion systems using extremum seeking. In *American Control Conference (ACC), 2013*, pages 2241–2246, 2013.

[31] S. Heier. *Grid Integration of Wind Energy*. Wiley, 2014.

[32] M. Hernandez–Gomez, R. Ortega, F. Lamnabhi–Lagarrigue, and G. Escobar. Adaptive PI stabilization of switched power converters. *IEEE Transactions on Control Systems Technology*, 18(3):688–698, 2010.

[33] D. P. Hohm and M. E. Ropp. Comparative study of maximum power point tracking algorithms. *Progress in Photovoltaics: Research and Applications*, 11(1):47–62, 2003.

[34] A. Isidori, S. M. Joshi, and A. G. Kelkar. Asymptotic stability of interconnected passive non-linear systems. *International Journal of Robust and Nonlinear Control*, 9(5):261–273, 1999.

[35] B. Jayawardhana, R. Ortega, E. García-Canseco, and F. Castanos. Passivity of nonlinear incremental systems: Application to PI stabilization of nonlinear RLC circuits. *Systems & Control Letters*, 56(9—10):618–622, 2007.

[36] K. Johnson, L. Pao, M. Balas, and L. Fingersh. Control of variable speed wind turbines. *IEEE Control Systems Magazine*, 26(3):70–81, June 2006.

[37] M. Karimi–Ghartemani. A unifying approach to single–phase synchronous reference frame PLLs. *IEEE Transactions on Power Electronics*, 28(10):4550–4556, 2013.

[38] E. Kaszkurewicz and A. Bhaya. *Matrix diagonal stability in systems and computation*. Birkhauser, 1991.

[39] H. K. Khalil. *Nonlinear Systems*. Prentice Hall, 2002.

[40] M. Komatsu, H. Miyamoto, H. Ohmori, and A. Sano. Output maximization control of wind turbine based on extremum control strategy. In *American Control Conference, 2001. Proceedings of the 2001*, volume 2, pages 1739–1740 vol.2, 2001.

[41] I. Kortabarria, J. Andreu, I. M. de Alegría, E. Ibarra, and E. Robles. Maximum power extraction algorithm for a small wind turbine. In *Power Electronics and Motion Control Conference (EPE/PEMC), 2010 14th International*, pages T12–49–T12–54, 2010.

[42] P. C. Krause. *Analysis of Electric Machinery*. McGraw Hill, New York, 1986.

[43] P. Lancaster and M. Tismenetsky. *The theory of matrices*. Academic Press, 1985.

[44] S. Li, A. H. Timothy, and L. Xu. Conventional and novel control designs for direct driven PMSG wind turbines. *Electric Power Systems Research*, 80(3):328–338, 2010.

[45] Y. Li, K. H. Ang, and G. Chong. PID control system analysis and design. *IEEE Control Systems*, 26(1):32–41, Feb 2006.

[46] F. Mancilla–David and R. Ortega. Adaptive passivity–based control for maximum power extraction of stand–alone windmill systems. *Control Engineering Practice*, 20(2):173–181, 2012.

[47] G. E. Marmidis and A. T. Alexandridis. A passivity-based PI control design for DC-drives. In *Control and Automation, 2009. MED '09. 17th Mediterranean Conference on*, pages 1511–1516, June 2009.

[48] MathWorks. Simpowersystems blockset user's guide. Hydro–Québec and The MathWorks, Inc. [Online]. Available: http://www.mathworks.com, 2011.

[49] J. L. Meza and V. Santibañez. Analysis via passivity theory of a class of nonlinear PID global regulators for robot manipulators. In *IASTED international conference on robotics and applications*, October 1999.

[50] N. Mohan, T. Undeland, and W. Robbins. *Power Electronics: Converters, Applications, and Design*. John Wiley & Sons, Inc., New Jersey, 2003.

[51] R. Mohler. *Encyclopedia of Physical Science and Technology*. Academic Press, New York, third edition edition, 2003.

[52] Josep M. Olm, Xavier Ros-Oton, and Yuri B. Shtessel. Stable inversion of abel equations: Application to tracking control in DC-–DC nonminimum phase boost converters. *Automatica*, 47(1):221–226, 2011.

[53] R. Ortega and P. Borja. New results on control by interconnection and energy-balancing passivity-based control of port-Hamiltonian systems. In *Decision and Control (CDC), 2014 IEEE 53rd Annual Conference on*, pages 2346–2351, Dec 2014.

[54] R. Ortega and E. García-Canseco. Interconnection and damping assignment passivity-based control: A survey. *European Journal of Control*, 10(5):432 – 450, 2004.

[55] R. Ortega, D. Jeltsema, and J. M. A. Scherpen. Power shaping: A new paradigm for stabilization of nonlinear RLC circuits. *Automatic Control, IEEE Transactions on*, 48(10):1762–1767, Oct 2003.

[56] R. Ortega and R. Kelly. PID self-tuners: Some theoretical and practical aspects. *Industrial Electronics, IEEE Transactions on*, IE-31(4):332–338, Nov 1984.

[57] R. Ortega, Z. Liu, and H. Su. Control via interconnection and damping assignment of linear time-invariant systems: A tutorial. *International Journal of Control*, 85(5):603–611, 2012.

[58] R. Ortega, A. Loria, P. Nicklasson, and H. Sira-Ramírez. *Passivity-based control of Euler-Lagrange systems: Mechanical, electrical and electromechanical applications*. Communications and Control Engineering. Springer Verlag, London, 1998.

[59] R. Ortega, F. Mancilla-David, and F. Jaramillo. A globally convergent wind speed estimator for wind turbine systems. *International Journal of Adaptive Control and Signal Processing*, 27(5):413–425, May 2013.

[60] R. Ortega and J. G. Romero. Robust integral control of port–Hamiltonian systems: The case of non-passive outputs with unmatched disturbances. *Systems & Control Letters*, 61(1):11 – 17, 2012.

[61] R. Ortega and M. Spong. Adaptive motion control of rigid robots: A tutorial. *Automatica*, 25(6):877–888, November 1989.

[62] R. Ortega, A. van der Schaft, F. Castaños, and A. Astolfi. Control by interconnection and standard passivity-based control of port-Hamiltonian systems. *Automatic Control, IEEE Transactions on*, 53(11):2527–2542, 2008.

[63] R. Ortega, A.J. van der Schaft, I. Mareels, and B. Maschke. Putting energy back in control. *Control Systems Magazine, IEEE*, 21(2):18–33, Apr 2001.

[64] A. Pavlov, A. Pogromsky, N. van de Wouw, and H. Nijmeijer. Convergent dynamics, a tribute to Boris Pavlovich Demidovich. *Systems & Control Letters*, 52(3–4):257 – 261, 2004.

[65] M. Perez, R. Ortega, and J. R. Espinoza. Passivity-based PI control of switched power converters. *IEEE Transactions on Control Systems Technology*, 12(6):881–890, Nov 2004.

[66] S. Prajna, A. van der Schaft, and G. Meinsma. An LMI approach to stabilization of linear port-Controlled Hamiltonian systems. *Systems & Control Letters*, 45(5):371 – 385, 2002.

[67] REN21. 2015 renewable global status report. Available on: http://www.ren21.net/.

[68] J. G. Romero, A. Donaire, and R. Ortega. Robust energy shaping control of mechanical systems. *Systems & Control Letters*, 62(9):770 – 780, 2013.

[69] S. R. Sanders and George C. Verghese. Lyapunov-based control for switched power converters. *Power Electronics, IEEE Transactions on*, 7(1):17–24, 1992.

[70] S. Sastry and M. Bodson. *Adaptive Control: Stability, convergence, and robustness*. Prentice Hall, 1994.

[71] C. Schaper, Y. Cho, P. Gyugyi, G. Hoffmann, S. Norman, P. Park, S. Boyd, G. Franklin, T. Kailath, and K. Saraswat. Dynamics and control of a rapid thermal multiprocessor. In *Proceedings SPIE Conference on Rapid Thermal and Integrated Processing*, pages 2–17, 1992.

[72] C. D. Schaper, Y. M. Cho, and T. Kailath. Low-order modeling and dynamic characterization of rapid thermal processing. *Applied Physics A*, 54(4), 1992.

[73] R. Sepulchre, M. Jankovic, and P. Kokotovic. *Constructive Nonlinear Control*. Springer London Ltd, 2011.

[74] R. Shorten, O. Mason, and C. King. An alternative proof of the Barker, Berman, Plemmons (BBP) result on diagonal stability and extensions. *Linear Algebra and its Applications*, 430(1):34– 40, 2009.

[75] H. Sira-Ramírez and R. Silva-Ortigoza. *Control Design Techniques in Power Electronics Devices*. Power systems. Springer, 2006.

[76] M. N. Soltani, T. Knudsen, M. Svenstrup, R. Wisniewski, P. Brath, R. Ortega, and K. Johnson. Estimation of rotor effective wind speed: A comparison. *IEEE Transactions on Control Systems Technology*, PP(99):1–1, 2013.

[77] M. Takegaki and S. Arimoto. A new feedback method for dynamic control of manipulators. *ASME. J. Dyn. Sys., Meas., Control.*, 103(2):119–125, June 1981.

[78] R. J. Talj, R. Ortega, and M. Hilairet. A controller tuning methodology for the air supply system of a PEM fuel-cell system with guaranteed stability properties. *International Journal of Control*, 61:1706–1719, 2009.

[79] G. Tao. A simple alternative to the barbalat lemma. *Automatic Control, IEEE Transactions on*, 42(5):698, May 1997.

[80] F. Valenciaga, P. F. Puleston, and P. E. Battaiotto. Power control of a solar/wind generation system without wind measurement: A passivity/sliding mode approach. *IEEE Transactions on Energy Conversion*, 18(4):501–507, 2003.

[81] A. van der Schaft. *L_2-Gain and Passivity Techniques in Nonlinear Control*. Springer-Verlag New York, Inc., 1996.

[82] G. Venkataramanan, B. Milkovska, V. Gerez, and H. Nehrir. Variable speed operation of permanent magnet alternator wind turbines using a single switch power converter. *ASME Journal of Solar Energy Engineering, Special Issue on Wind Energy*, 118(4):235–238, 1996.

[83] A. Venkatraman and A. van der Schaft. Energy shaping of port-Hamiltonian systems by using alternate passive input-output pairs. *European Journal of Control*, 16(6):665 – 677, 2010.

[84] M. Vidyasagar. Decomposition techniques for large–scale systems with non–additive interactions: Stability and stabilizability. *IEEE Transactions on Automatic Control*, 25(4):773–779, April 1980.

[85] M. Vidyasagar and C. A. Desoer. *Feedback Systems: Input-Output Properties*. Academic Press, 1975.

[86] R. J. Wai and C. Y. Lin. Implementation of novel maximum-power- extraction algorithm for PMSG wind generation system without mechanical sensors. In *Robotics, Automation and Mechatronics, 2006 IEEE Conference on*, pages 1–6, 2006.

[87] Y. Xia, K. H. Ahmed, and B. W. Williams. Wind turbine power coefficient analysis of a new maximum power point tracking technique. *IEEE Transactions on Industrial Electronics*, 60(3):1122–1132, March 2013.

[88] A. Yazdani and R. Iravani. *Voltage–Sourced Converters in Power Systems*. Wiley–IEEE Press, Massachusetts, 2010.

[89] Q. Zeng, L. Chang, and R. Shao. Fuzzy-logic-based maximum power point tracking strategy for PMSG variable-speed wind turbine generation systems. In *Electrical and Computer Engineering, 2008. CCECE 2008. Canadian Conference on*, pages 405–410, 2008.

[90] D. Zonetti, R. Ortega, and A. Benchaib. Modeling and Control of HVDC Transmission Systems from Theory to Practice and Back. *Control Engineering Practice*, 45:133 – 146, 2015.

[91] Y. Zou, M.E. Elbuluk, and Y. Sozer. Stability analysis of maximum power point tracking (mppt) method in wind power systems. *Industry Applications, IEEE Transactions on*, 49(3):1129–1136, 2013.

université PARIS-SACLAY
ÉCOLE DOCTORALE
Sciences et technologies de l'information et de la communication (STIC)

Titre : Commande PI basée sur la Passivité : Application aux Systèmes Physiques.

Mots clés : Commande PI basée sur la Passivité, PI-PBC pour systèmes physiques, Commande d'éoliens, Commande de convertisseurs, PI-PBC pour le problème de suivi.

Résumé : Le régulateur PID (Proportionnel-Intégral-Dérivée) est la commande par retour d'état la plus connue. Elle permet d'aborder un bon nombre de problèmes de commande, particulièrement pour des systèmes faiblement non linéaire et dont la performance requise est relativement modeste. En plus, en raison de sa simplicité, la commande PID est largement utilisée dans l'industrie. Étant donné que les méthodes de réglage de la commande PID sont basées sur la linéarisation du système, la synthèse d'un contrôleur autour d'un point d'équilibre est relativement simple, néanmoins, la performance sera faible dans des modes de fonctionnement loin du point d'équilibre. Pour surmonter ce désavantage, une pratique courante consiste à adapter les gains du PID, procédure connue comme Séquencement de gain (ou Gain-scheduling en anglais). Il y a plusieurs désavantages à cette procédure, comme la commutation des gains de la commande et la définition - non triviale - des régions de l'espace d'état dans lesquelles cette commutation aura lieu. Ces deux problèmes se compliquent quand la dynamique est fortement non linéaire.
Dans ce contexte, ce travail de thèse a pour objectif de synthétiser des commandes PI, basés sur la passivité, de telle sorte que la stabilité globale du système non-linéaire en boucle fermé soit garantie. L'un des avantages à utiliser la passivité est son caractère intuitif, qui exploite les propriétés physiques des systèmes en introduisant le concept d'énergie dans la synthèse de la loi de commande. La méthodologie de commande PI présentée dans ce travail est constructive et motivée par des applications aux systèmes physiques.

Title : PI Passivity-Based Control : Application to Physical Systems.

Keywords : PI-PBC for physical systems, Passivity-based Control, Control for power converters, Control of windmill, Tracking PI-PBC.

Abstract : One of the best known forms of feeding back a system is through a three-term control law called PID (Proportional-Integral-Derivative) controller. PID controllers are sufficient for many control problems, particularly when process dynamics are not highly nonlinear and the performance requirements are modest. Besides, because of its simple structure, the PID controller is the most adopted control scheme by industry and practitioners, being the PI the form mostly employed. Since the PI tuning methods are based on the linearization, commissioning a PI to operate around a single operating point is relatively easy, however, the performance will be below par in wide operating regimes. To overcome this drawback the current practice is to re-tune the gains of the PI controllers based on a linear model of the plant evaluated at various operating points, a procedure known as Gain-scheduling. There are several disadvantages of gain-scheduling including the need to switch (or interpolate) the controller gains and the non-trivial definition of the regions in the plants state space where the switching takes place - both problems are exacerbated if the dynamics of the plant is highly nonlinear. In this context, the current thesis work is aimed at the designing of PI controllers, based on the passivity theory, such that the stability of the closed-loop non-linear system is guaranteed.
The methodology for deriving PI controllers presented in this work is constructive and motivated by the applicaton to physical systems.

Université Paris-Saclay
Espace Technologique / Immeuble Discovery
Route de l'Orme aux Merisiers RD 128 / 91190 Saint-Aubin, France